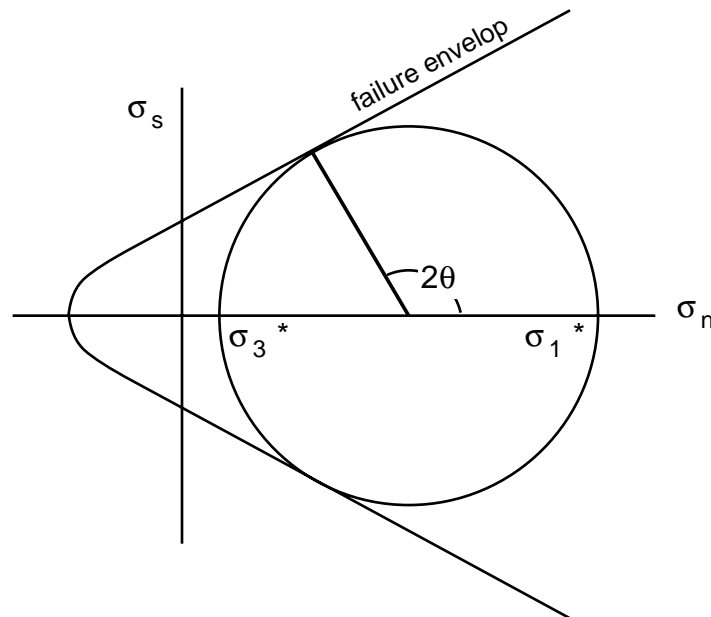


LECTURE 21—FAULTS III: DYNAMICS & KINEMATICS

21.1 Introduction

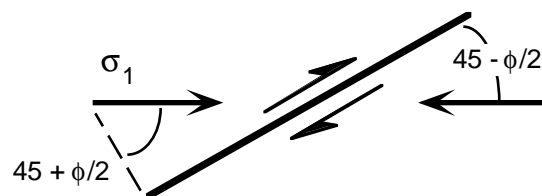
Remember that the process of making a fault in unfractured, homogeneous rock mass could be described by the Mohr's circle for stress intersecting the failure envelope.



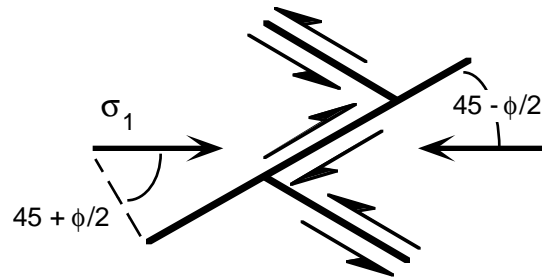
Under upper crustal conditions, the failure envelope has a constant slope and is referred to as the Coulomb failure criteria:

$$\sigma_s = S_0 + \sigma_n^* \mu, \text{ where } \mu = \tan \phi.$$

What this says is that, under these conditions, faults should form at an angle of $45^\circ - \phi/2$ with respect to σ_1 . Because for many rocks, $\phi \approx 30^\circ$, fault should form at about 30° to the maximum principal stress, σ_1 :



Furthermore the Mohr's Circle shows that, in two dimensions, there will be two possible fault orientations which are symmetric about σ_1 .

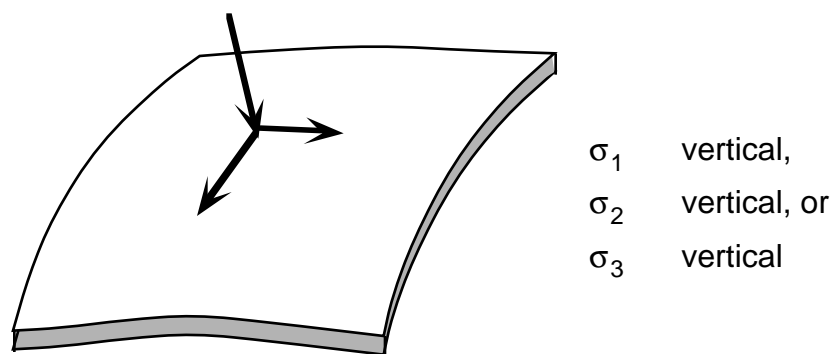


Such faults are called **conjugate fault sets** and are relatively common in the field. The standard interpretation is that σ_1 bisects the acute angle and σ_3 bisects the obtuse angle between the faults.

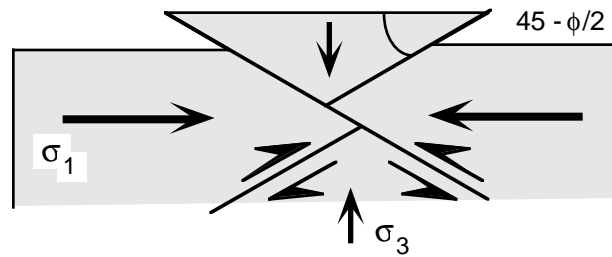
21.2 Anderson's Theory of Faulting

Around the turn of the century, Anderson realized the significance of Coulomb failure, and further realized that, *because the earth's surface is a "free surface" there is essentially no shear stress parallel to the surface of the Earth.* [The only trivial exception to this is when the wind blows hard.]

Therefore, one of the three principal stresses must be perpendicular to the Earth's surface, because a principal stress is always perpendicular to a plane with no shear stress on it. The other two principal stresses must be parallel to the surface:

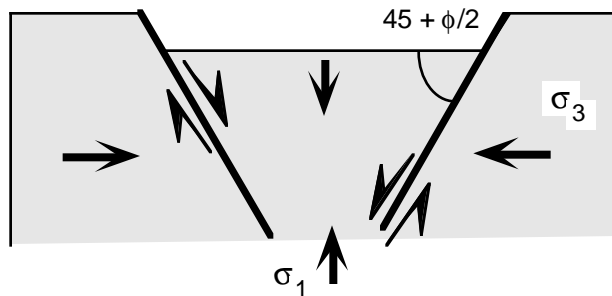


This constraint means that there are very few possible fault geometries for near surface deformation. They are shown below:



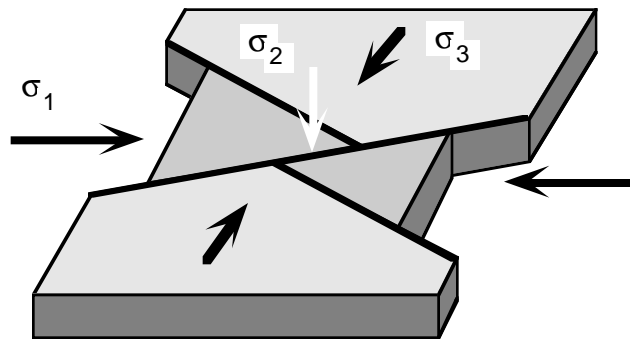
Thrust faults

dip < 45°



Normal faults

dip > 45°



Strike-slip

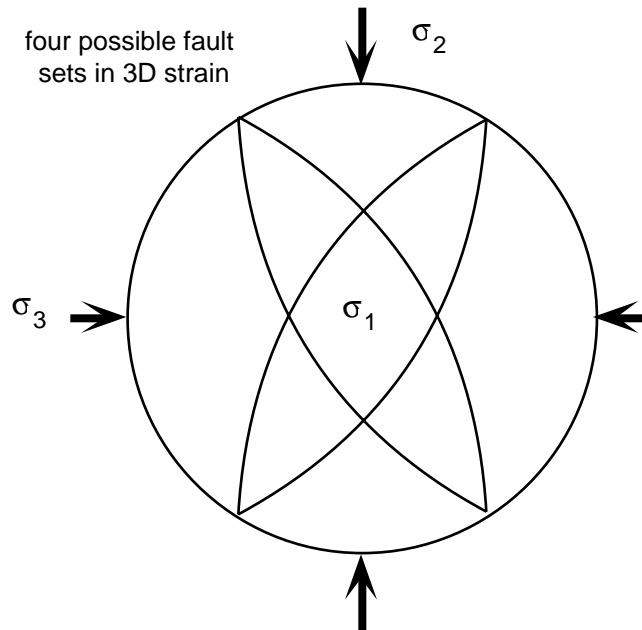
Anderson's theory has proved to be very useful but it is not a universal rule. For example, the theory predicts that we should never see low-angle normal faults near the Earth's surface but, as we shall see later in the course, we clearly do see them. Likewise, high-angle reverse faults exist, even if they are not predicted by the theory.

There are two basic problems with Anderson's Theory:

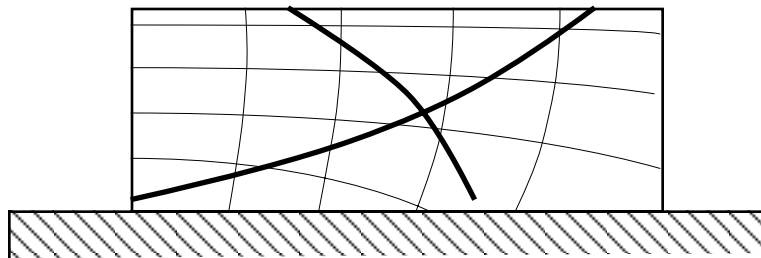
- Rocks are not homogeneous as implied by Coulomb failure but commonly have planar anisotropies. These include bedding, metamorphic foliations, and pre-existing fractures. If σ_1 is greater than about 60° to the planar anisotropy then it doesn't matter; otherwise the slip will probably occur parallel to the

anisotropy.

- There is an implicit assumption of plane strain in Anderson's theory -- no strain is assumed to occur in the σ_2 direction. Thus, only two fault directions are predicted. In three-dimensional strain, there will be two pairs of conjugate faults as shown by the work of Z. Reches.



Listric faults and steepening downward faults would appear to present a problem for Anderson's theory, but this is not really the case. They are just the result of curving stress trajectories beneath the Earth's surface:



Because the stress trajectories curve, the faults must curve. The only requirement is that they intersect the surface at the specified angles

21.3 Strain from Fault Populations

Anderson's law is commonly too restrictive for real cases where the Earth contains large numbers of pre-existing fractures of various orientations in a variety of rock materials. Thus, structural geologists have developed a number of new techniques to analyze fault populations. There are two basic ways to study populations of faults: (1) to look at them in terms of the *strain* that they produce — e.g. **kinematic analysis**, or (2) to interpret the faults in terms of the stress which produced them, or **dynamic analysis**. Both of these methods have their advantages and disadvantages and all require knowledge of the sense of shear of all of the faults included in the analysis.

21.3.1 Sense of Shear

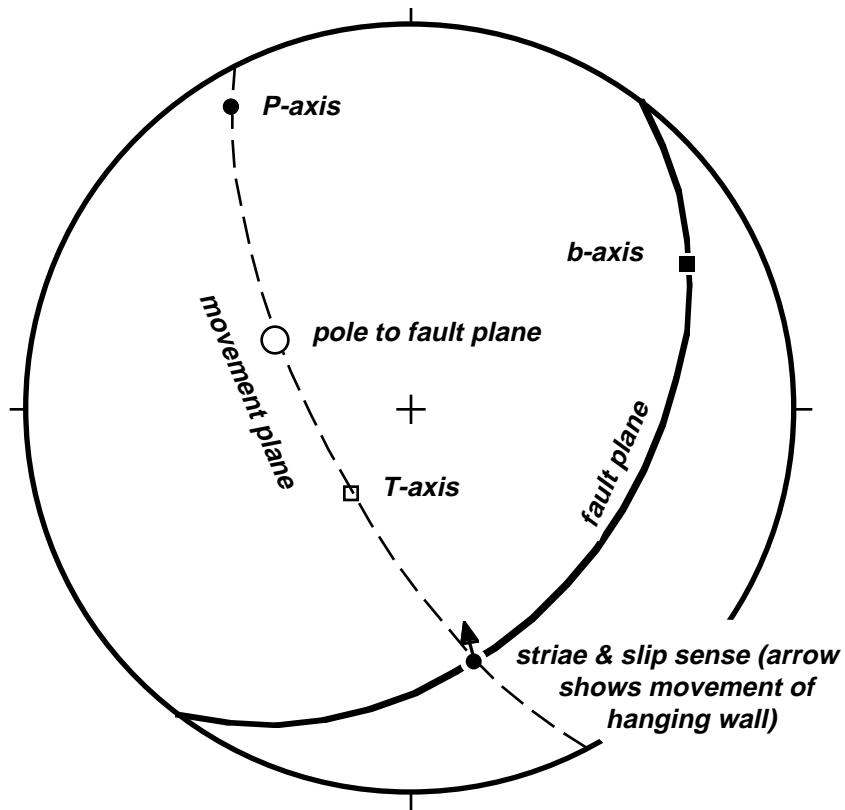
Brittle shear zones have been the focus of increasing interest during the last decade. Their analysis, either in terms of kinematics or dynamics, require that we determine the sense of shear. Because piercing points are rare, we commonly need to resort to an interpretation of minor structural features along, or within the shear zone itself. In general, these features include such things as (listed roughly in order of decreasing reliability):

- sigmoidal extension fractures
- steps with mineral fibers
- shear zone foliations (“brittle S-C fabrics”)
- drag folds
- Riedel shears (with sense-of shear indicators)
- tool marks

21.3.2 Kinematic Analysis of Fault Populations

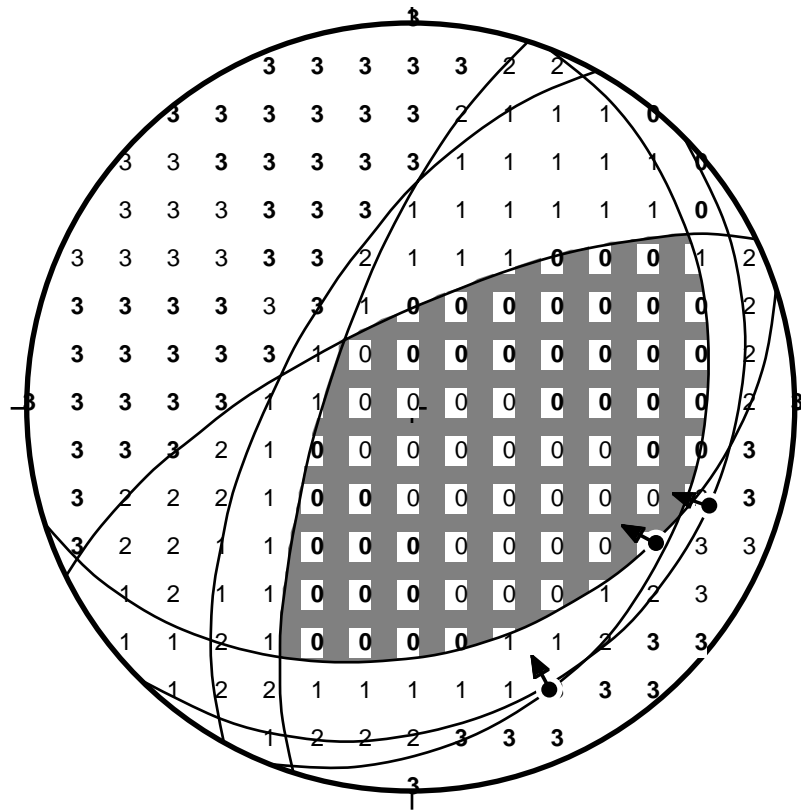
The simplest kinematic analysis, which takes its cue from the study of earthquake fault plane solutions is the graphical **P & T axis analysis**. Despite their use in seismology as “pressure” and “tension”, respectively, P and T axes are the infinitesimal strain axes for a fault. Perhaps the greatest advantage of P and T axes are that, independent of their kinematic or dynamic significance, they are a simple, direct representation of fault geometry and the sense of slip. That is, one can view them as simply a compact alternative way of displaying the original data on which any further analysis is based. The results of most of the more sophisticated analyses commonly are difficult to relate to the original data; such is not the problem for P and T axes. For any fault zone, you can identify a **movement plane**, which

is the plane that contains the vector of the fault and the pole to the fault. The P & T axes are located in the movement plane at 45° to the pole:

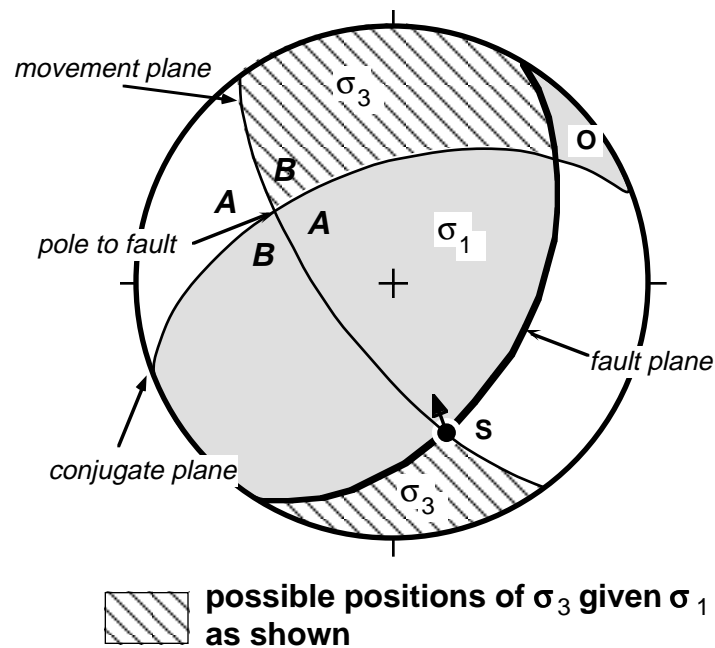


21.3.3 The P & T Dihedra

MacKenzie (1969) has pointed out, however, that particularly in areas with pre-existing fractures (which is virtually everywhere in the continents) there may be important differences between the principal stresses and P & T. In fact, the greatest principal stress may occur virtually anywhere within the P-quadrant and the least principal stress likewise anywhere within the T-quadrant. The P & T dihedra method proposed by Angelier and Mechler (1977) takes advantage of this by assuming that, in a population of faults, the geographic orientation that falls in the greatest number of P-quadrants is most likely to coincide with the orientation of σ_1 . The diagram, below, shows the P & T dihedra analysis for three faults:



In the diagram, the faults are the great circles with the arrow-dot indicating the striae. The conjugate for each fault plane is also shown. The number at each grid point shows the number of individual P-quadrants that coincide with the node. The region which is within the T-quadrants of all three faults has been shaded in gray. The bold face zeros and threes indicate the best solutions obtained using Lisle's (1987) AB-dihedra constraint. Lisle showed that the resolution of the P & T dihedra method can be improved by considering how the stress ratio, R , affects the analysis. The movement plane and the conjugate plane divide the sphere up into quadrants which Lisle labeled "A" and "B" (see figure below). If one principal stress lies in the region of intersection of the appropriate kinematic quadrant (i.e. either the P or the T quadrant) and the A quadrant then the other principal stress must lie in the B quadrant. In qualitative terms, this means that the σ_3 axis must lie on the same side of the movement plane as the σ_1 axis.



21.4 Stress From Fault Populations¹

Since the pioneering work of Bott (1959), many different methods for inferring certain elements of the stress tensor from populations of faults have been proposed. These can be grouped in two broad categories: graphical methods (Compton, 1966; Arthaud, 1969; Angelier and Mechler, 1977; Aleksandrowski, 1985; and Lisle, 1987) and numerical techniques (Carey and Brunier, 1974; Etchecopar et al., 1981; Armijo et al., 1982; Angelier, 1984, 1989; Gephart and Forsyth, 1984; Michael, 1984; Reches, 1987; Gephart, 1988; Huang, 1988).

21.4.1 Assumptions

Virtually all numerical stress inversion procedures have the same basic assumptions:

1. Slip on a fault plane occurs in the direction of resolved shear stress (implying that local heterogeneities that might inhibit the free slip of each fault plane -- including interactions with other fault planes -- are relatively insignificant).
2. The data reflect a uniform stress field (both spatially and temporally)—this

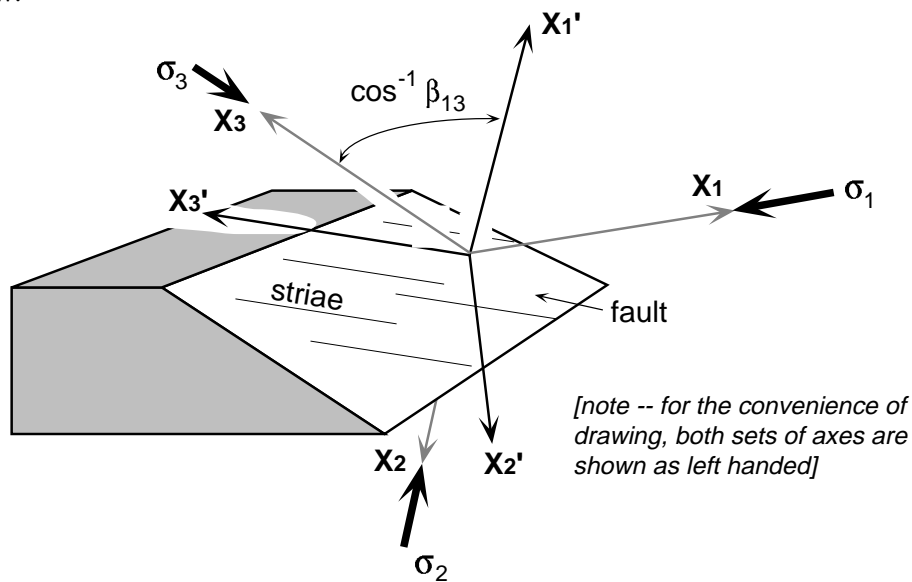
¹This supplemental section was co-written John Gephart and Rick Allmendinger and is adapted from the 1989 Geological Society of America shortcourse on fault analysis.

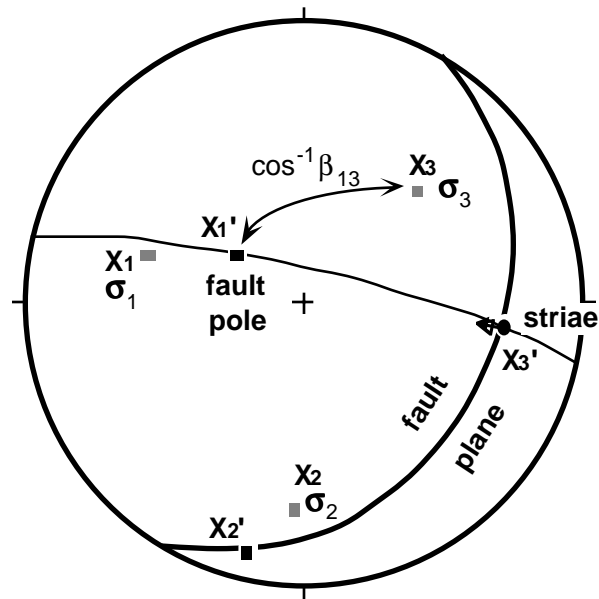
requires that there has been no post-slip deformation of the region which would alter the fault orientations.

While the inverse techniques may be applied to either fault/slickenside or earthquake focal mechanism data, these assumptions may apply more accurately to the latter than the former. Earthquakes may be grouped in geologically short time windows, and represent sufficiently small strains that rotations may be neglected. Faults observed in outcrop, on the other hand, almost certainly record a range of stresses which evolved through time, possibly indicating multiple deformations. If heterogeneous stresses are suspected, a fault data set can easily be segregated into subsets, each to be tested independently. In any case, to date there have been many applications of stress inversion methods from a wide variety of tectonic settings which have produced consistent and interpretable results.

21.4.2 Coordinate Systems & Geometric Basis

Several different coordinate systems are used by different workers. The ones used here are those of Gephart and Forsyth (1984), with an unprimed coordinate system which is parallel to the principal stress directions, and a primed coordinate system fixed to each fault, with axes parallel to the pole, the striae, and the B-axis (a line in the plane of the fault which is perpendicular to the striae) of the fault, as shown below:





The relationship between the principal stress and the stress on the one fault plane shown is given by a standard tensor transformation:

$$\sigma'_{ij} = \beta_{ik} \beta_{jl} \sigma_{kl}.$$

In the above equation, β_{ik} is the transformation matrix reviewed earlier, σ_{kl} are the regional stress magnitudes, and σ'_{ij} are the stresses on the plane. Expanding the above equation to get the components of stress on the plane in terms of the principal stresses, we get:

$$\sigma'_{11} = \beta_{11}\beta_{11}\sigma_1 + \beta_{12}\beta_{12}\sigma_2 + \beta_{13}\beta_{13}\sigma_3 \quad \text{[normal traction],}$$

$$\sigma'_{12} = \beta_{11}\beta_{21}\sigma_1 + \beta_{12}\beta_{22}\sigma_2 + \beta_{13}\beta_{23}\sigma_3 \quad \text{[shear traction } \perp \text{ striae],}$$

and

$$\sigma'_{13} = \beta_{11}\beta_{31}\sigma_1 + \beta_{12}\beta_{32}\sigma_2 + \beta_{13}\beta_{33}\sigma_3 \quad \text{[shear traction } // \text{ striae].}$$

From assumption #1 above we require that σ'_{12} vanishes, such that:

$$0 = \beta_{11}\beta_{21}\sigma_1 + \beta_{12}\beta_{22}\sigma_2 + \beta_{13}\beta_{23}\sigma_3.$$

Combining this expression with the condition of orthogonality of the fault pole and B axis:

$$0 = \beta_{11}\beta_{21} + \beta_{12}\beta_{22} + \beta_{13}\beta_{23}.$$

yields

$$\frac{\sigma_2 - \sigma_1}{\sigma_3 - \sigma_1} \equiv R = - \frac{\beta_{13} \beta_{23}}{\beta_{12} \beta_{22}}. \quad (21.1)$$

where the left-hand side defines the parameter, R, which varies between 0 and 1 (assuming that $\sigma_1 \geq \sigma_2 \geq \sigma_3$) and provides a measure of the magnitude of σ_2 relative to σ_1 and σ_3 . A value of R near 0 indicates that σ_2 is nearly equal to σ_1 ; a value near 1 means σ_2 is nearly equal to σ_3 ². Any combination of principal stress and fault orientations which produces $R > 1$ or $R < 0$ from the right-hand side of (21.1) is incompatible (Gephart, 1985). A further constraint is provided by the fact that the shear traction vector, σ_{13}' , must have the same direction as the slip vector (sense of slip) for the fault; this is ensured by requiring that $\sigma_{13}' > 0$.

Equation (21.1) shows that, of the 6 independent components of the stress tensor, only four can be determined from this analysis. These are the stress magnitude parameter, R, and three stress orientations indicated by the four β_{ij} terms (of which only three are independent because of the orthogonality relations).

21.4.3 Inversion Of Fault Data For Stress

Several workers have independently developed schemes for inverting fault slip data to obtain stresses, based on the above conditions but following somewhat different formulations. In all cases, the goal is to find the stress model (three stress directions and a value of R) which minimizes the differences between the observed and predicted slip directions on a set of fault planes.

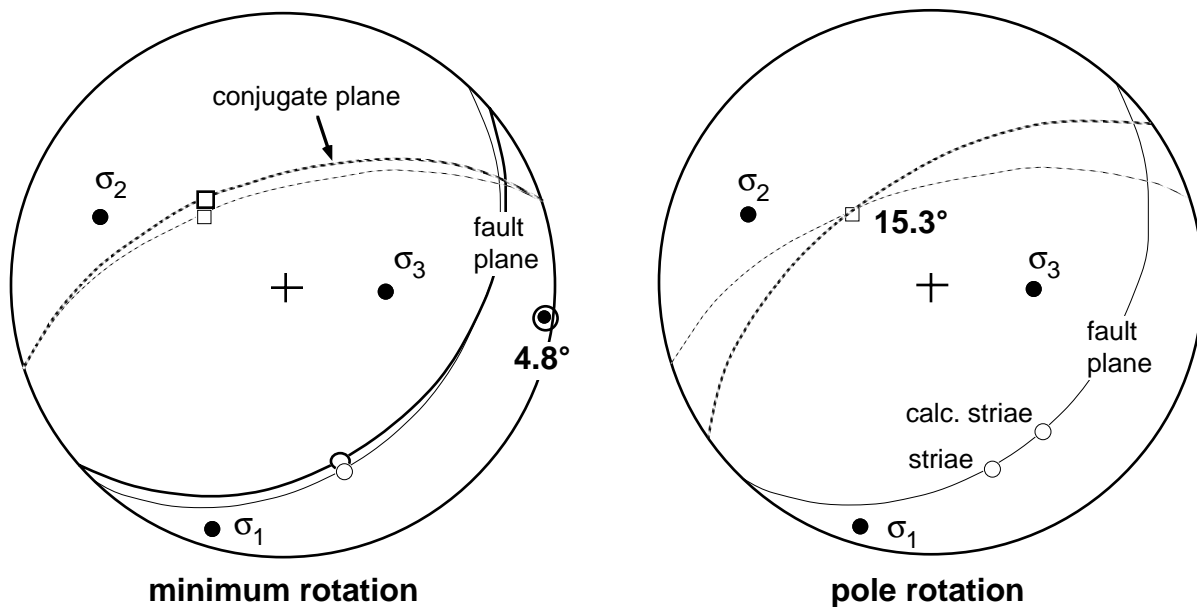
The first task is to decide: What parameter is the appropriate one to minimize in finding the optimum model? The magnitude of misfit between a model and fault slip datum reflects either: (1) the minimum observational error, or (2) the minimum degree of heterogeneity in stress orientations, in order to attain perfect consistency between model and observation. Two simple choices may be considered: Many workers (e.g. Carey and Brunier, 1974; Angelier, 1979, 1984) define the misfit as the angular difference between the observed and predicted slip vector measured in the fault plane (referred to as a

²An similar parameter was devised independently by Angelier and coworkers (Angelier et al., 1982; Angelier, 1984, 1989):

$$\Phi = \frac{\sigma_2 - \sigma_3}{\sigma_1 - \sigma_3}.$$

In this case, if $\Phi = 0$, then $\sigma_2 = \sigma_3$, and if $\Phi = 1$, then $\sigma_2 = \sigma_1$. Thus, $\Phi = 1 - R$.

“pole rotation” because the angle is a rotation angle about the pole to the fault plane). This implicitly assumes that the fault plane is perfectly known, such that the only ambiguity is in the orientation of the striae (right side of figure below). Such an assumption may be acceptable for fault data from outcrop for which it is commonly easier to measure the fault surface orientation than the orientation of the striae on the fault surface. Alternatively, one can find the smallest rotation of coupled fault plane and striae about *any* axis that results in a perfect fit between data and model (Gephart and Forsyth, 1984)—this represents the smallest possible deviation between an observed and predicted fault slip datum, and can be much smaller than the pole rotation, as shown in the left-hand figure below (from Gephart, in review). This “minimum rotation” is particularly useful for analyzing earthquake focal mechanism data for which there is generally similar uncertainties in fault plane and slip vector orientations.



Because of the extreme non-linearity of this problem, the most reliable (but computationally demanding) procedure for finding the best stress model relative to a set of fault slip data involves the application of an exhaustive search of the four model parameters (three stress directions and a value of R) by exploring sequentially on a grid (Angelier, 1984; Gephart and Forsyth, 1984). For each stress model examined the rotation misfits for all faults are calculated and summed; this yields a measure of the acceptability of the model relative to the whole data set—the best model is the one with the smallest sum of misfits. Following Gephart and Forsyth (1984), confidence limits on the range of acceptable models

can then be calculated using statistics for the one norm misfit, after Parker and McNutt (1980). In order to increase the computational efficiency of the inverse procedure, a few workers have applied some approximations which enable them to linearize the non-linear conditions in this analysis (Angelier, 1984; Michael, 1984); naturally, these lead to approximate solutions which in some cases vary significantly from those of more careful analyses. The inversion methods of Angelier et al. (1982, eq. 9 p. 611) and Michael (1984) make the arbitrary assumption that the first invariant of stress is zero ($\sigma_{11} + \sigma_{22} + \sigma_{33} = 0$). Gephart (in review) has noted that this implicitly prescribes a fifth stress parameter, relating the magnitudes of normal and shear stresses (which should be mutually independent), the effect of which is seldom evaluated.

Following popular convention in inverse techniques, many workers (e.g. Michael, 1984; Angelier et al., 1982) have adopted least squares statistics in the stress inversion problem (e.g. minimizing the sum of the squares of the rotations). A least squares analysis, which is appropriate if the misfits are normally distributed, places a relatively large weight on extreme (poorly-fitting) data. If there are erratic data (with very large misfits), as empirically is often the case in fault slip analyses, then too much constraint is placed on these and they tend to dominate a least squares inversion. One can deal with this by rejecting anomalous data (Angelier, 1984, suggests truncating the data at a pole rotation of 45°), or by using a one-norm misfit, which minimizes the sum of the absolute values of misfits (rather than the squares of these), thus placing less emphasis on such erratic data, and achieving a more robust estimate of stresses (Gephart and Forsyth, 1984).

21.5 Scaling Laws for Fault Populations

Much work over the last decade has shown that fault populations display power law scaling characteristics (i.e., “fractal”). In particular, the following features have been shown to be scale invariant:

- trace length vs. cumulative number
- displacement vs. cumulative number
 - trace length vs. displacement
- geometric moment vs. cumulative number

If the power law coefficients were known with certainty, then these relationships would have important predictive power. Unfortunately, there are very few data sets which have been sample with sufficient completeness to enable unambiguous determination of the coefficients.

LECTURE 22—FAULTS IV: MECHANICS OF THRUST FAULTS

22.1 The Paradox of Low-angle Thrust Faults

In many parts of the world, geologists have recognized very low angle thrust faults in which older rocks are placed over younger. Very often, the dip of the fault surface is only a few degrees. Such structures were first discovered in the Alps around 1840 and have intrigued geologists ever since. The basic observations are:

1. Faults are very low angle, commonly $< 10^\circ$;
2. Overthrust blocks of rock are relatively thin, ~ 5 - 10 km;
3. The map trace of individual faults is very long, 100 - 300 km; and
4. The blocks have been displaced large distances, 10s to 100s of km.

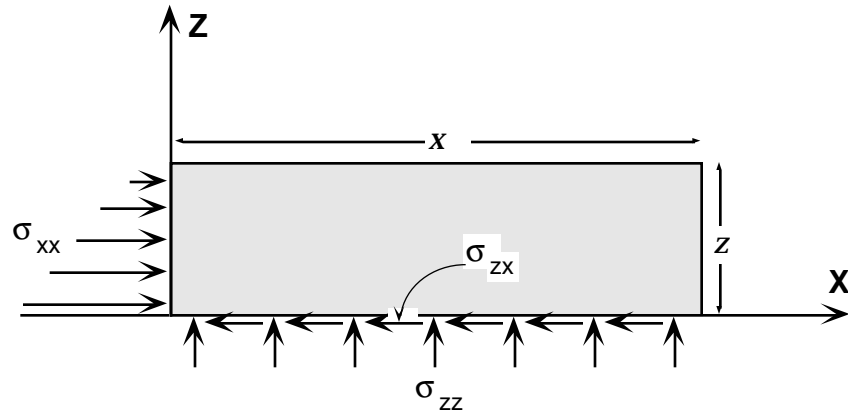
What we have is a very thin sheet of rock that has been pushed over other rocks for 100s of kilometers. This process has been likened to trying to push a wet napkin across a table top: There's no way that the napkin will move as a single rigid unit.

The basic problem, and thus the "paradox" of large overthrusts, is that rocks are apparently too weak to be pushed from behind over long distances without deforming internally. That rocks are so weak has been noted by a number of geologists, and was well illustrated in a clever thought experiment by M. King Hubbert in the early 1950's. He posed the simple question, "if we could build a crane as big as we wanted, could we pick up the state of Texas with it?" He showed quite convincingly that the answer is no because the rocks that comprise the state (any rock in the continental crust) are too weak to support their own weight.

22.2 Hubbert & Rubey Analysis

In 1959, Hubbert along with W. Rubey wrote a classic set of papers which clearly laid out the mechanical analysis of the paradox of large overthrusts. I want to go through their analysis because it is a superb illustration of the simple mechanical analysis of a structural problem.

The simplest expression of the problem is to imagine a rectangular block sitting on a flat surface. When we push this block on the left side, the friction along the base, which is a function of the weight of the block times the coefficient of friction, will resist the tendency of the block to slide to the right. The basic boundary conditions are:



Note that indices used in the diagram above are the standard conventions that were used when we discussed stress.

When the block is just ready to move, the applied stress, σ_{xx} , must just balance the shear stress at the base of the block, σ_{zx} . We can express this mathematically as:

$$\int_0^z \sigma_{xx} dz = \int_0^x \sigma_{zx} dx \quad (22.1)$$

We can get an expression for σ_{zx} easily enough because it's just the frictional resistance to sliding, which from last time is

$$\sigma_s = \mu \sigma_n,$$

or, in our notation, above

$$\sigma_{zx} = \mu \sigma_{zz}. \quad (22.2)$$

The normal stress, σ_{zz} , is just equal to the lithostatic load:

$$\sigma_{zz} = \rho g z.$$

So,

$$\sigma_{zx} = \mu \rho g z.$$

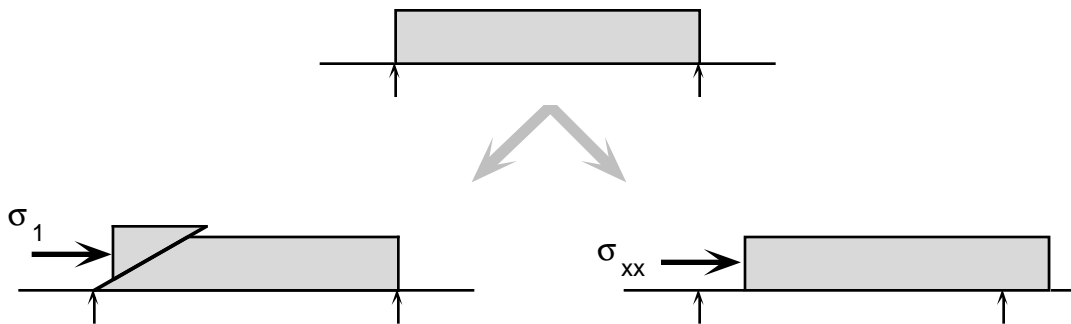
We can now solve the right hand side of equation **22.1** (p. 171):

$$\int_0^z \sigma_{xx} dz = \int_0^x \mu \rho g z dx$$

and

$$\int_0^z \sigma_{xx} dz = \mu \rho g z x .$$

Now we need to evaluate the left side of the equation. Remember that we want to find the largest stress that the block can support without breaking internally as illustrated in the diagram below.

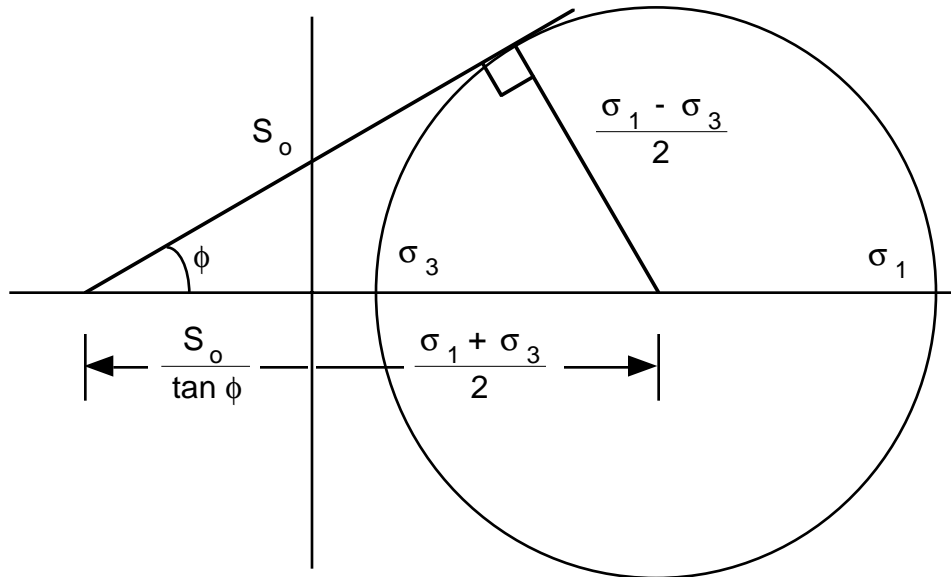


The limiting case then, is where the block does fracture internally, in which case there is no shear on the base. So, in this limiting case

$$\sigma_1 = \sigma_{xx} \quad \text{and} \quad \sigma_3 = \sigma_{zz} .$$

Now to solve this problem, we need to derive a relationship between σ_1 and σ_3 at failure, which we can get from Mohr's circle for stress. From the geometry of the Mohr's Circle, below, we see that:

$$\frac{\sigma_1 - \sigma_3}{2} = \left(\frac{\sigma_1 + \sigma_3}{2} + \frac{S_o}{\tan \phi} \right) \sin \phi$$



Solving for σ_1 in terms of σ_3 we get:

$$\sigma_1 = C_o + K \sigma_3, \quad (22.3)$$

where

$$C_o = 2S_o \sqrt{K} \quad \text{and} \quad K = \frac{1 + \sin \phi}{1 - \sin \phi}. \quad (22.4)$$

So,

$$\sigma_{xx} = \sigma_1 = C_o + K \sigma_3 = C_o + K \sigma_{zz}.$$

But $\sigma_{zz} = \rho g z$ so

$$\sigma_{xx} = C_o + K \rho g z.$$

Now, we can evaluate the left side of equation **22.1** (p. 171):

$$\int_0^z \sigma_{xx} dz = \mu \rho g z x$$

$$\int_0^z (C_o + K \rho g z) dz = \mu \rho g z x$$

$$C_o z + \frac{K \rho g z^2}{2} = \mu \rho g z x .$$

Dividing through by z and solving for x , we see that the maximum length of the block is a linear function of its thickness:

$$x = \frac{C_o}{\mu \rho g} + \frac{Kz}{2\mu} . \tag{22.5}$$

Now, let's plug in some realistic numbers. Given

$$\begin{aligned} \phi &= 30^\circ \\ \mu &= 0.58 \\ S_o &= 20 \text{ Mpa} \\ \rho &= 2.3 \text{ gm/cm}^3, \end{aligned}$$

we can calculate that

$$\begin{aligned} C_o &= 69.4 \text{ Mpa} \\ K &= 3. \end{aligned}$$

With these values, equation 20-5 becomes:

$$x_{max} = 5.4 \text{ km} + 2.6 z .$$

Thus,

Thickness	Maximum Length
5 km	18.4 km
10 km	31.4 km

22.3 Alternative Solutions

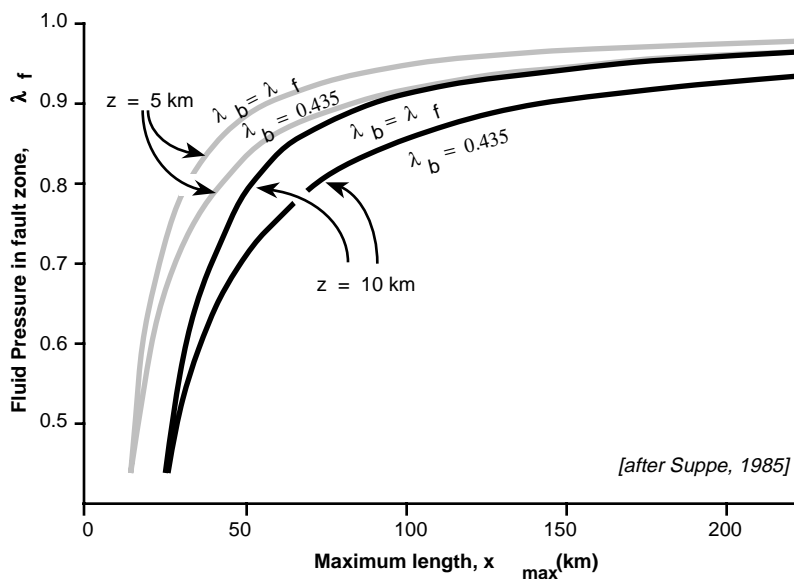
These numbers are clearly too small, bearing out the paradox of large thrust faults which we stated at the beginning of this lecture. Because large thrust faults obviously do exist, there must be something wrong with the model. Over the years, people have suggested several ways to change it.

1. Rheology of the basal zone is incorrect—In our analysis, above, we assumed that friction governed the sliding of the rock over its base. However, it is likely that in some rocks, especially shales or evaporites, or where higher temperatures are involved, plastic or viscous rheologies are more appropriate. This would change the problem significantly because the yield strengths in those cases is independent of the normal stress.

2. Pore Pressure—Pore pressure could reduce the effective normal stress on the fault plane [$\sigma_{zz}^* = \sigma_{zz} - P_f$] and therefore it would also reduce the frictional resistance due to sliding, σ_{zx} (from equation 20-2). There is, however, a trade off because, unless you somehow restrict the pore pressure to *just* the fault zone, excess fluid pressure will make the block weaker as well (and we want the block as strong as possible).

Hubbert and Rubey proposed that pore pressure was an important part of the answer to this problem and they introduced the concept of the fluid pressure ratio:

$$\lambda_f = \frac{P_f}{\rho g z} = \frac{\text{pore fluid pressure}}{\text{lithostatic stress}}$$



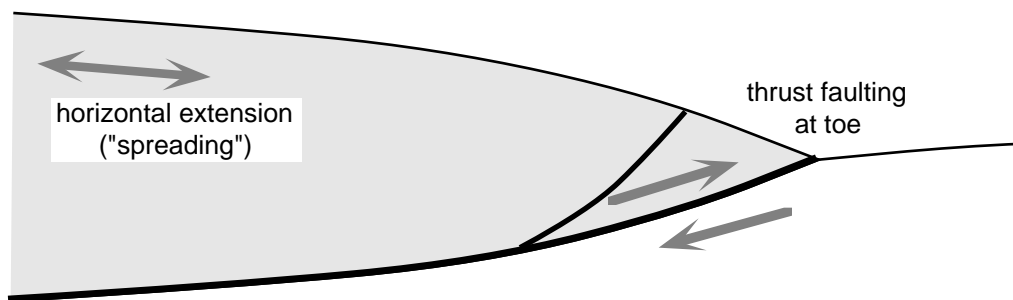
The graph above show how pore pressure in the block (plotted as λ_b) and pore pressure along the fault (λ_f) affect the maximum length of the block. For blocks 5 and 10 km thick, two cases are shown, one where there is no difference in pore pressure between block and fault, and the other where the pore pressure is hydrostatic (assuming a density, $\rho = 2.4 \text{ gm/cm}^3$). The diagram was constructed assuming C_0

50 MPa and $K = 3$.

3. Thrust Plates Slide Downhill—This was the solution that Hubbert and Rubey favored (aided by pore pressure), but the vast amount of seismic reflection data in thrust belts which has been collected since they wrote their article shows that very few thrust faults move that way. Most major thrust faults moved up a gentle slope of $2 - 10^\circ$.

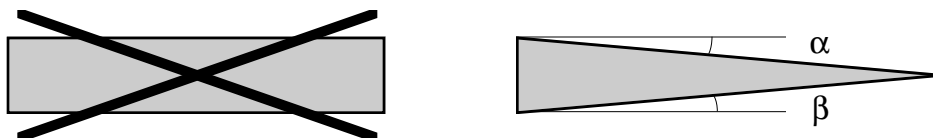
There are major low-angle fault bounded blocks that slide down hill. The Heart Mountain detachment in NW Wyoming is a good example.

4. Thrust Belts Analogous to Glaciers—Several geologists, including R. Price (1973) and D. Elliott (1976) have proposed that thrust belts basically deform like glaciers. Like gravity sliding, the spreading of a glacier is driven by its own weight, rather than being pushed from behind by some tectonic interaction. Glaciers, however, can flow uphill as long as the topographic slope is inclined in the direction of flow.

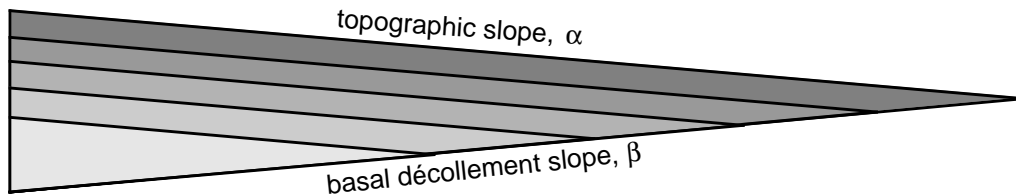


This model was very popular in the 1970's, but the lack of evidence for large magnitude horizontal extension in the rear of the thrust belt, or "hinterland" has made it decline in popularity.

5. Rectangular Shape Is Not Correct—This is clearly an important point. Thrust belts and individual thrust plates within them are wedge-shaped rather than rectangular as originally proposed by Hubbert and Rubey. Many recent workers, including Chapple (1978) and Davis, Suppe, & Dahlen (1983, and subsequent papers) have emphasized the importance of the wedge.



The wedge taper is defined the sum of two angles, the topographic slope, α , and the slope of the basal décollement, β , as shown above. Davis et al. (1983) proposed that the wedge grows “*self-similarly*”, maintaining a constant taper.



In their wedge mechanics, they propose the following relation between α and β when the wedge is a critical taper:

$$\alpha + \beta = \frac{(1 - \lambda)\mu + \beta}{(1 - \lambda)k + 1}$$

where μ is the coefficient of friction, λ is the Hubbert-Rubey pore pressure ratio, and k is closely related to the “earth pressure coefficient” which was derived above in equations 20-3 and 20-4.

If the basal friction increases, either by changing the frictional coefficient, μ , or by increasing the normal stress across the fault plane (which is the same as decreasing λ), the taper of the wedge will increase. Note that, as $\lambda \rightarrow 1$, $\alpha \rightarrow 0$. In other words, when there is no normal stress across the fault because the lithostatic load is entirely supported by the pore pressure, there should be no topographic slope.

If the wedge has a taper *less than* the critical taper, then it will deform internally by thrust faulting in order to build up the taper. If its taper is *greater than* the critical taper, then it will deform by normal faulting to reduce the taper.

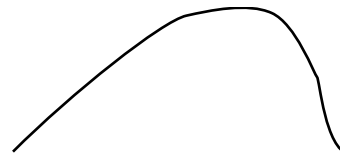
LECTURE 23—FOLDS I: GEOMETRY

Folding is the bending or flexing of layers in a rock to produce frozen waves. The layers may be any planar feature, including sedimentary bedding, metamorphic foliation, planar intrusions, etc. Folds occur at all scales from microscopic to regional. This first lecture will probably be mostly review for you, but it's important that we all recognize the same terminology.

23.1 Two-dimensional Fold Terminology

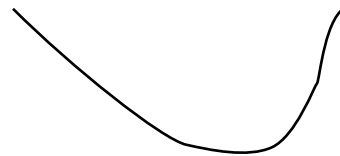
Antiform

Folds that are convex upward:

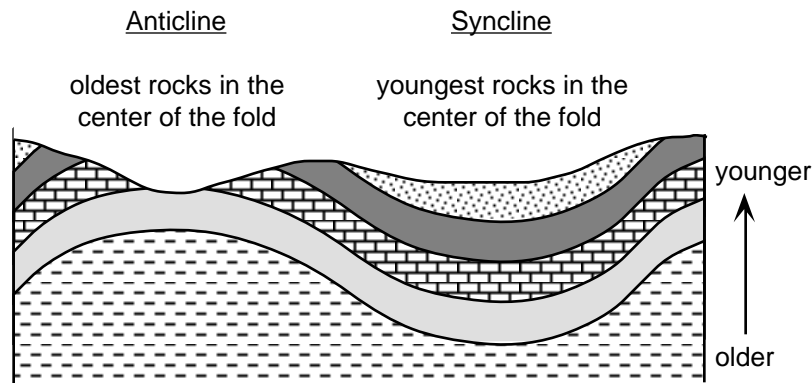


Synform

Folds that are concave upward:



To use the more common terms, anticline and syncline, we need to know which layers are older and which layers are younger. Many folds of metamorphic and igneous rocks should only be described using the terms antiform and synform.

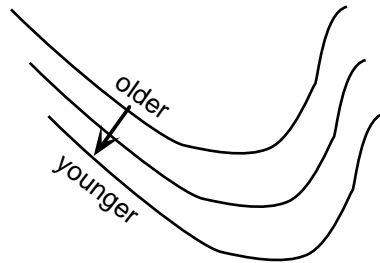


It may, at first, appear that there is no significant difference between antiforms and anticlines and synforms and synclines, but this is not the case. You can easily get antiformal synclines and synformal anticlines,

for example:

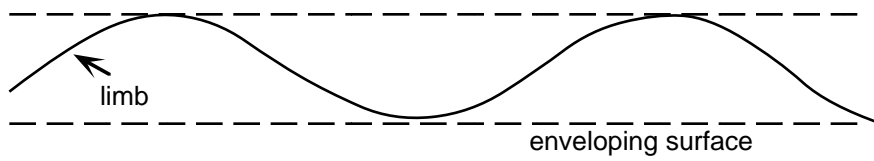
Synformal anticline

Folds that are concave upward, but the oldest beds are in the middle:

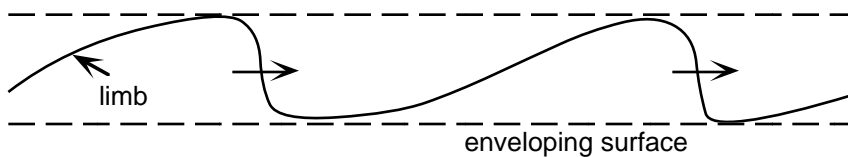


Folds can also be symmetric or asymmetric. The former occurs when the limbs of the folds are the same length and have the same dip relative to their enveloping surface. In asymmetric folds, the limbs are of unequal length and dip:

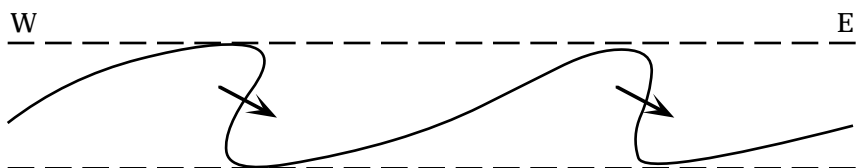
Symmetric folds:



Asymmetric folds:



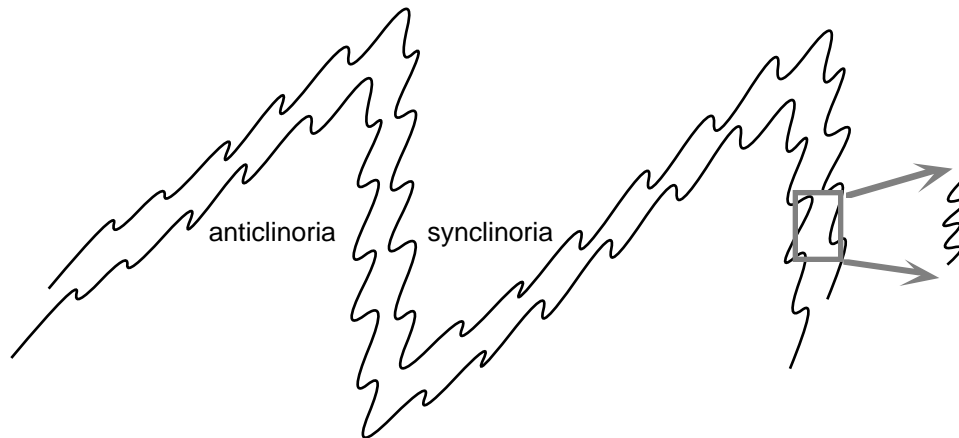
Overturned folds:



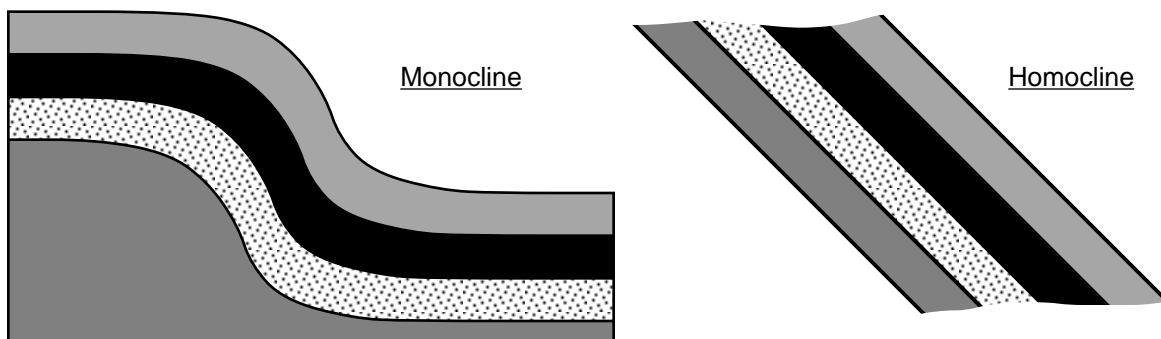
the tops of the more steeply dipping beds are facing or verging to the east in this picture

In asymmetric and overturned folds the concept of vergence or facing is quite important. This is the direction that the shorter, more steeply dipping asymmetric limb of the fold faces, or the arrows in the above pictures.

Numerous different scales folds can be superimposed on each other producing what are known as anticlinoria and synclinoria:



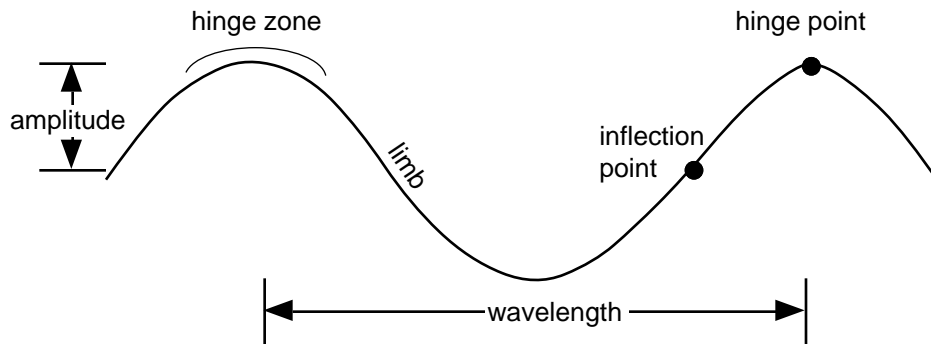
Two final terms represent special cases of tilted or folded beds:



23.2 Geometric Description of Folds

23.2.1 Two-dimensional (Profile) View:

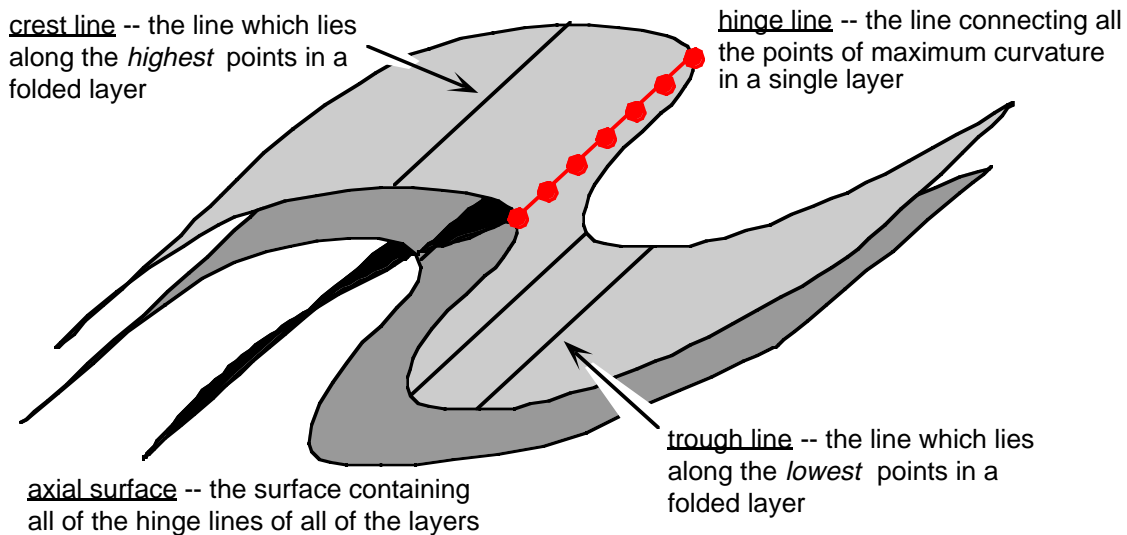
The most important concept is that of the hinge, which is the point or zone of maximum curvature in the layer. Other terms are self-explanatory:



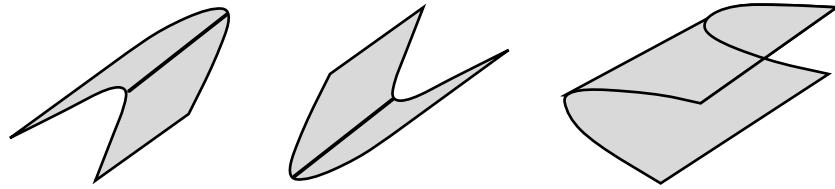
Note that the amplitude is the distance from the top (or bottom) of the folds to the inflection point.

23.2.2 Three-dimensional View:

In three dimensions, we can talk about the hinge line, which may be straight or curved, depending on the three-dimensional fold geometry. The axial surface contains all of the hinge lines. It is more commonly referred to as the “axial plane” but this is a special case where all of the hinge lines lie in a single plane.



In practice, you specify the orientation of the hinge line by measuring its *trend and plunge*. This information, alone, however, is insufficient to totally define the orientation of the fold. For example, all of the folds below have identical hinge lines, but are clearly quite different:

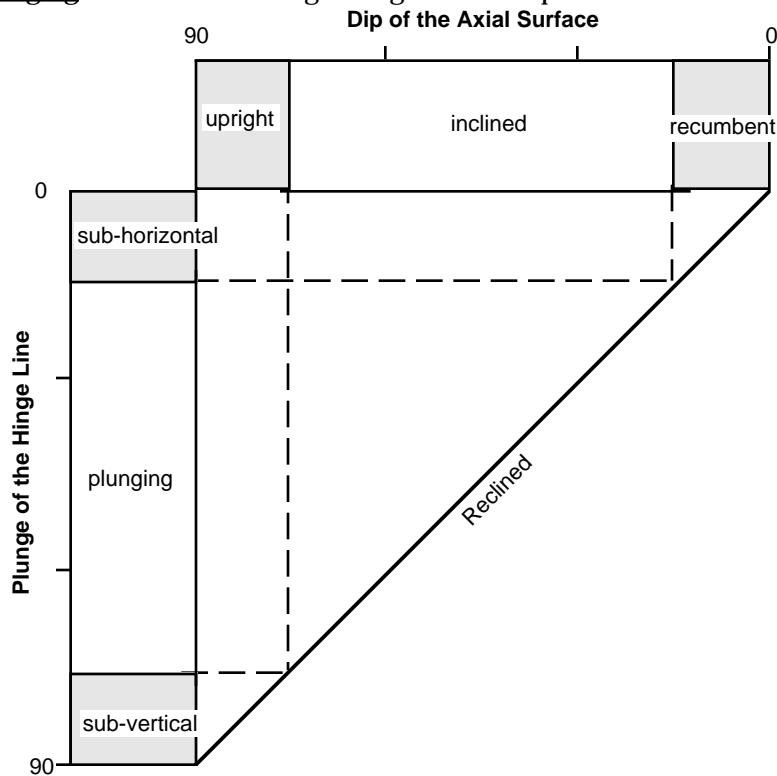


To completely define the orientation of a fold you need to specify both the trend and plunge of the hinge line and the strike and dip of the axial surface. The orientation of the axial surface alone is not sufficient either.

Most of the time, you will be representing the fold in two-dimensional projections: cross-sections, structural profiles or map views. In these cases what you show is the trace of the axial surface, or the axial trace. This is just the intersection between the axial surface and the plane of your projection.

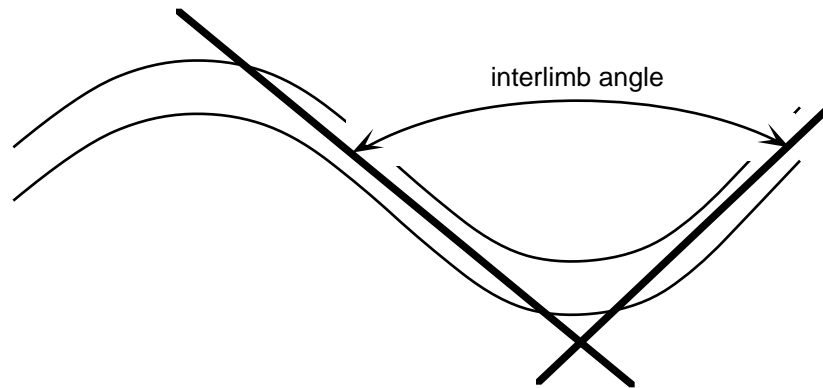
23.3 Fold Names Based on Orientation

The hinge line lies within the axial plane, but the trend of the hinge line is only parallel to the strike of the axial surface when the hinge line is horizontal. If the hinge line is not horizontal, then we say that the fold is a plunging fold. The following table give the complete names for fold orientations:



23.4 Fold Tightness

Another measure of fold geometry is the interlimb angle, shown in the diagram below.



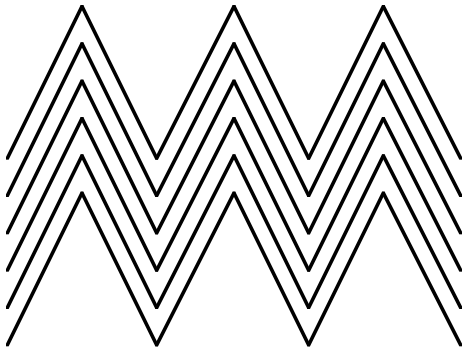
With this concept, there are yet more descriptive terms for folded rocks:

<u>Name</u>	<u>Interlimb Angle</u>
Flat lying, Homocline	180°
Gentle	170 - 180°
Open	90 - 170°
Tight	10 - 90°
Isoclinal	0 - 10°

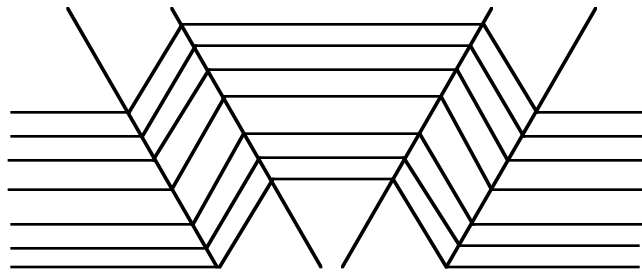
LECTURE 24 — FOLDS II: GEOMETRY & KINEMATICS

24.1 Fold Shapes

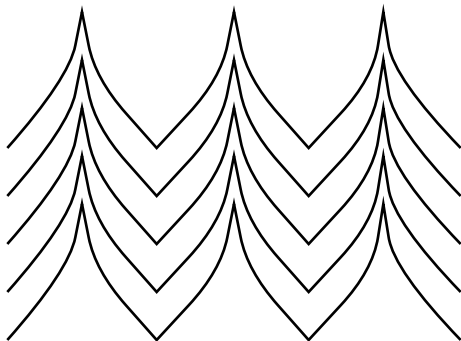
We have been drawing folds only one way, with nice smooth hinges, etc. But, there are many different shapes that folds can take:



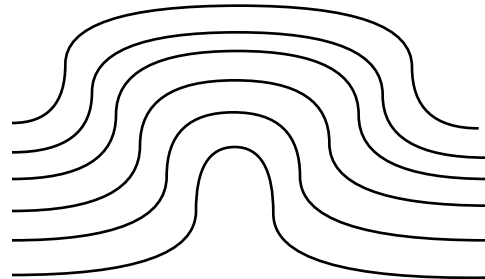
Chevron folds



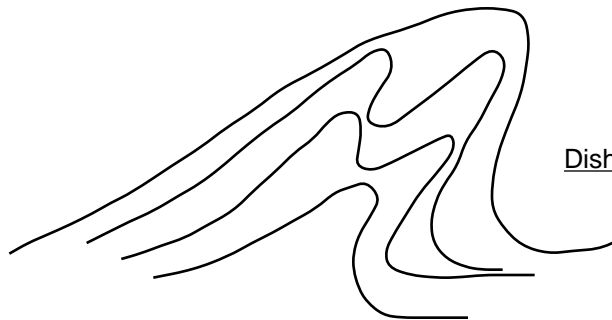
Kink Bands



Cusped folds



Box folds

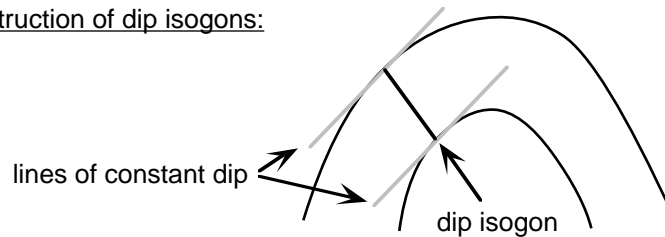


Disharmonic folds

24.2 Classification Based on Shapes of Folded Layers

One way of quantifying fold shape is by construction dip isogon diagrams. Dip isogons are lines which connect points of the same dip on different limbs of folds:

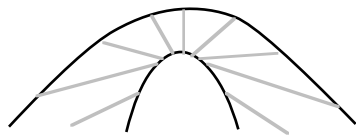
Construction of dip isogons:



By plotting dip isogons, you can identify three basic types of folds:

Class 1:

Inner beds more curved than outer beds. Dip Isogons fan outward



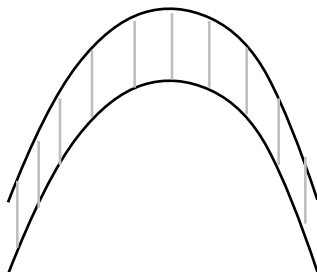
1A -- isogons on limbs make an obtuse angle with respect to the axial surface



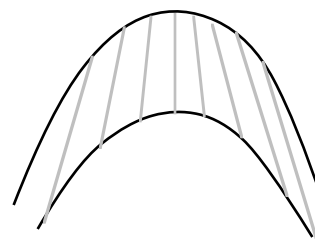
1B -- isogons are everywhere perpendicular to the beds, on both inner and outer surfaces. These are Parallel folds



1C -- isogons on limbs make an acute angle with respect to the axial surface



Class 2: Inner and outer surfaces have the same curvature. Dip isogons are parallel to each other and to the axial surface. These are Similar folds



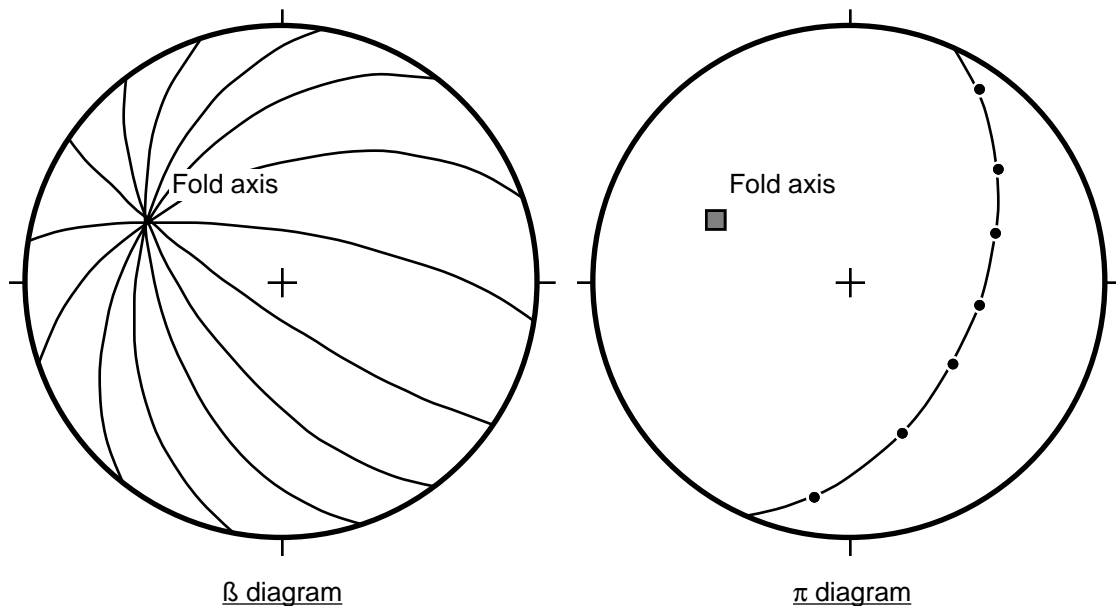
Class 3: Inner surface is less curved than the outer surface. Dip isogons fan inwards

24.3 Geometric-kinematic Classification:

24.3.1 Cylindrical Folds

Cylindrical folds are those in which the surface can be generated or traced by moving a line parallel to itself through space. This line is parallel to the hinge line and is called the fold axis. *Only cylindrical folds have a fold axis*. Thus, the term fold axis is properly applied only to this type of fold.

If you make several measurements of bedding on a perfectly cylindrical fold and plot them as great circles on a stereonet, all of the great circles will intersect at a single point. That point is the fold axis. The poles to bedding will all lie on a single great circle. This is the practical test of whether or not a fold is cylindrical:

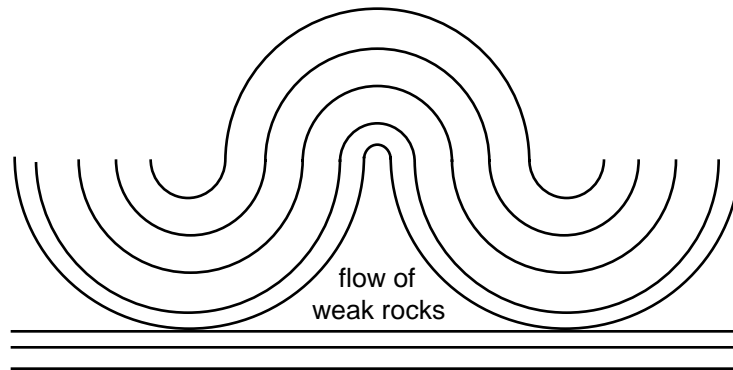


There are two basic types of cylindrical folds:

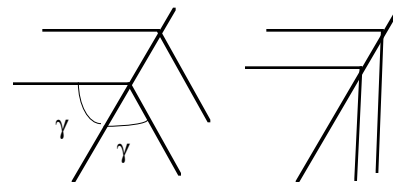
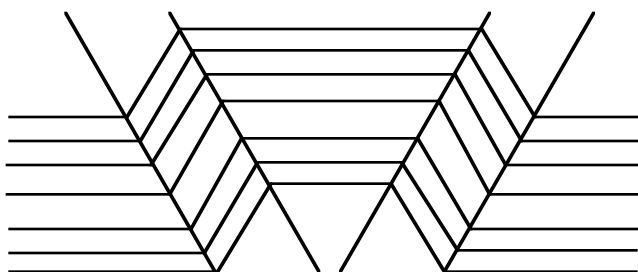
Parallel Folds -- In parallel folds, the layer thickness, measured perpendicular to bedding remains constant. Therefore, parallel folds are equivalent to class 1B folds described above. Some special types of parallel folds:

Concentric folds are those in which all folded layers have the same center of curvature and the radius of curvature decreases towards the cores of the folds. Therefore, concentric folds get tighter towards the cores and more open towards the anticlinal crests and synclinal troughs. The Busk method

of cross-section construction is based on the concept of concentric folds. These types of folds eventually get so tight in the cores that the layers are “lifted-off” an underlying layer. The French word for this is “*décollement*” which means literally, “unsticking”.

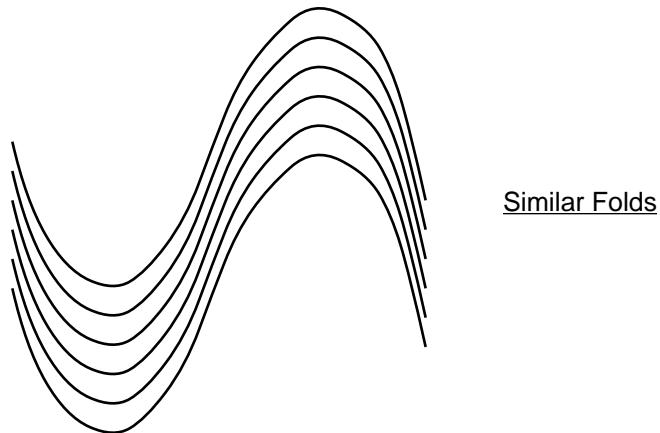


Kink Folds have angular axes and straight limbs. The layers do not have a single center of curvature. As we will see later in the course, these are among the easiest to analyze quantitatively



The axis of the kink has to bisect the angles between the two dip panels or the layer thickness will not be preserved

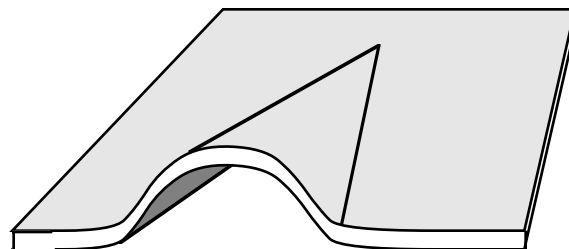
Similar Folds -- The other major class of cylindrical folds is similar folds. These are folds in which the layer thickness parallel to the axial surface remains constant but thickness perpendicular to the layers does not. They are called similar because each layer is “similar” (ideally, identical) in curvature to the next. Thus, they comprise class 2 folds. In similar folds, there is never a need for a *décollement* because you can keep repeating the same shapes forever without pinching out the cores:



24.3.2 Non-Cylindrical Folds

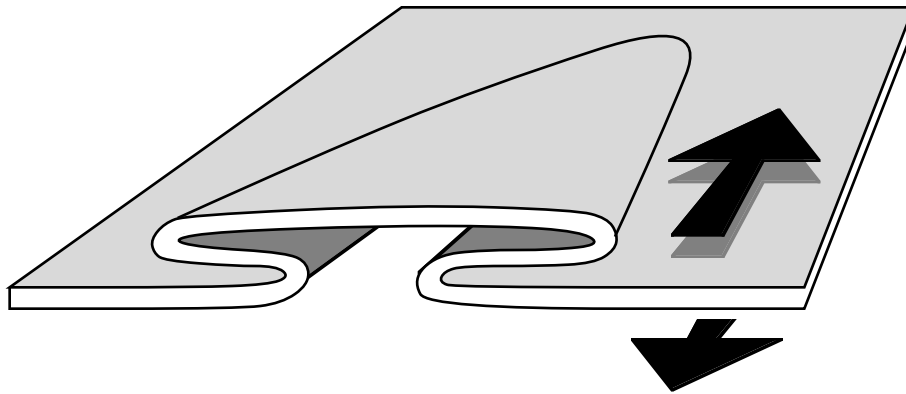
These folded surfaces cannot be traced by a line moving parallel to itself. In practice what this means is that the fold shape changes geometry as you move parallel to the hinge line. Thus, they are complex, three dimensional features. Some special types:

Conical folds -- the folded surfaces in these folds are in the shape of a cone. In other words, the folded layers converge to a point, beyond which the fold does not exist at all.



There is a very distinct difference between plunging cylindrical fold and conical folds. The conical fold simply does not exist beyond the tip of the cone. Thus, the shortening due to fold of the layers changes along strike of the hinge. Conical folds are commonly found at the tip lines of faults.

Sheath folds -- These are a special type of fold that forms in environments of high shear strain, such as in shear, or mylonite, zones. They are called “sheath” because they are shaped like the sheath of a knife.



Sheath folds are particularly useful for determining the sense of shear in mylonite zones. The upper plate moved in the direction of closure of the sheath. They probably start out as relatively cylindrical folds and then get distorted in the shear zone.

24.4 Summary Outline

- Cylindrical
 - Parallel
 - Concentric
 - Kink
 - Similar

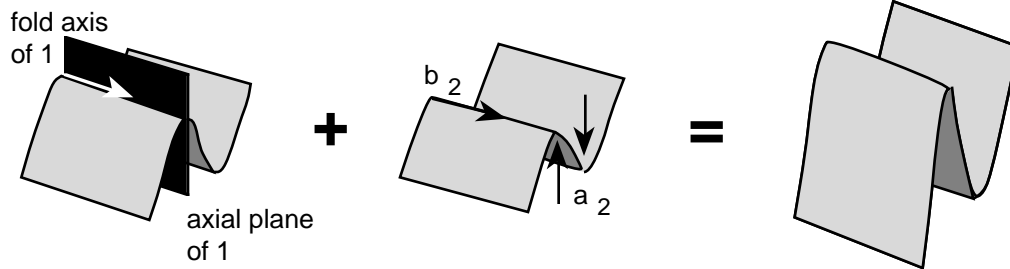
- Non-cylindrical
 - Conical
 - Sheath

24.5 Superposed Folds

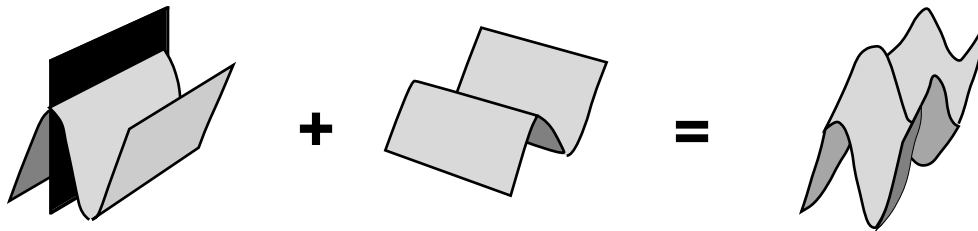
Multiple deformations may each produce their own fold sets, which we label F_1 , F_2 , etc., in the order of formation. This superposition of folds can produce some very complex geometries, which can be very difficult to distinguish on two dimensional exposures. Ramsay (1967; Ramsay & Huber, 1985) have come up with a classification scheme based on the orientations of the fold axis (labeled F_1 , below) and axial surface (the black plane, below) of the first set of folds with respect to the fold axis (labeled b_2 ,

below) and the sense of displacement of the layer during the second folding (labeled a_2 , below). With this approach, there are four types of superposed fold geometries:

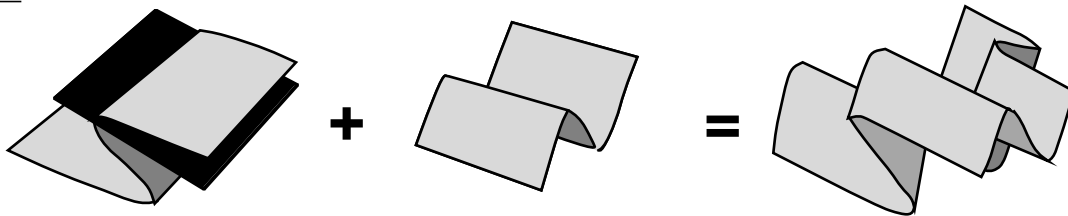
Type 0:



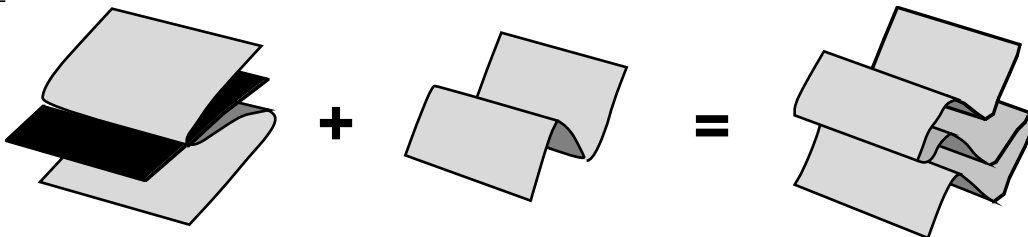
Type 1:



Type 2:



Type 3:



Type 0 results in folds which are indistinguishable from single phase folds. Type 1 produces the classic "dome and basin" or "egg-carton" pattern. Type 2 folds in cross-section look like boomerangs. Type 3 folds are among the easiest to recognize in cross-section.

LECTURE 25—FOLDS III: KINEMATICS

25.1 Overview

Kinematic models of fold development can be divided into five types:

1. Gaussian Curvature,
2. Buckling,
3. Layer parallel shear,
4. Shear oblique to layers, and
5. Pure shear passive flow.

The first two treat only single layers while the third and fourth address multilayers. The final one treats layers as passive markers, only. All are appropriate only to cylindrical folds. Thus, you should not think of these as mutually exclusive models. For example, you can have buckling of a single layer with shear between layers.

25.2 Gaussian Curvature

The curvature of a line, C , is just the inverse of the radius of curvature:

$$C = \frac{1}{r_{\text{curvature}}} .$$

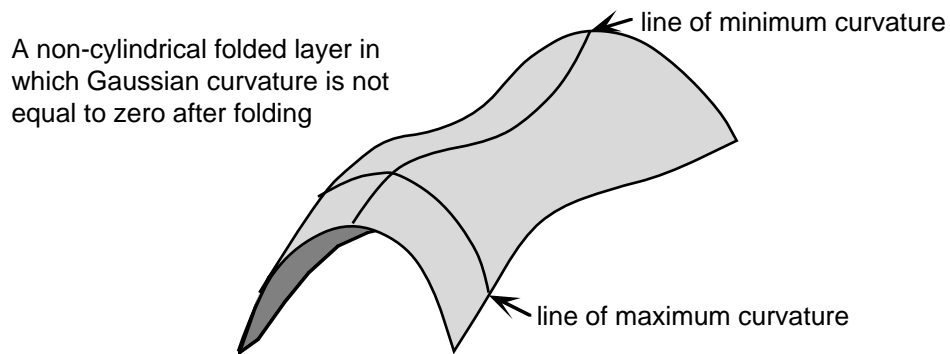
In any surface, you can identify a line (really a family of parallel lines) with maximum curvature and a line of minimum curvature. These two are called the “principal curvatures.” The product of the maximum and minimum curvatures is known as the Gaussian curvature, a single number which describes the overall curvature of a surface:

$$C_{\text{Gauss}} = C_{\text{max}} C_{\text{min}} .$$

There is a universal aspect to this: *the Gaussian curvature of a surface before and after a deformation remains constant unless the surface is stretched or compressed* (and thereby distorted internally). Although few people realize it, we deal with this fact virtually daily: corrugated cardboard boxes get their strength from the fact that the middle layer started out flat before it folded and sandwiched between the two flat outer

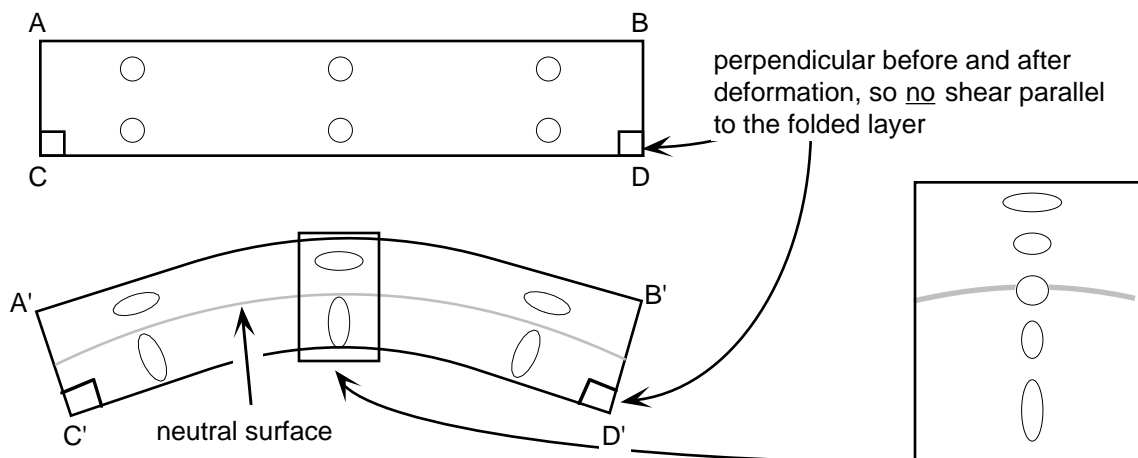
layers. Because its Gaussian curvature started out at zero, it must be zero after folding, meaning that bending it perpendicular to the folds is not possible without internally deforming the surface. Corrugated tin roofs are the same. In general, by folding a flat layer in one direction, you give the layer great resistance to bending in any other direction.

Because bedding starts out flat or nearly so, its minimum curvature after folding must be zero if the layer is not to have significant internal deformation. In other words, *the fold axis must be a straight line*. The folds which meet this criteria are cylindrical folds; non-cylindrical folds do not because their hinge lines (the line of minimum curvature) are not straight. [Now you see why we distinguish between axes and hinges!]



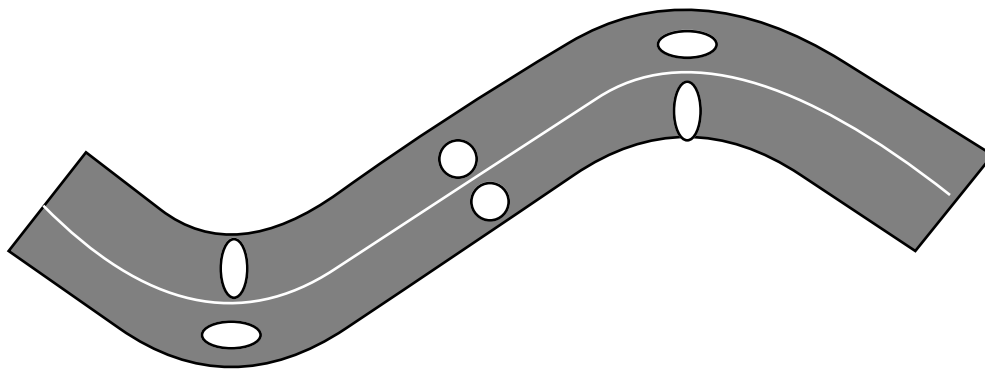
25.3 Buckling

Buckling applies to a single folded layer of finite thickness, or to multiple layers with high cohesive strength between layers:

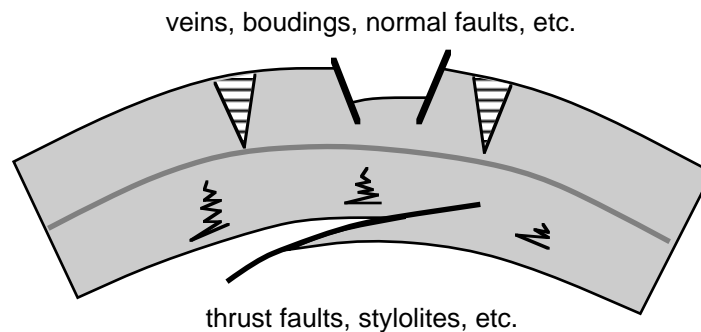


Note how in the above picture the outer arc gets longer (i.e. $A'B' > AB$) and the inner arc gets shorter ($C'D' < CD$). In the middle, there must be a line that is the same length before and after the folding. In three dimensions, this is called the neutral surface.

Bedding thickness remains constant; thus, the type of fold produced is a parallel or class 1b fold. Because a line perpendicular to the layer remains perpendicular, there can be no shear strain parallel to the layer. In an anticline-syncline pair, the maximum strains would be in the cores of the folds, with zero strain at the inflection point on the limbs:



You can commonly find geological evidence of buckling of individual beds during folding:

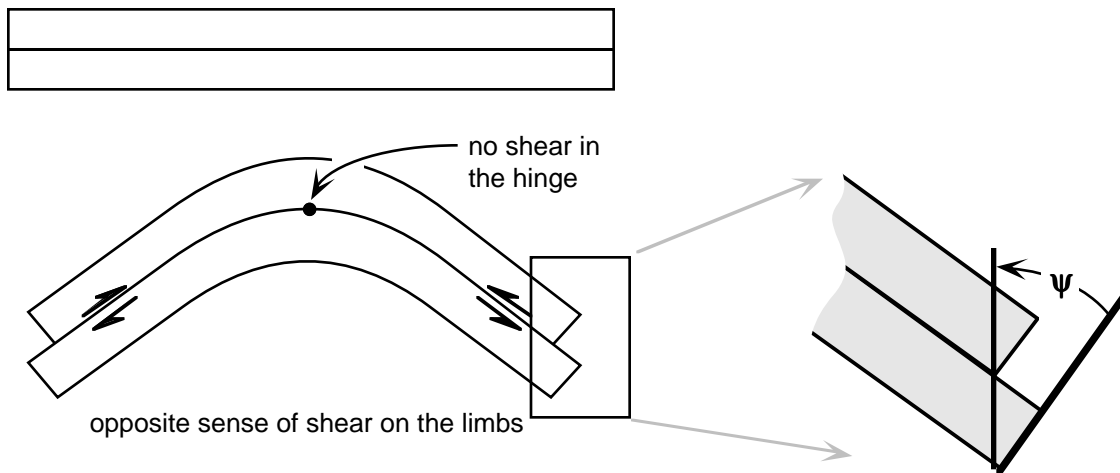


25.4 Shear Parallel to Layers

There are two end member components to this kinematic model. The only difference between them is the layer thickness:

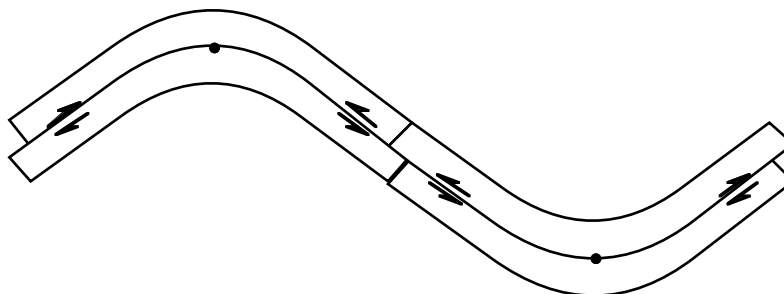
- Flexural Slip -- multiple strong stiff layers of finite thickness with low cohesive strength between the layers
- Flexural Flow -- The layer thickness is taken to be infinitesimally thin.

Because they're basically the same, we'll mostly concentrate on flexural slip.

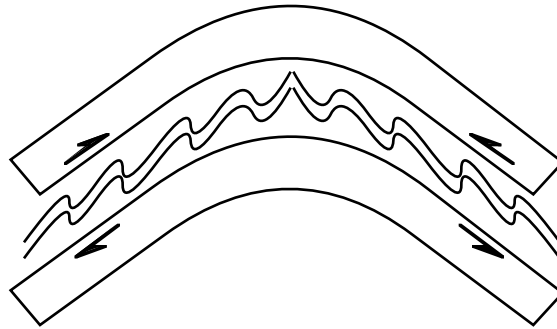


Because shear is parallel to the layers, it means that one of the two lines of no finite and no infinitesimal elongation will be parallel to the layers. Thus, the layers do not change length during the deformation. The slip between the layers is perpendicular to the fold axis. You can think of this type of deformation as “telephone book” deformation. When you bend a phone book parallel to its binding, the pages slide past one another but the individual pages don’t change dimensions; they are just as wide (measured in the deformed plane) as they started out.

Note that the sense of shear changes only across the hinge zones but is consistent between anticlinal and synclinal limbs:



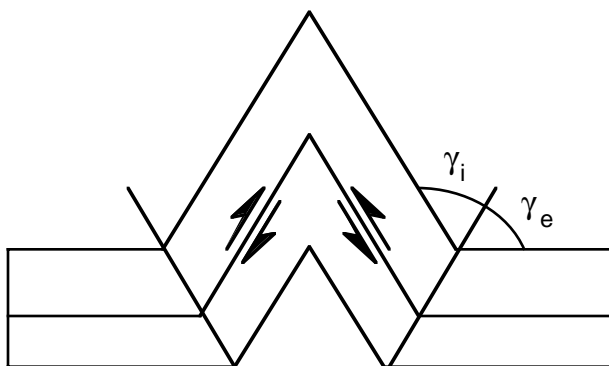
When you have an incompetent layer, such as a shale, between two more competent layers which are deforming by this mechanism, the shear between the layers can produce drag folds, or parasitic folds, on the limbs of the larger structure:



Because the layers of flexural slip (as opposed to flexural flow) folds have finite thickness, you can see that they must deform *internally* by some other mechanism, such as buckling. Thus, buckling and flexural slip are not by any means mutually exclusive.

25.4.1 Kink folds

Kink folds are a special type of flexural slip fold in which the fold hinges have *infinite curvature* (because the radius of curvature is equal to zero).



if layer thickness is constant, then

$$\gamma_i = \gamma_e$$

no shear in horizontal layers, only in dipping layers

If the internal kink angle $\gamma_i < \gamma_e$ then you will have thinning of the beds in the kink band; if $\gamma_i > \gamma_e$ then the beds in the kink band will thicken.

25.4.2 Simple Shear during flexural slip

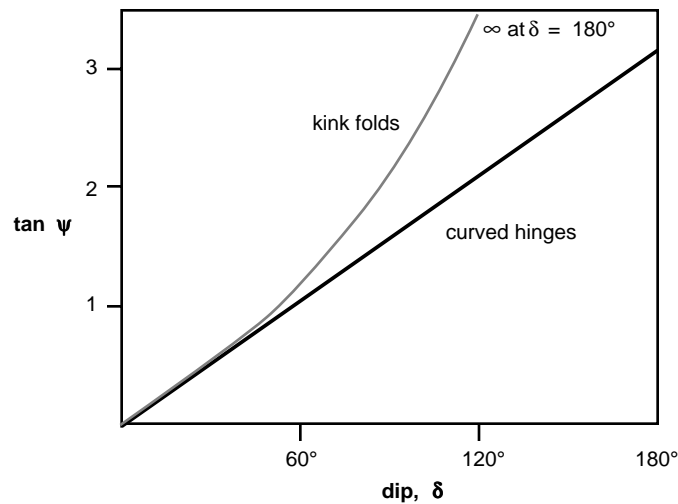
For kink bands: $\tan \psi = 2 \tan\left(\frac{\delta}{2}\right)$ [δ = dip of bedding]

average slip = $\bar{s} = 2\bar{h} \tan\left(\frac{\delta}{2}\right)$

For curved hinges: $\tan \psi = \frac{\pi}{180^\circ} \delta = 0.0175 \delta$

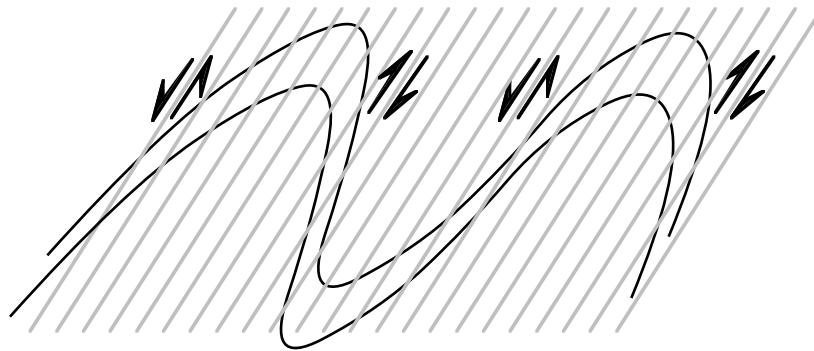
average slip = $\bar{s} = \frac{\pi}{180^\circ} \bar{h} \delta$

The following graph show the relationship between bedding dip and shear on the limbs for kink and curved hinge folds:

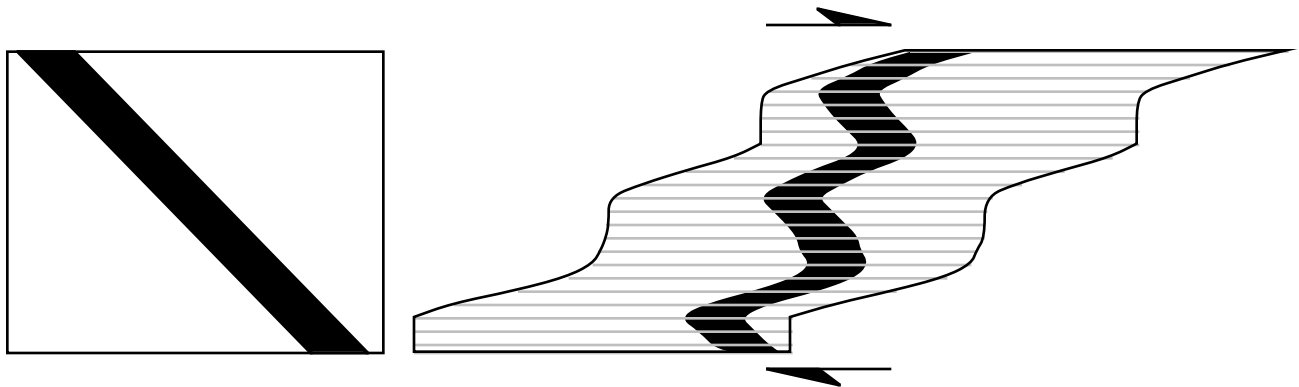


25.5 Shear Oblique To Layers

This type of mechanism will produce similar folds. In this case, the shear surfaces, which are commonly parallel to the axial surfaces of the folds, are parallel to the lines of no finite and infinitesimal elongation.

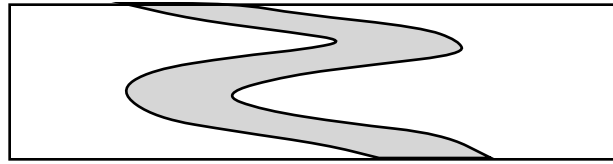
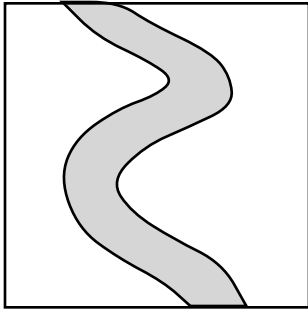


To make folds by simple shear without reversing the shear sense, you have to have heterogeneous simple shear zone with the layer dipping in the same direction as the sense of shear in the zone.

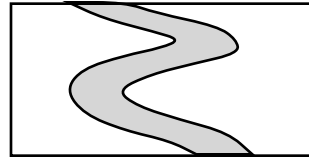


25.6 Pure Shear Passive Flow

In this type of mechanism, the layers, which have already begun to fold by some other mechanism behave as passive markers during a pure shear shortening and elongation. The folds produced can be geometrically identical to the previous kinematic model:



volume constant, pure shear



volume reduction, no extension pure shear
(e.g. pressure solution)

LECTURE 26—FOLDS IV: DYNAMICS

26.1 Basic Aspects

There are two basic factors to be dealt with when one attempts to make a theoretical analysis of folding:

1. Folded layers do not maintain original thickness during folding, and
2. Folded rocks consist of multiple layers or “multilayers” in which different layers have different mechanical properties.

These two basic facts about folding have the following impact:

1. There is layer-parallel shortening before folding and homogeneous shortening during folding. The latter will tend to thin the limbs of a fold and thicken the hinges.
2. In multilayers, the first layers that begin to fold will control the wavelength of the subsequent deformation. Incompetent layers will conform to the shape, or the distribution and wavelength, of the more competent layers.

26.2 Common Rock Types Ranked According to “Competence”

The following list shows rock types from most competent (or stiffest) at the top to least at the bottom:

Sedimentary Rocks

dolomite
arkose
quartz sandstone
greywacke
limestone
siltstone
marl
shale
anhydrite, halite

Metamorphic Rocks

meta-basalt
granite
qtz-fspar-mica gneiss
quartzite
marble
mica schist

26.3 Theoretical Analyses of Folding

In general, theoretical analyses of folding involve three assumptions:

1. Folds are small, so gravity is not important
2. Compression is parallel to the layer to start
3. Plane strain deformation

26.3.1 Nucleation of Folds

If layers of rock were perfect materials and they were compressed exactly parallel to their layering, then folds would never form. The layers would just shorten and thicken uniformly. Fortunately (at least for those of us who like folds) layers of rock are seldom perfect, but have irregularities in them. Folds nucleate, or begin to form, at these irregularities.

Bailey Willis, a famous structural geologist earlier in this century performed a simple experiment while studying Appalachian folds. He showed that changes in initial dip of just 1 - 2° were sufficient to nucleate folds.

As folds begin to form at irregularities, a single wave length will become dominant. Simple theory shows that the dominant wavelength is a linear function of layer thickness:

$$\text{for elastic deformation: } L_d = 2\pi t \sqrt[3]{\frac{E}{6E_o}}$$

$$\text{for viscous deformation: } L_d = 2\pi t \sqrt[3]{\frac{\eta}{6\eta_o}}$$

where

L_d = dominant wavelength

t = thickness of the stiff layer

E = Young's modulus of the stiff layer

E_o = Young's modulus of the confining medium

η = viscosity modulus of the stiff layer

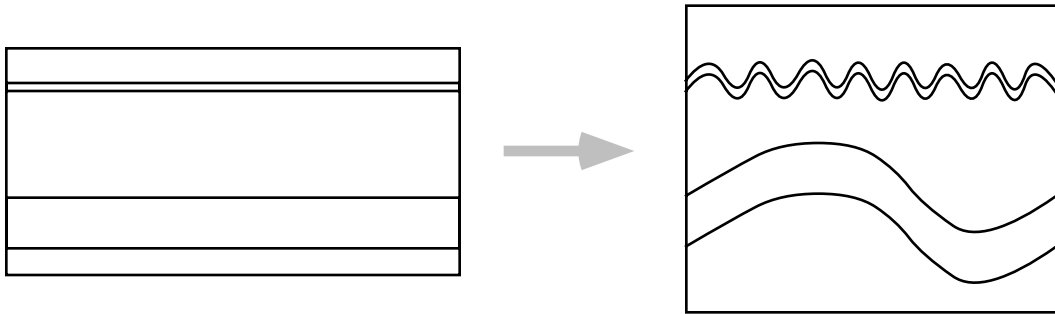
η_o = viscosity modulus of the confining medium

Viscous deformation will also depend on the layer parallel shortening:

$$L_d = 2\pi t \sqrt[3]{\frac{\eta(S-1)}{6\eta_o(2S^2)}}$$

$$S = \sqrt{\frac{\lambda_1}{\lambda_3}}$$

where λ is the quadratic elongation. Thus, the thicker the layer, the longer the wavelength of the fold:



For a single layer,

$$4 \leq \frac{L_d}{t} \leq 6 ,$$

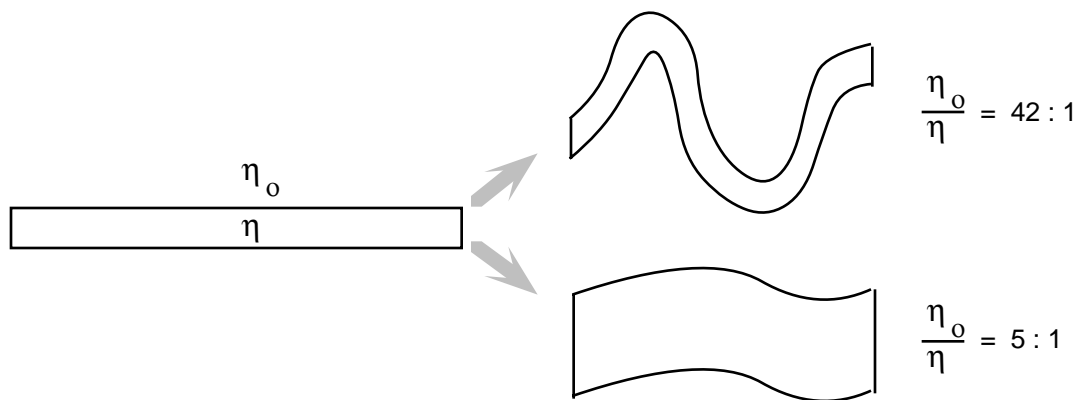
and for multilayers:

$$\frac{L_d}{t} \approx 27 .$$

26.3.2 Growth of Folds

At what stage does this theory begin to break down? Generally around limb dips of $\sim 15^\circ$ [small angle assumptions were used to derive the above equations]. For more advanced stages of folding, it is common to use a numerical rather than analytical approach.

A general result of numerical folding theory: As the viscosity contrast between the layers decreases, layer parallel shortening increases and folding becomes less important:



26.3.3 Results for Kink Folds

Experimental work on kink folds indicates that kinks form in multilayers with high viscosity contrast and bonded contacts (i.e. high frictional resistance to sliding along the contacts). Compression parallel to the layers produces conjugate kink bands at 55 - 60° to the compression. Loading oblique to the layering (up to 30°) produces asymmetric kinks.

LECTURE 27—LINEAR MINOR STRUCTURES

27.1 Introduction to Minor Structures

Minor structures are those that we can see and study at the outcrop or hand sample scale. We use these features because they contain the most kinematic information. In other words, the strain and strain history of the rock is most commonly recorded in the minor structures.

There are several types of minor structures, but they fall into two general classes: linear and planar, which we refer to as lineations and foliations, respectively.

Lineations

mineral fibers
minor fold axes
boudins
intersection lineations
rods & mullions

Foliations

veins
stylolites
joints
cleavage
S-C fabrics

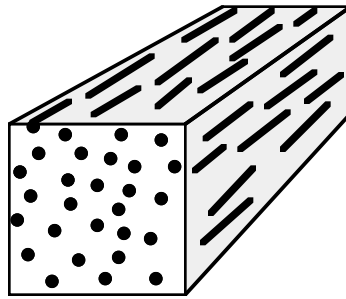
The lineations and foliations in a rock comprise what is known as the **rock fabric**. This term is analogous to cloth fabric. Rocks have a texture, an ordering of elements repeated over and over again, just like cloth is composed of an orderly arrangement of threads.

27.2 Lineations

Any linear structure that occurs repeatedly in a rock is called a lineation; it is a *penetrative* linear fabric. Lineations are very common in igneous and sedimentary rocks, where alignment of mineral grains and other linear features results from flow during emplacement of the rock. However, we're most interested in those lineations which arise from, and reflect, deformation. Of primary importance is to remember that *there is no one explanation for the origin of lineations*.

27.2.1 Mineral Lineations

These are defined by elongations of inequant mineral grains or aggregates of grains.



common minerals:

hornblende
sillimanite
feldspar
quartz
biotite

Mineral lineations can form in

Folds

parallel to the hinge

perpendicular to the hinge

anywhere in between

Fault zones -- parallel to the slip direction

Regional metamorphism

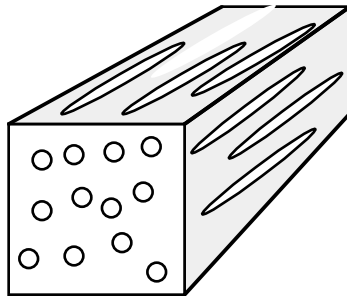
The preferred orientation of elongate mineral grains can form by three different mechanisms:

1. Deformation of grains -- straining the grains into ellipsoidal shapes
2. Preferential growth -- no strain of the mineral crystal but may, nonetheless, reflect the regional deformation
3. Rigid body rotation -- the mineral grains themselves are not strained but they rotate as the matrix which encloses them is strained.

It is, occasionally, difficult to tell these mechanisms apart.

27.2.2 Deformed Detrital Grains (and related features)

This category differs from the previous only in that pre-existing sedimentary features, or features formed in sedimentary rocks are deformed. The basic problem with their interpretation is that such features commonly have very different mechanical properties than the matrix of the rock. thus the strain of the deformed object which you measure may not reflect the strain of the rock as a whole.



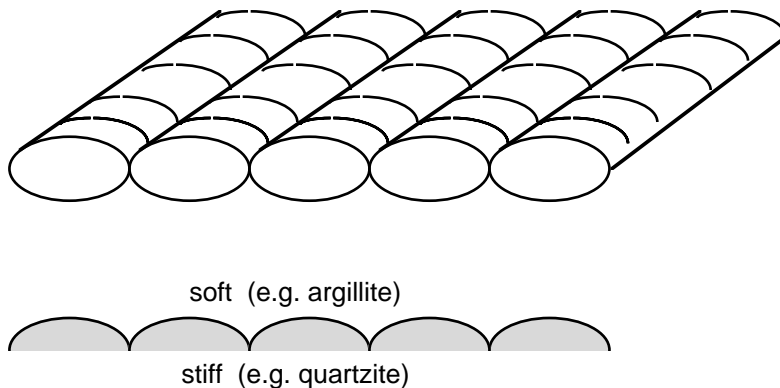
common features:

- ooids
- pebbles
- reduction spots

27.2.3 Rods and Mullions

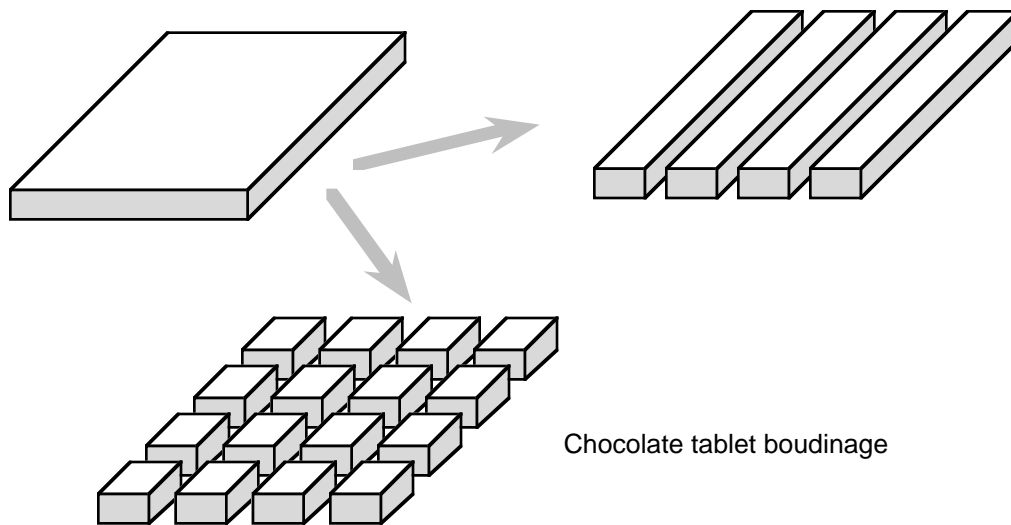
Rods are any elongate, essentially monomineralic aggregate not formed by the disruption of the original rock layering. They are generally cylindrical shaped and striated parallel to their length. They are almost always oriented parallel to fold hinge lines and occur in the hinge zones of minor folds. Rods are thought to form by metamorphic or fluid flow processes during tectonic deformation.

Mullions are elongate bodies of rock, partly bounded by bedding planes and partly by newer structures. They generally have a cylindrical, ribbed appearance and are oriented parallel to the fold hinges. They form at the interface between soft and stiff layers.



27.3 Boudins

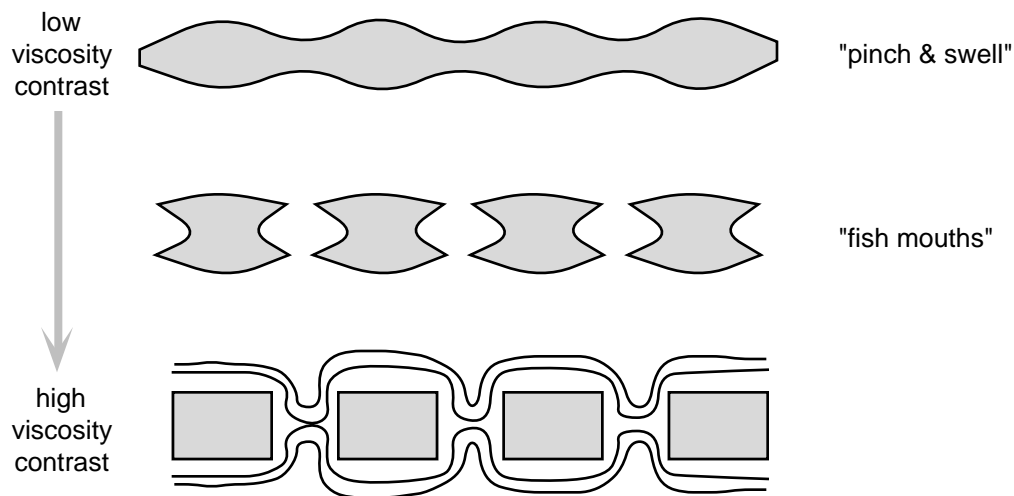
Boudin is the French word for sausage. They are formed by the segmentation of pre-existing layers and appear similar to links of sausages. The segmented layers certainly can be, but need not be, sedimentary layering. The segmentation can occur in two or three dimensions.



Chocolate tablet boudinage

For simple boudinage (upper right), the long axis of the boudin is perpendicular to the extension direction. Chocolate tablet boudinage forms when you have extensions in two directions.

The shapes of boudins in cross section are a function of the viscosity contrast between the layers:



27.4 Lineations Due to Intersecting Foliations

A type of lineation can form when two foliations, usually bedding and cleavage, intersect. When this occurs in fine-grained, finely bedded rocks, the effect is to produce a multitude of splinters. The resulting structure is called **pencil structure**. There are good examples at Portland Pt. quarry. Pencils are usually oriented parallel to fold hinges.

LECTURE 28—PLANAR MINOR STRUCTURES I

28.1 Introduction to Foliations

The word foliation comes from the Latin word folium which means “leaf” (folia = leaves). In structural geology, we use foliation to describe any planar structure in the rocks. Under the general term foliation there are several more specific terms:

- bedding
- cleavage
- schistosity
- gneissic layering

These collective foliations were sometimes referred to in older literature as “*S-surfaces*”. Geologists would determine the apparent relative age relations between foliations and then assign them numbers from oldest to youngest (with bedding, presumably being the oldest, labeled S_0). In the last decade, this approach has fallen out of favor because, among other things, we know that foliations can form simultaneously (as well will see with “S-C fabrics” in a subsequent lecture). Furthermore, structural geologists used to correlate deformational events based on their relative age (e.g. correlating S_3 in one are with S_3 in another are 10s or 100s of kilometers away). With the advent of more accurate geochronologic techniques, we now know that such correlation is virtually worthless in many cases.

28.2 Cleavage

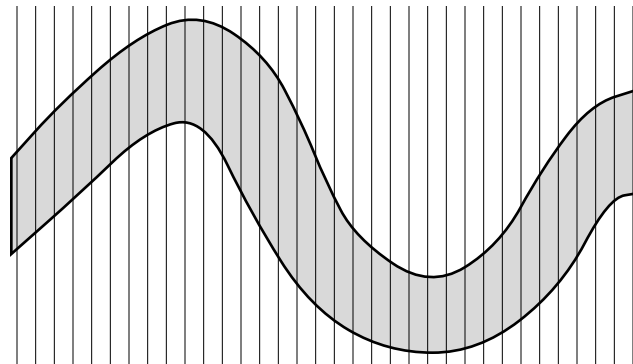
Many rocks have the tendency to split along certain regular planes that are not necessarily parallel to bedding. Such planes are called **cleavage**. Roofing slates are an excellent example. Cleavage is a type of foliation that can be penetrative or non-penetrative. An important point to remember is that:

rock cleavage \neq mineral cleavage

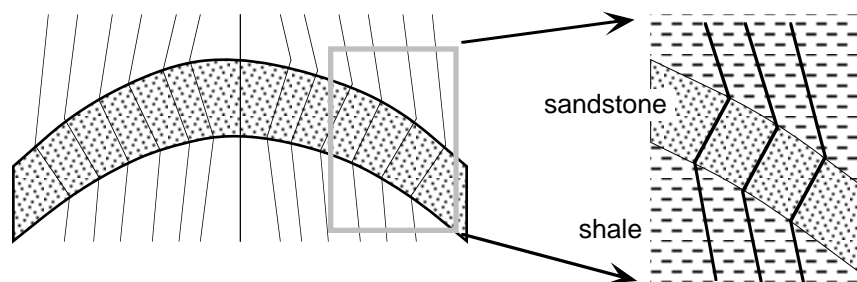
The two are generally unrelated.

28.2.1 Cleavage and Folds

Cleavage is commonly seen to be related in a systematic way to folds. When this occurs, the cleavage planes are nearly always parallel or sub-parallel to the axial surfaces of the folds. This is known as **axial planar cleavage**.

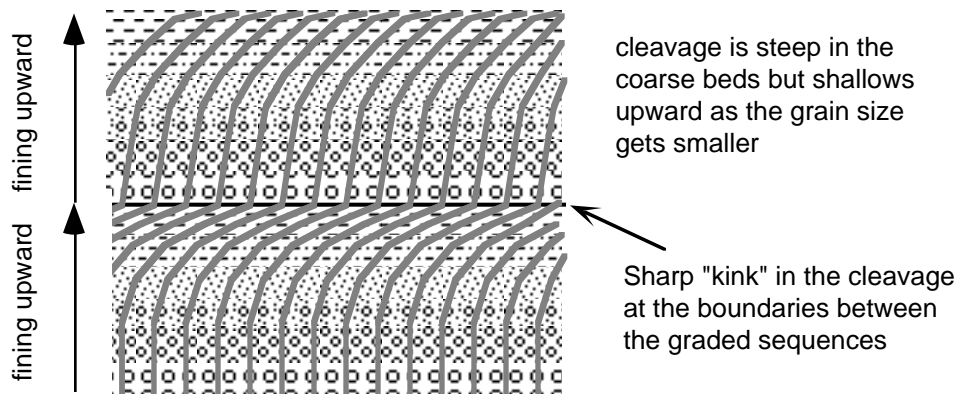


If examined in detail, the cleavage usually is not exactly parallel to the axial surface every where but changes its orientation as it crosses beds with different mechanical properties. This produces a fanning of the cleavage across the fold. In a layered sandstone and shale sequence, the cleavage is more nearly perpendicular to bedding in the sandstone and bends to be at a more acute angle in the shale. This is known as **cleavage refraction**.

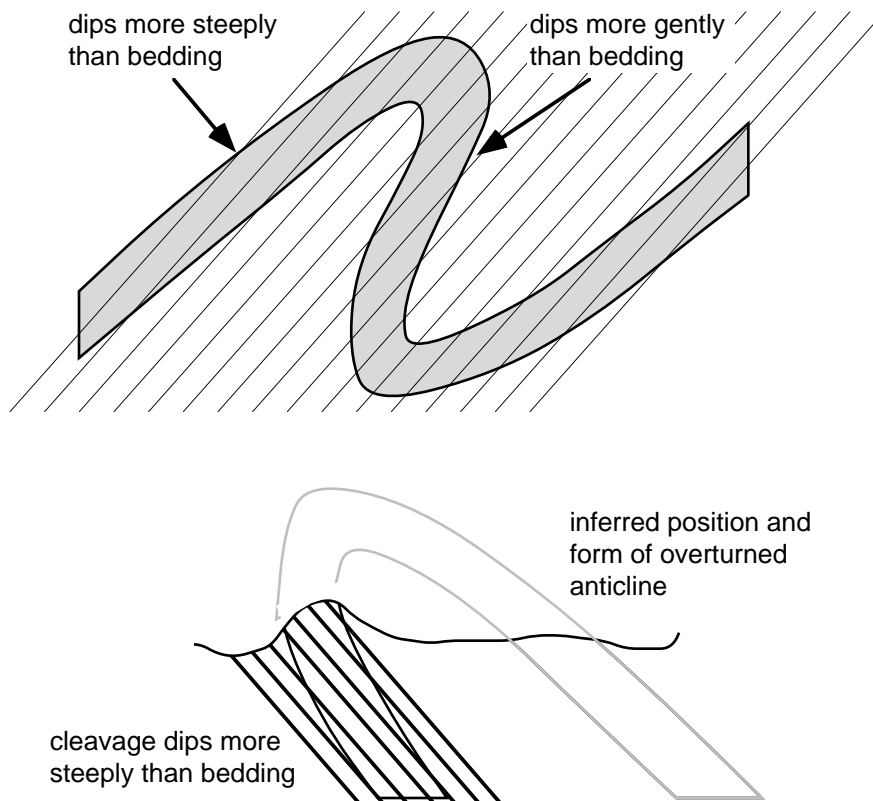


Cleavage Fanning & Refraction

As we will see next time, cleavage refraction is related to the relative magnitudes of strain in the different layers and the orientation of the lines of maximum shear strain. As a side light, cleavage refraction can be used to tell tops in graded beds. This property can be very useful in metamorphic terranes where the grading includes only medium sand and finer.



Cleavage can also be very useful when doing field work in a poorly exposed region with overturned folds. If the cleavage is axial planar, then the cleavage will dip more steeply than bedding on the upright limbs of the folds but will dip more gently than bedding on the overturned limbs:



28.3 Cleavage Terminology

Cleavage can take on a considerable variety of appearances, but at its most basic level, there are two types of cleavage:

- **Continuous cleavage** occurs in rocks which have an equal tendency to cleave (or split) throughout, at the scale of observation. In other words, the cleavage is *penetrative*.
- **Spaced or Discontinuous cleavage** is *not* penetrative at the scale of observation.

28.3.1 Problems with Cleavage Terminology

Because of its economic importance (i.e. in quarries, etc.) some of the names for various types of cleavage are very old and specific to a particular rock type. Furthermore, cleavage terminology has been overrun with *genetic terms*, which are still used by some, long after the particular processes implied by the name have been shown to not be important. The following is an incomplete list of existing terms *which should not be used when describing cleavage because they are all genetic*:

- fracture cleavage
- stylolitic or pressure solution cleavage
 - Shear foliation
- strain-slip cleavage

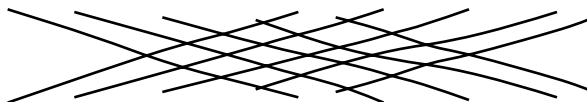
These terms have their place in the literature, but only after you have proven that a particular process is important.

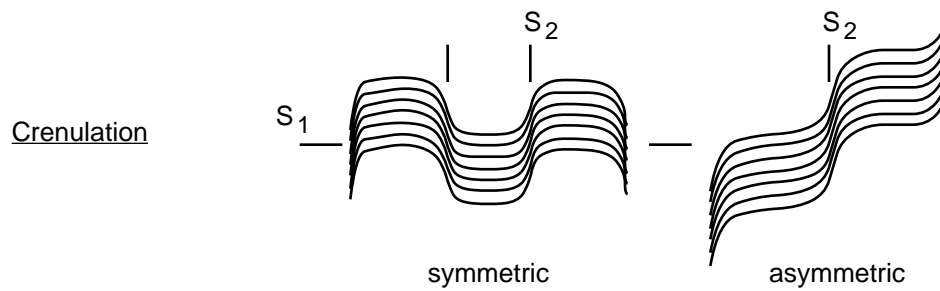
28.3.2 Descriptive Terms

Anastomosing



Conjugate

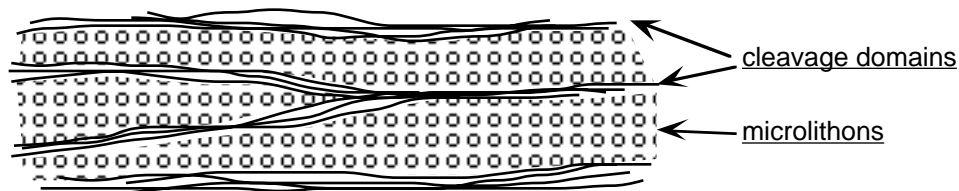




Crenulation is particularly interesting. In it, a pre-existing alignment of mineral grains is deformed into microfolds. This is accompanied by mineral differentiation such that the mineral composition in the zones of second foliation (or crenulation cleavage, labeled “ S_2 ” above) is different than that part of the rock between the cleavage planes. Crenulation cleavage has been called “strain slip cleavage” but that term has now thankfully fallen into disuse.

28.4 Domainal Nature of Cleavage

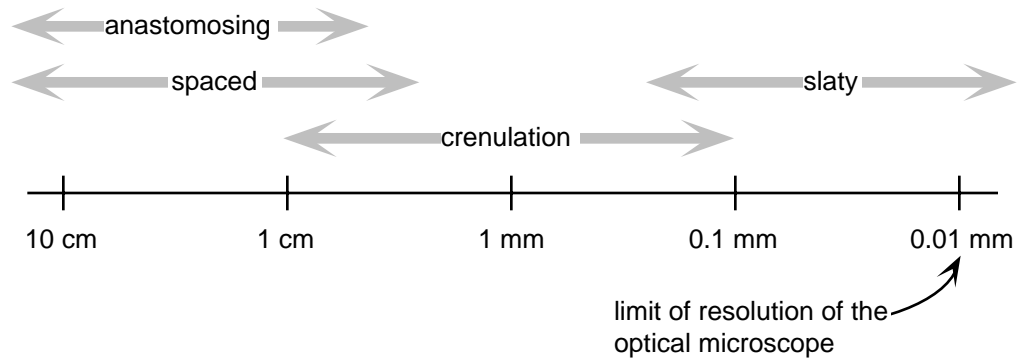
Most cleaved rocks have a domainal structure at one scale or another which reflects the mechanical and chemical processes responsible for their formation.



The rocks tend to split along the cleavage domains, which have also been called “folia”, “films”, or “seams”.

In fine-grained rocks, cleavage domains are sometimes called “M-domains” because mica and other phyllosilicates are concentrated there, whereas the lenticular microlithons are the “QF-domains” because of the concentration of quartz and feldspar. As in the discussion of crenulation cleavage, above, we see that mineralogical and chemical differentiation is a common aspect of cleavage.

28.4.1 Scale of Typical Cleavage Domains



LECTURE 29—PLANAR MINOR STRUCTURES II: CLEAVAGE & STRAIN

29.1 Processes of Foliation Development

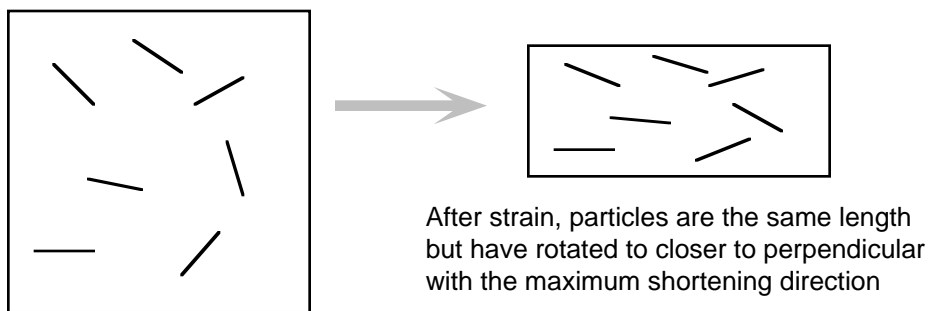
There are four basic processes involved in the development of a structural foliation:

1. Rotation of non-equant grains,
2. Change in grain shape through pressure solution,
3. Plastic deformation via dislocation mechanisms, and
4. Recrystallization.

The first two are the most important in the development of cleavage at low to moderate metamorphic grades and will be the focus of this lecture.

29.2 Rotation of Grains

This process is very important in compaction of sediments and during early cleavage development. The basic idea is:



There are two similar models which have been devised to describe this process. Both attempt to predict the degree of preferred orientation of the platy minerals (how similarly oriented they are) as a function of strain. The preferred orientation is usually displayed as poles to the platy particles; the more oriented they are, the higher the concentration of poles at a single space on the stereonet.

29.2.1 March model

rotation of purely passive markers that have no mechanical contrast with the confining medium. We solved this problem already for two-dimensional deformation when we talked about strain.

$$\tan \theta'_{xz} = \tan \theta_{xz} \frac{S_z}{S_x} = \frac{\tan \theta_{xz}}{R_{xz}}$$

In three dimensions it is a little more complex but still comprehensible:

$$\tan \delta' = \tan \delta \left(R_{xy}^2 \sin^2 \phi_{yz} + R_{xz}^2 \sin^2 \phi_{xy} \right)$$

where ϕ_{yz} is the azimuth with respect to the y axis, δ and δ' are the dips of the markers before and after the strain, and R is the ellipticity measured in a principal plane of the strain ellipse (i.e. a plane that contains two of the three principal axes, as indicated by the subscripts).

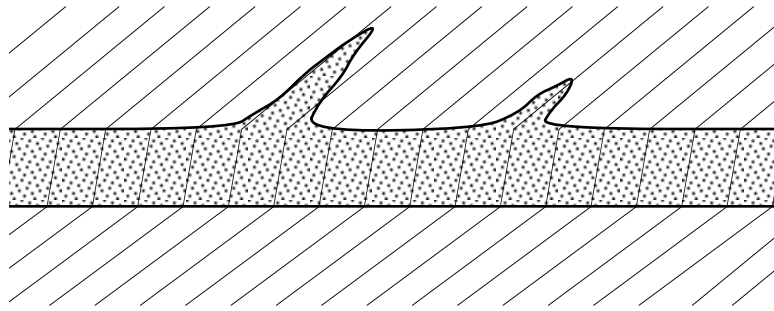
29.2.2 Jeffery Model

Rotation of rigid bodies in a viscous fluid (the former modeled as rigid ellipsoidal particles). For elongate particles, there is little difference between the Jeffery and March models. For example, detrital micas in nature have aspect ratios between 4 and 10. For this range of dimensions, the Jeffery model predicts 12 to 2 % lower concentrations than a March model.

Both of these models work only for loosely compacted material (i.e. with high porosity). At lower porosities, the grains interfere with each other, resulting in lots of kinking, bending and breaking of grains.

29.2.3 A Special Case of Mechanical Grain Rotation

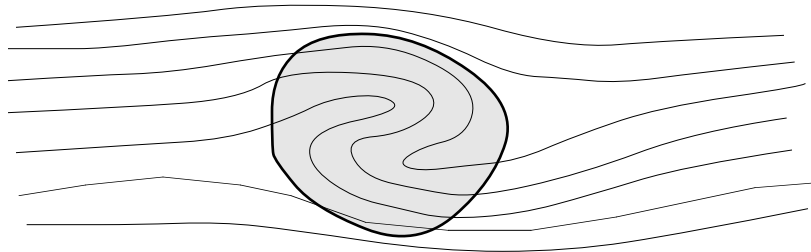
In 1962, John Maxwell of Princeton proposed that the cleavage in the Martinsburg Formation at the Delaware Water Gap was formed during dewatering of the sediments and thus this theory of cleavage formation has come to be known as the **dewatering hypothesis**. He noted that the cleavage was parallel to the sandstone dikes in the rocks:



Maxwell suggested that expulsion of water from the over-pressured sandstone during dewatering resulting in alignment of the grains by mechanical rotation. We now know that this is incorrect for the Martinsburg because

1. Cleavage in the rocks there is really due to pressure solution, and
2. Internal rotations during strain naturally results in sub-parallelism of cleavage and the dikes.

Mechanical rotation does occur during higher grade metamorphism as well. The classic example is the rolled garnet:



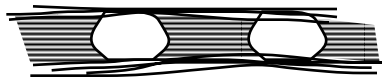
29.3 Pressure Solution and Cleavage

We've already talked some about the mechanical basis for pressure solution. The basic observation in the rocks which leads to an interpretation of pressure solution is grain truncation in the microlithons:



Most people associate pressure solution with carbonate rocks, but it is very common in siliceous rocks as well.

There are two general aspects that pressure solution and related features that you can observe in the rocks:



local overgrowths and vein formation means limited fluid circulation. Volume is more-or-less conserved

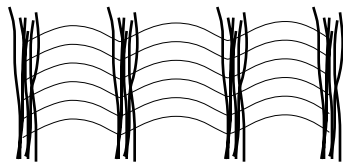


more commonly, you see no evidence for redeposition, which means bulk circulation and volume reduction were important

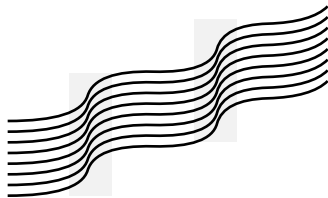
In the Martinsburg Formation that Maxwell studied, a volume reduction of greater than 50% has been documented by Wright and Platt.

29.4 Crenulation Cleavage

Crenulation cleavage is probably a product of both pressure solution and mechanical rotation. It has two end member morphologies:



Discrete -- truncation of grains against the cleavage domains. Very strong alignment of grains within cleavage domains



Zonal -- initial fabric is continuous across the cleavage domains. Clearly a case of microfolding

Both types of the same characteristics:

1. No cataclastic textures in cleavage domains (i.e. they are not faults),
2. There is mineralogical and chemical differentiation. Quartz is lacking from the cleavage

domains and there is enrichment of Al_2O_3 and K_2O in the cleavage domains relative to the microlithons,

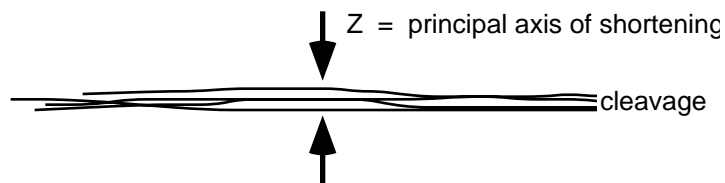
3. Thinning and truncation are common features, and
4. No intracrystalline plastic deformation.

Probably what occurs is rotation of phyllosilicates by microfolding accompanied by pressure solution of quartz and/or carbonate.

29.5 Cleavage and Strain

There are two opposing views of how cleavage relates to strain:

1. J. Ramsay, D. Wood, S. Treagus -- *Cleavage is always parallel to the XY plane of the finite strain ellipsoid* (i.e. it is perpendicular to the Z-axis). Thus, there can be no shear parallel to the planes.



The basis for this assertion is mostly observational. These workers have noted in many hundreds of instances that the cleavage is essentially perpendicular to the strain axes as determined by other features in the rock.

2. P. Williams, T. Wright, etc. -- *cleavage is commonly close to the XY-plane but can deviate significantly* and, at least at some point during its history, may be parallel to a plane of shear.

There are two issues here which are responsible for this debate:

First, at high strains the planes of maximum shear are very close to the planes of maximum elongation (the X-axis). Thus it is very difficult in the field to measure angles precisely enough that you can resolve the difference between a plane of maximum shear and a principal plane.

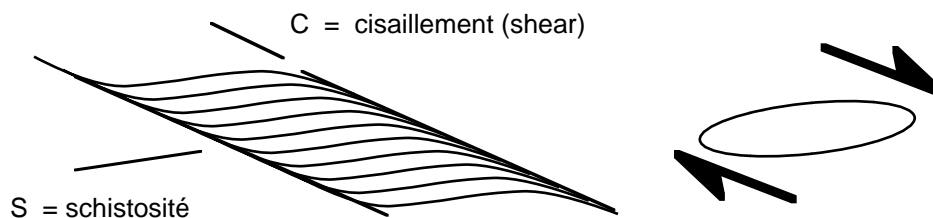
Second, cleavage becomes a material line. If the deformation is by pure shear then it could be that cleavage remains perpendicular to the Z-axis. However, in a progressive simple shear, it cannot remain perpendicular to the Z-axis all the time (because it is a material plane) and thus must experience shear along it at some point.

LECTURE 30—SHEAR ZONES & TRANSPOSITION

30.1 Shear Zone Foliations and Sense of Shear

Within ductile shear zones, a whole array of special structures develop. Because of the progressive simple shear, the structures that develop are inherently asymmetric. It is this asymmetry that allows us to determine the sense of shear in many shear zones.

30.1.1 S-C Fabrics



S-C fabrics are an example of two planar foliations which formed at the same time (although there are many examples of the S-foliation forming slightly or considerably earlier than the C-foliation). The S planes are interpreted to lie in the XY plane of the finite strain ellipsoid and contain the maximum extension direction (as seen in the above figure). The C-planes are planes of shear. As the S-planes approach the C-planes they curve into and become sub-parallel (but technically never completely parallel) to the C-planes.

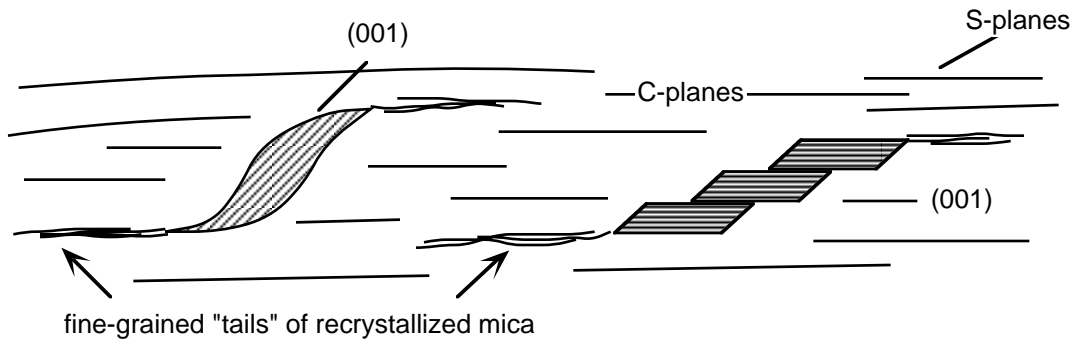
Two types of S-C fabrics have been identified:

- **Type I** -- found in granitoid rocks rich in quartz, feldspar, and biotite. Both the S- and C-planes are well developed.
- **Type II** -- form in quartzites. The foliation is predominantly comprised of C-planes, with S-planes recorded by sparse mica grains (see below)

30.1.2 Mica "Fish" in Type II S-C Fabrics

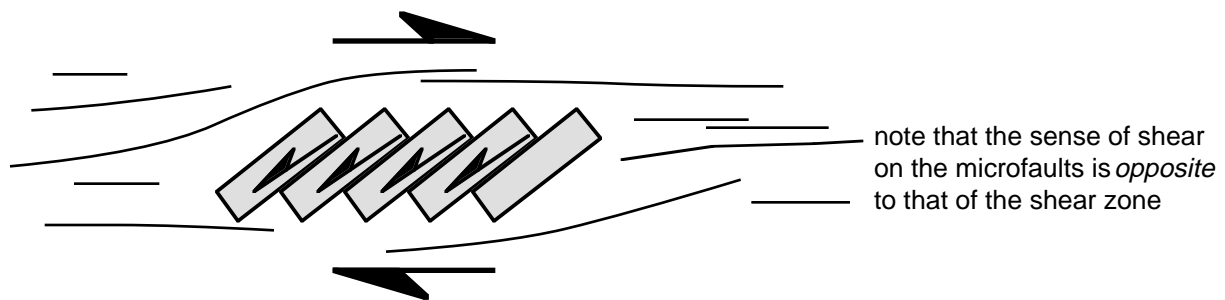
The S-planes are recorded by mica grains in rock. In general, the cleavage planes of all the mica

grains are similarly oriented so that when you shine light on them (or in sunlight) they all reflect at the same time. This effect is referred to somewhat humorously as “fish flash”.



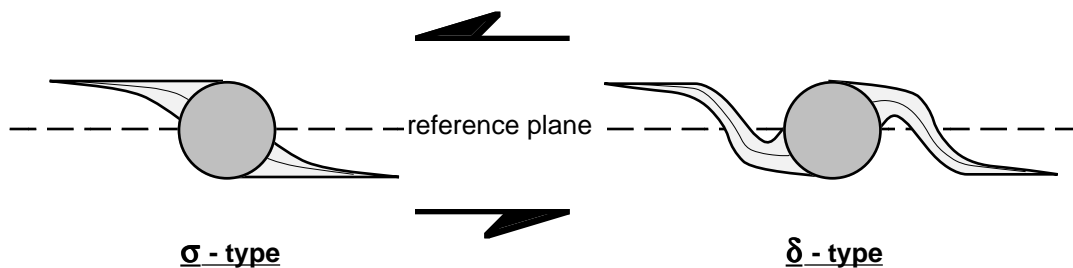
30.1.3 Fractured and Rotated Mineral Grains

Minerals such as feldspar commonly deform by fracture rather than by crystal plastic mechanisms. One common mode of this deformation is the formation of domino blocks. The fractured pieces of the mineral shear just like a collapsing stack of dominos:



30.1.4 Asymmetric Porphyroclasts

There are two basic types of asymmetric porphyroclasts:

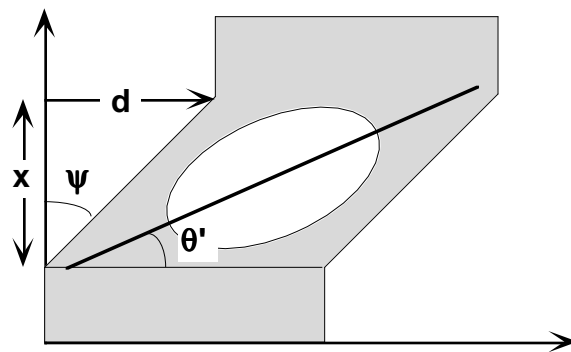


In the σ -type, the median line of the recrystallizing tails does not cross the reference plane, whereas in the δ -type, the median line of the recrystallizing tails does cross the reference plane. The ideal conditions for the development of asymmetric porphyroclasts are:

1. Matrix grain size is small compared to the porphyroclasts,
2. Matrix fabric is homogeneous,
3. Only one phase of deformation,
4. Tails are long enough so that the reference plane can be constructed, and
5. Observations are made on sections perpendicular to the foliation and parallel to the lineation.

30.2 Use of Foliation to Determine Displacement in a Shear Zone

Consider a homogeneous simple shear zone:



$$\gamma = \tan \psi$$

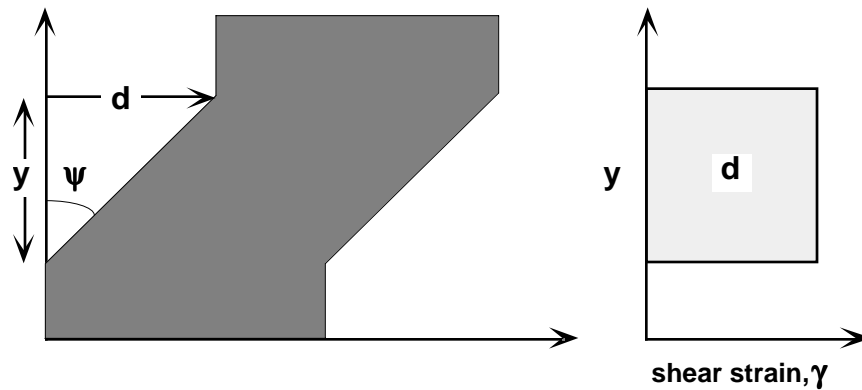
$$d = \gamma x$$

In the field, we can't measure ψ directly, but we can measure θ' , which is just the angle between the foliation (assumed to be kinematically similar to S-planes) and the shear zone boundary. If the foliation is parallel to the XY plane of the strain ellipsoid then there is a simple relationship between θ' and γ :

$$\tan 2\theta' = \frac{2}{\gamma}$$

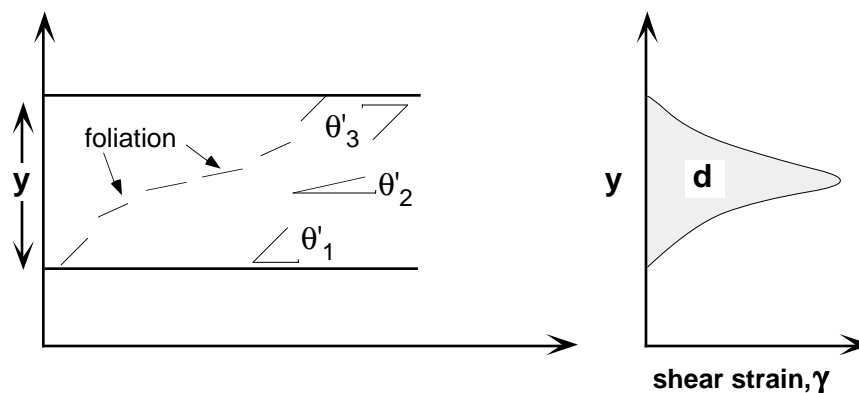
Although it is trivial in the case of a homogeneous shear zone, we could compute the displacement graphically by plotting γ as a function of the distance across the shear zone x and calculating the area

under the curve (i.e. the integral shown):



$$d = \int_0^y \gamma dy$$

For a heterogeneous shear zone -- the usual case in geology -- the situation is more complex, but you can still come up with a graphical solution as above. The basic approach is to (1) measure the angle between the foliation and the shear zone boundary, θ' , at a number of places, (2) convert those measurements to the shear strain, γ , (3) plot γ as a function of perpendicular distance across the shear zone, and (4) calculate the displacement from the area under the resulting curve:

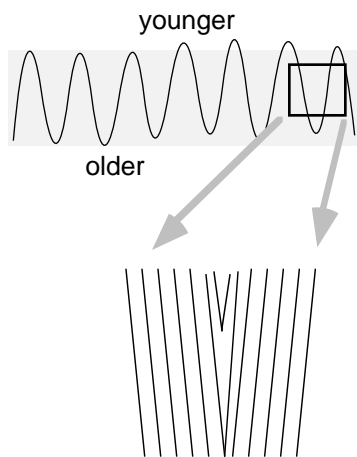


30.3 Transposition of Foliations

In many rocks, you see a compositional layering that looks like bedding, but in fact has no stratigraphic significance. The process of changing one foliation into another -- thereby removing the frame of reference provided by the first foliation -- is known as transposition. There are two basic

processes involved:

1. Isoclinal folding of the initial foliation (i.e. bedding) into approximate parallelism with the axial surfaces, and
2. attenuation and cutting out of the limbs by simple shear.



macroscopically, the bedding trends E-W, with the younger and older relations as indicated

On the outcrop, the bedding trends N-S. If the fold hinges are very obscure, then you may interpret the layering as a normal stratigraphic sequence

Obscuring of the fold hinges is an important part of the process of transposition:



This sequence of deformation would produce transposed layering in which all of the beds (really just a single bed) were right side up

Transposition is most common in metamorphic rocks, but can also occur in mélanges. It is difficult to recognize where extreme deformation is involved. In general one should look for the following:

- look for the fold hinges

- look for cleavage parallel to compositional layering
 - Walk the rocks out to a less deformed area.

LECTURE 31—THRUST SYSTEMS I: OVERVIEW & TECTONIC SETTING

31.1 Basic Thrust System Terminology

Before starting on the details of thrust faults we need to introduce some general terms. Although these terms are extensively used with respect to thrust faults, they can, in fact, be applied to any low angle fault, whether thrust or normal.

Décollement -- a French word for “unsticking”, “ungluing”, or “detaching”. Basically, it is a relatively flat, sub-horizontal fault which separates deformed rocks above from undeformed rocks, below.

Thin-skinned -- Classically, this term has been applied to deformation of sedimentary strata above undeformed basement rocks. A décollement separates the two. My own personal use applies the term to any deformation with a décollement level in the upper crust. This definition includes décollement within shallow basement. In general, the term comes from Chamberlain in 1910 and 1919; he termed the Appalachians a “thin-shelled” mountain range. John Rodgers, a well known Yale structural geologist gave the term its present form in the 1940’s.

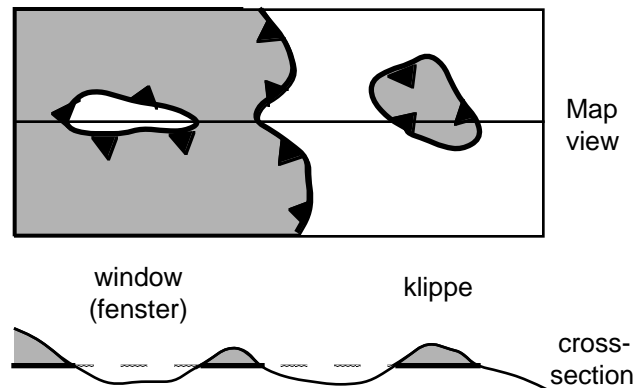
Thick-skinned -- Again, the classic definition involves deformation of basement on steep reverse faults. My own definition -- involves décollement at middle or deep crustal levels, if within the crust at all.

Allochthon -- A package of rocks which has been moved a long way from their original place of deposition. The word is commonly used as an adjective as in: “these rocks are allochthonous with respect to those...”

Autochthon -- Rocks that have moved little from their place of formation. These two terms are commonly used in a relative sense, as you might expect given that the plates have moved around the globe! You will also see the term “parautochthon” used for rocks that probably have moved, but not as much as some other rocks in the area you are studying.

Klippe -- An isolated block of rocks, once part of a large allochthon, which has become separated from the main mass, usually by erosion but sometimes by subsequent faulting.

Fenster -- This is the German word for “window”, and it means literally that: a window or a hole through an allochthon, in which the underlying autochthon is exposed. A picture best illustrates these last two terms:



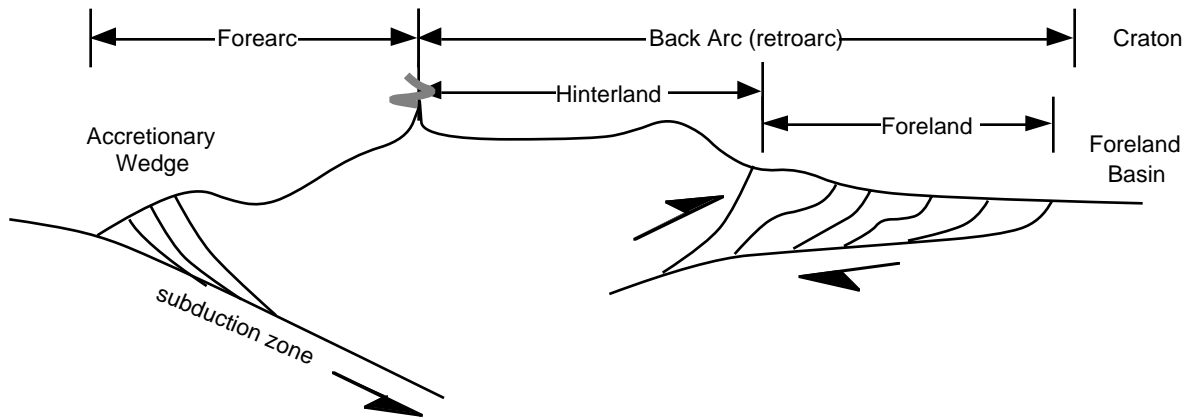
31.2 Tectonic Setting of Thin-skinned Fold & Thrust Belts

Long linear belts of folds and thrusts, known as foreland thrust belts, occur in virtually all major mountain belts of the world. Characteristically, they lie between the undeformed craton and the main part of the mountain belt itself. Some well-known examples include:

- Valley & Ridge Province (Appalachians)
- Jura Mountains (Alps)
- Canadian Rockies (Foothills, Front & Main Ranges)
- Sub-Himalayan Belt
- Subandean belt

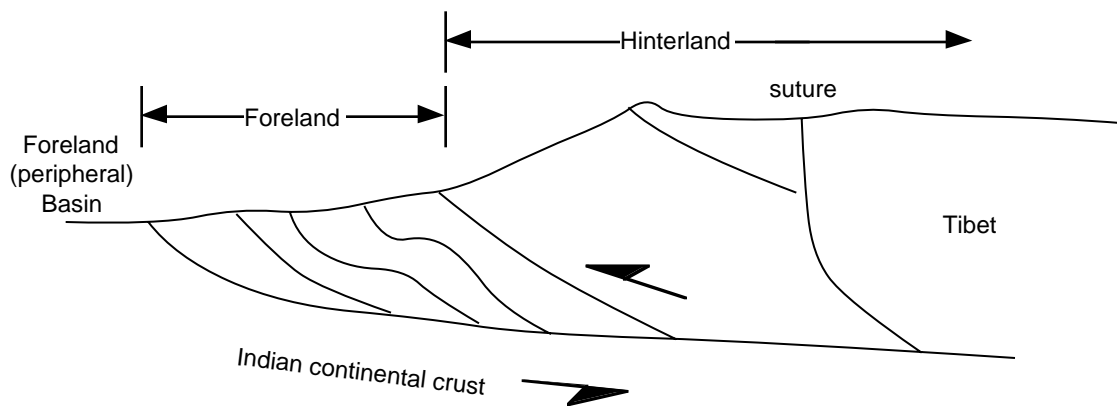
Foreland thrust belts occur in two basic types of plate settings:

31.2.1 Andean Type:



This type of foreland thrust belt is sometimes called an antithetic belt because the sense of shear is opposite to that of the coeval plate margin subduction zone.

31.2.2 Himalayan Type:



The Himalayan type is sometimes called a synthetic thrust belt because the sense of shear is the same as the plate margin that preceded it. At this point, we need to introduce two additional terms:

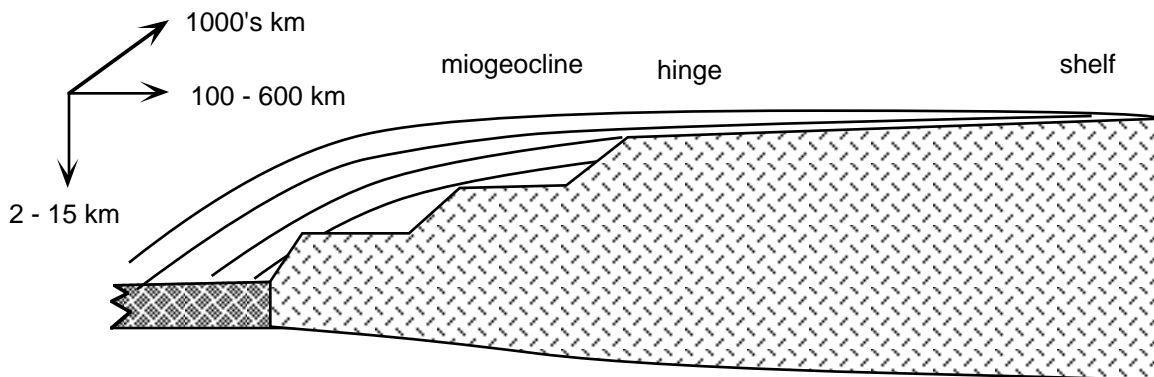
Foreland is a stable area marginal to an orogenic belt toward which rocks of the belt were folded and thrust. It includes thin-skinned thrusting which does not involve basement. In active mountain belts, such as the Andes or the Himalaya, the foreland is a region of low topography.

Hinterland refers to the interior of the mountain belt. There, the deformation involves deeper

structural levels. In active mountain belts, the hinterland is a region of high topography which includes everything between the thrust belt and the magmatic arc (where there is one). “Hinterland” in particular is a poorly defined term about which there is no general agreement. You should always state what you mean by it.

31.3 Basic Characteristics of Fold-thrust Belts

1. Linear or arcuate belts of folds and low-angle thrust faults
2. Form in subhorizontal or wedge-shaped sedimentary prisms
3. Vergence (or facing) generally toward the continent
4. Décollement zone dips gently ($1 - 6^\circ$) toward the interior of the mountain belt
5. They are the result of horizontal shortening and thickening.



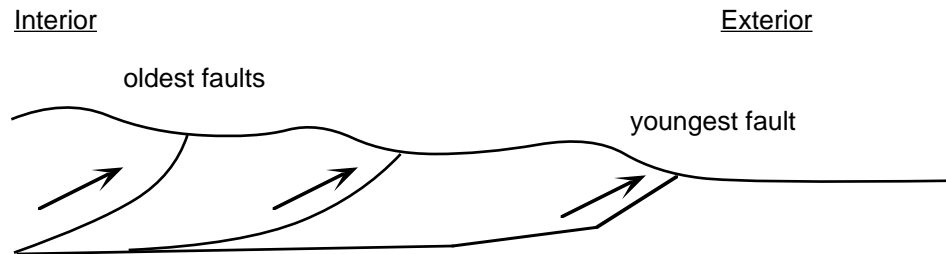
The typical fold-thrust belt in North America and many other parts of the world is formed in a passive margin sequence (or “miogeocline”) deposited on a rifted margin.

This geometry is responsible for numbers one through four in the list above because:

- miogeocline is laterally continuous
- wedge-shape responsible for the vergence
- planar anisotropy of layers produces décollement

31.4 Relative and Absolute Timing in Fold-thrust Belts

A general pattern in mountain belts is that deformation proceeds from the interior to the exterior (or from hinterland to foreland):



This progression has been demonstrated both directly and indirectly. The more interior faults are seen to be folded and deformed by the more exterior ones and the erosion of the individual thrust plates produces an inverted stratigraphy in the foreland basin in which deposits derived from the oldest thrust plate are found at the bottom of the sedimentary section.

The duration of thrust belts is quite variable. In the western North America, the thrust belt spanned nearly 100 my; in the Andes it has been active for only the last 10 - 15 my, and in Taiwan it is only 4 my old.

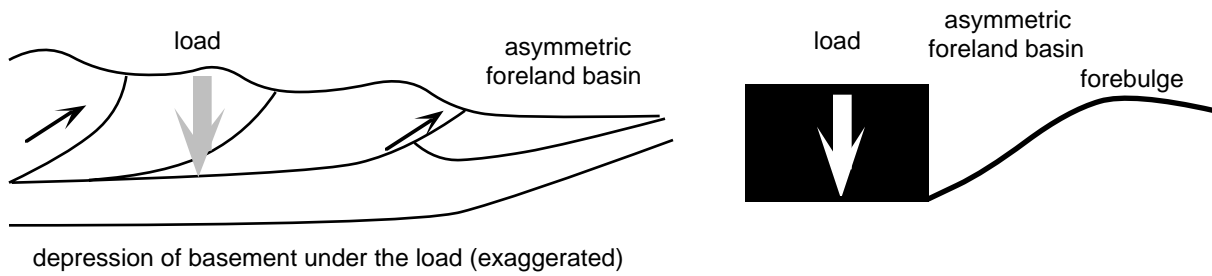
Rates of shortening in foreland thrust belts is similarly variable. In general, they range from mm/yr to cm/yr. Antithetic thrust belts are 1 to 2 orders of magnitude slower than plate convergence rates whereas synthetic thrust belts are 30 - 70% of the total convergence rate.

31.5 Foreland Basins

The horizontal shortening of the rocks in a thrust belt is accompanied by vertical thickening. This thickening means that there is more weight resting on the upper part of the continental lithosphere than there was before. Thus, the lithosphere bends or flexes under this load, just like a diving board does when you stand on the end of it. As we will see in a few lectures (last week of classes), this large scale, broad wavelength deformation of the lithosphere is known as flexural isostasy.

The loading by the thrust belt produces an asymmetric depression, with its deepest point right next to the belt. Material eroded from the uplifted thrust belt is deposited in the depression, forming a

type of sedimentary basin known as a foreland basin.



The Cretaceous deposits of western Wyoming and eastern Idaho are perhaps some of the best known foreland basin deposits.

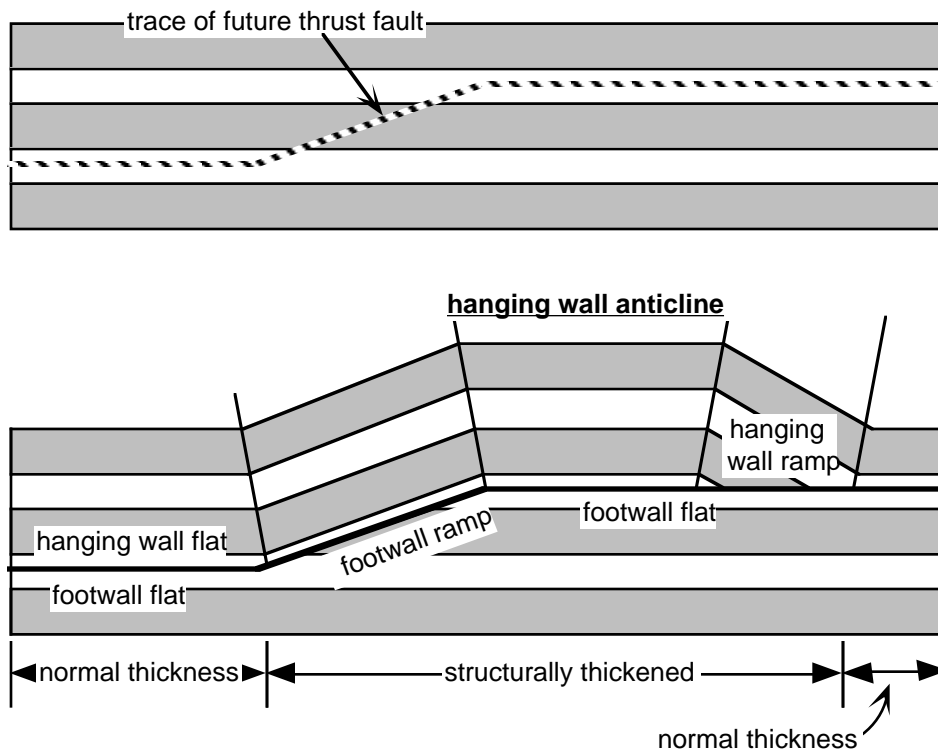
LECTURE 32—THRUST SYSTEMS II: BASIC GEOMETRIES

32.1 Dahlstrom's Rules and the Ramp-flat (Rich Model) Geometry

The basic geometries of fold and thrust belts are summarized in three “rules” proposed by Dahlstrom (1969, 1970), based on his work in the Canadian Rockies:

1. Thrusts tend to cut up-section in the direction of transport
2. Thrusts parallel bedding in incompetent horizons and cut across bedding in competent rocks
3. Thrusts young in the direction of transport

Deformation following these rules produces a stair step or “ramp and flat” geometry. This geometry was first recognized by J. L. Rich (a former Cornellian) in 1934:



The important points to remember about this “ramp-flat” model are:

- structural thickening occurs only between the footwall and the hanging wall ramps
- thrusts cut up-section in both the footwall and the hanging wall ramps
- Stratigraphic throw is not a good indication of the amount of thrust displacement
- Anticline is only in the hanging wall, not the footwall
- Thrust puts older rocks on younger rocks

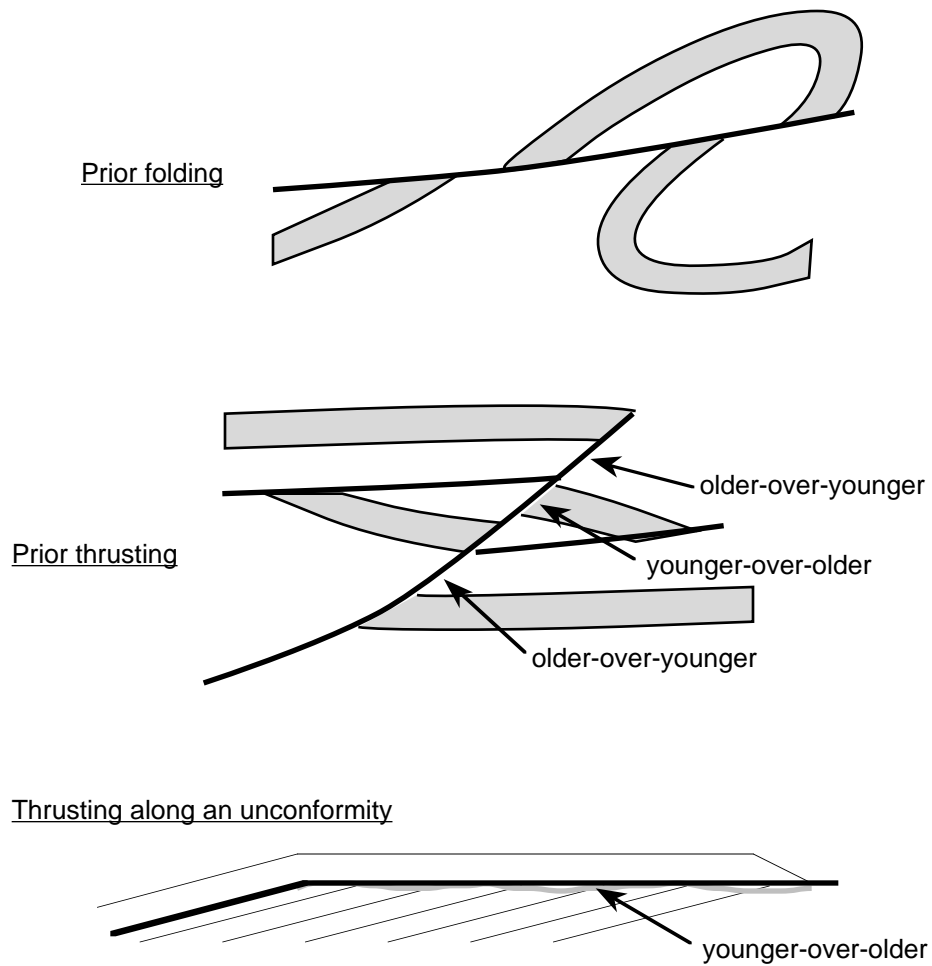
Suppe calls this process “Fault bend folding”. He has made it more quantitative by assuming a strict kink geometry. In his terminology, the dipping beds located over the footwall ramp are referred to as the “back-limb” and those over the hanging wall ramp the “forelimb”. These limbs define kink bands which help you find where the ramps are located in the subsurface. Suppe has derived equations to show that the forelimb dips (or “fore-dips”) should be steeper than the back limb dips (or “back-dips”).

It is important to remember that the conclusions we have listed above do not depend on having a kink geometry. You get the same results with curved folds and listric faults.

32.2 Assumptions of the Basic Rules

Before we get too carried away with this elegantly simple geometry, let's explore an important underlying assumption of Dahlstrom's rules:

- *Thrusts cut through a previously undeformed, flat-lying sequence of layered sedimentary rock* As long as this is true, a thrust fault will place older rocks over younger rocks. However, you can easily conceive of geometries where this will not be true:

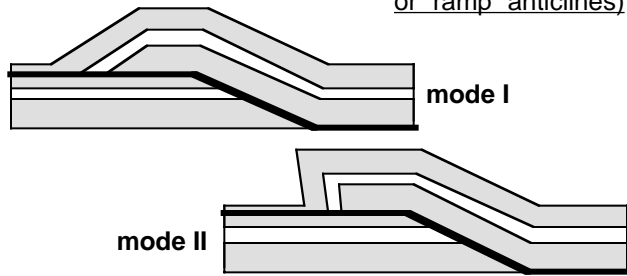


32.3 Types of Folds in Thrust Belts

The hanging-wall anticline shown above is not the only type of fold which can form in thrust belts. In general, there are four types which are commonly found:

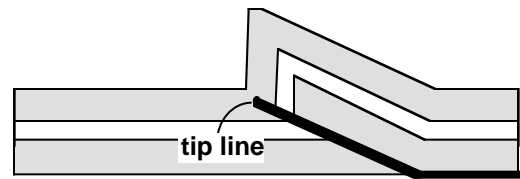
I. Fault Bend Folds

(also "hanging wall"
or "ramp" anticlines)

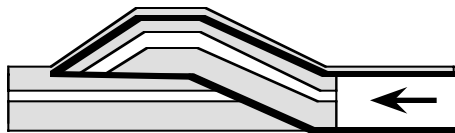


II. Fault Propagation Folds

(also "tip-line folds")

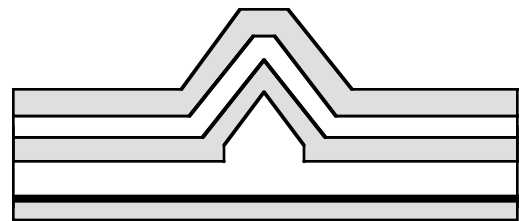


III. Wedge Fault-folds



IV. Detachment Folds

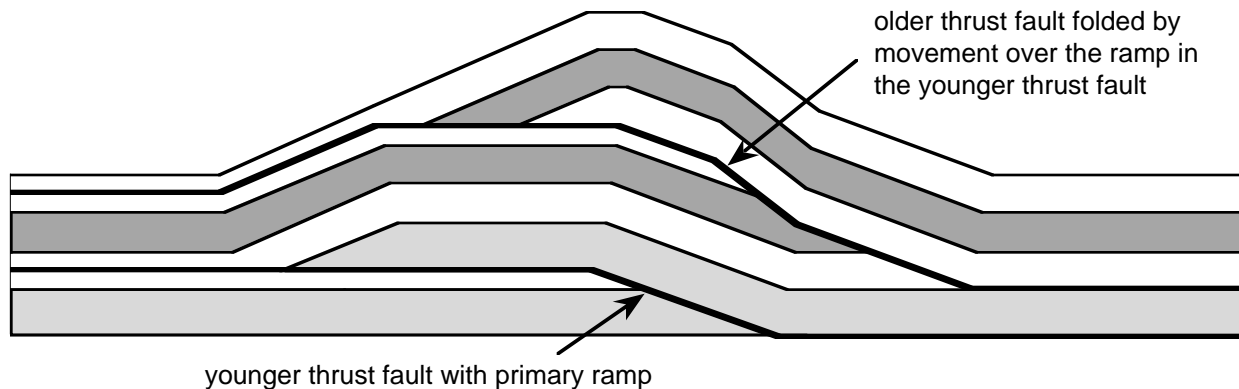
(also "Lift-off" or
"pop-up" folds)



32.4 Geometries with Multiple Thrusts

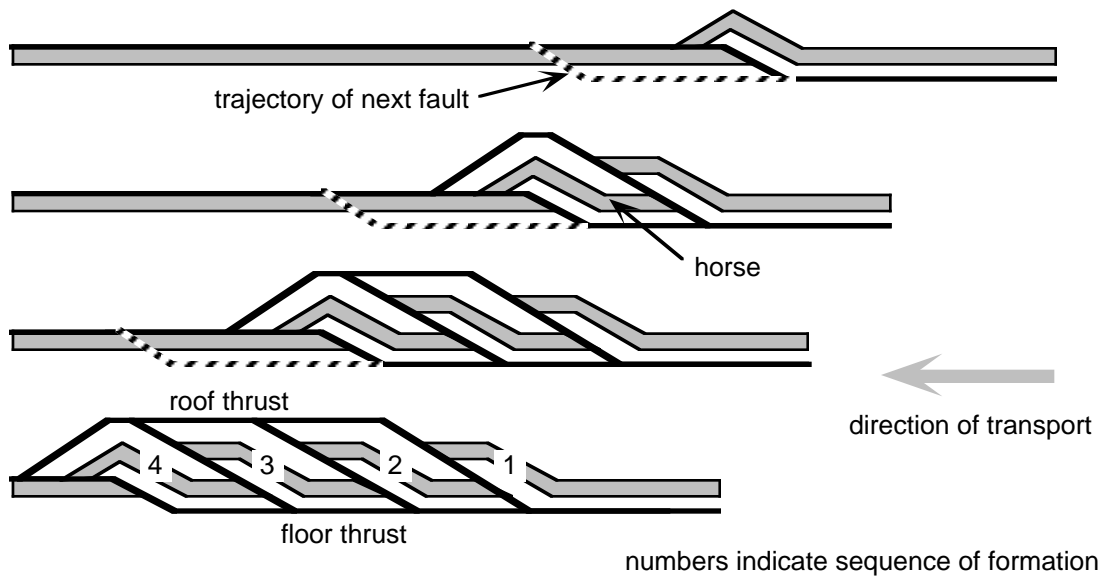
32.4.1 Folded thrusts

In general, younger faults will form at lower levels and cut into undeformed layering. When they move over ramps, they will deform any older thrusts higher in the section as illustrated in the diagram below. This provides one of the best ways to determine relative ages of faults.

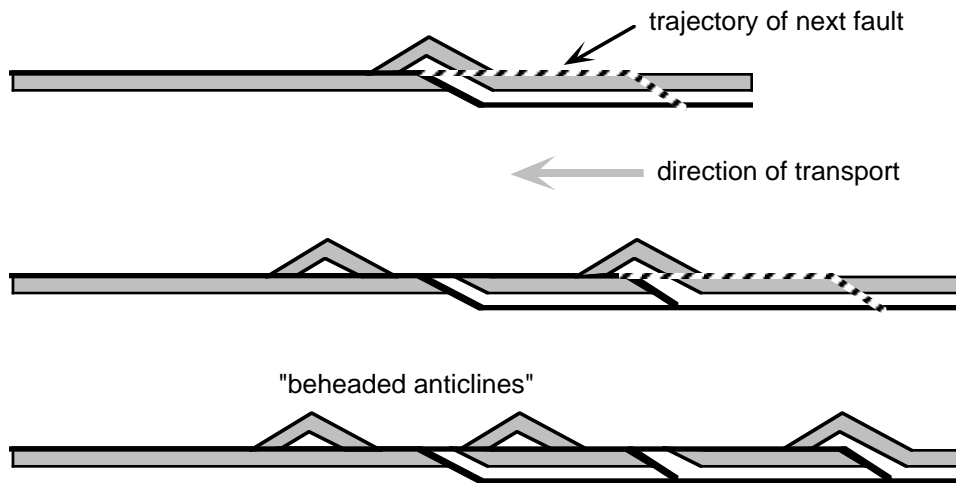


32.4.2 Duplexes

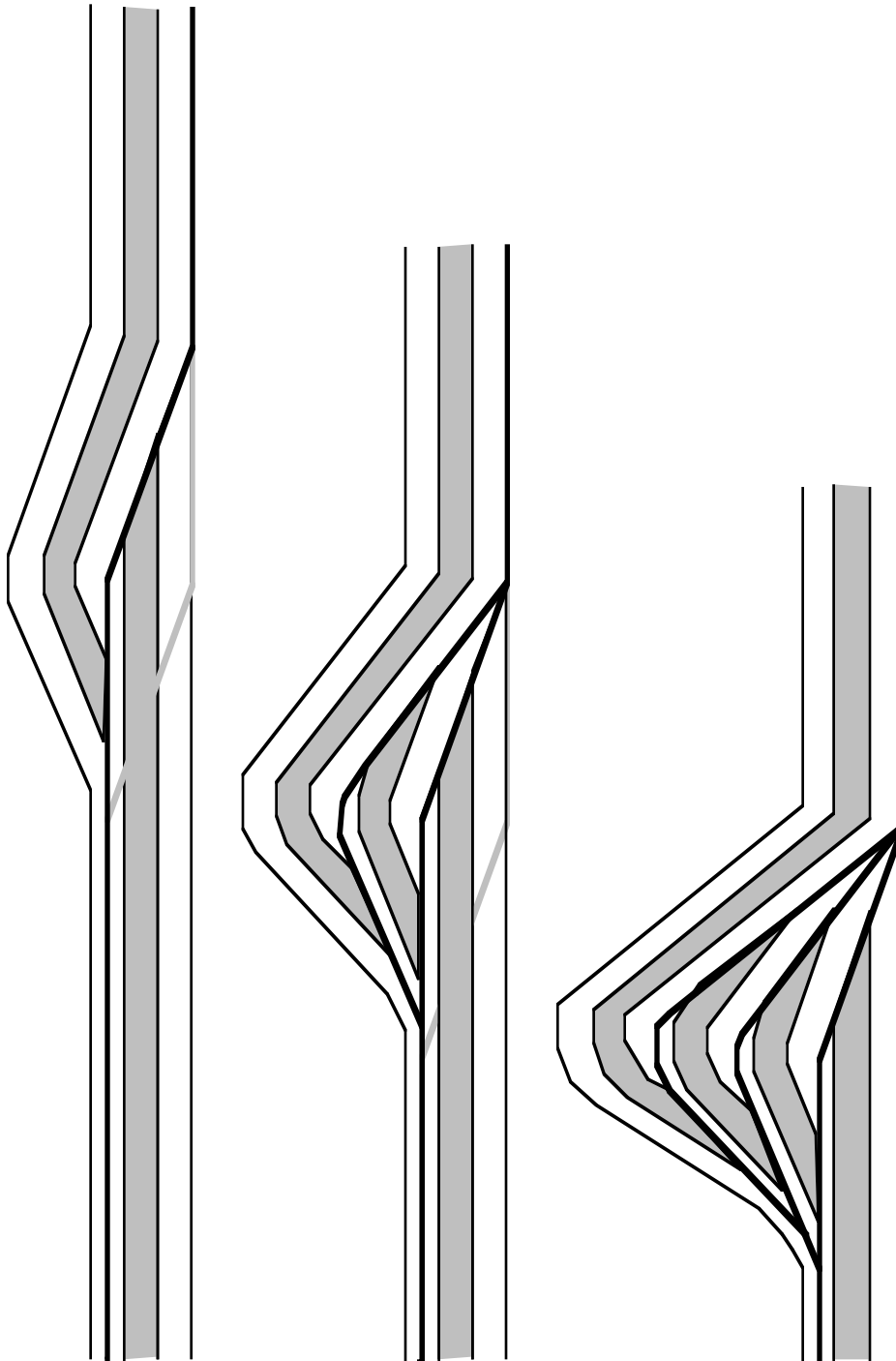
Commonly, a fault will splay off of an older thrust fault but then will rejoin the older fault again. This produces a block of rock complete surrounded by faults, which is known as a **horse**. Several horses together make a **duplex**.



Notice that the sequence of formation of the horses is in the direction of transport (i.e. from the hinterland to the foreland). This is mostly observational. If the horses formed in the other direction, then you would see "beheaded" anticlines:



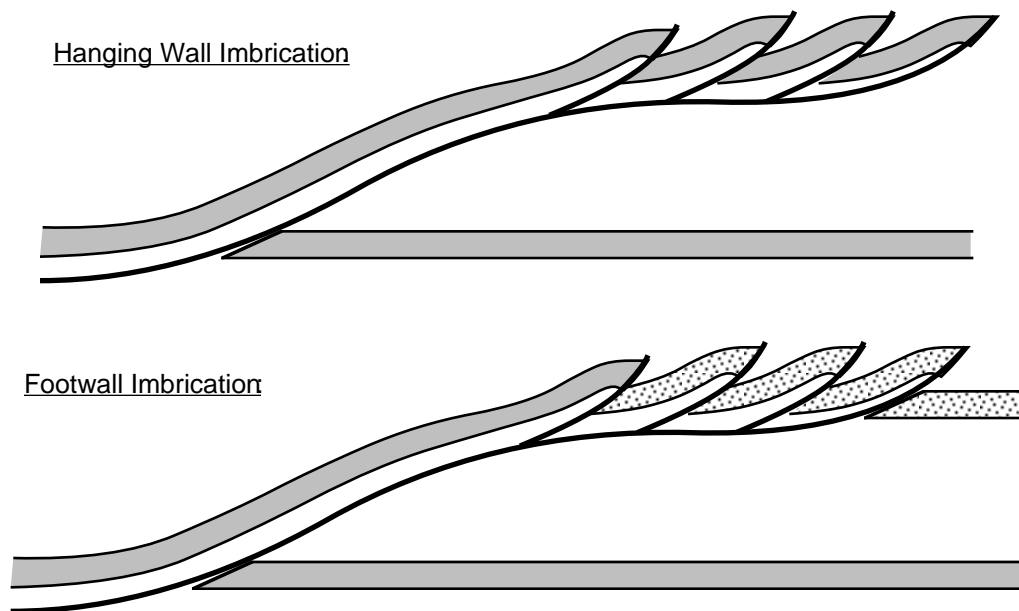
The exact shape of a duplex depends upon the height of the ramps, the spacing of the ramps, and the displacement of the individual horses. For example, as shown on the next page, if the displacement is equivalent to the initial spacing of the ramps you get a compound antiformal structure known as an **antiformal stack**:



Formation of an antiformal stack by movement on a series of horses, each with displacement equivalent to the initial spacing between the ramps. The top section formed first.

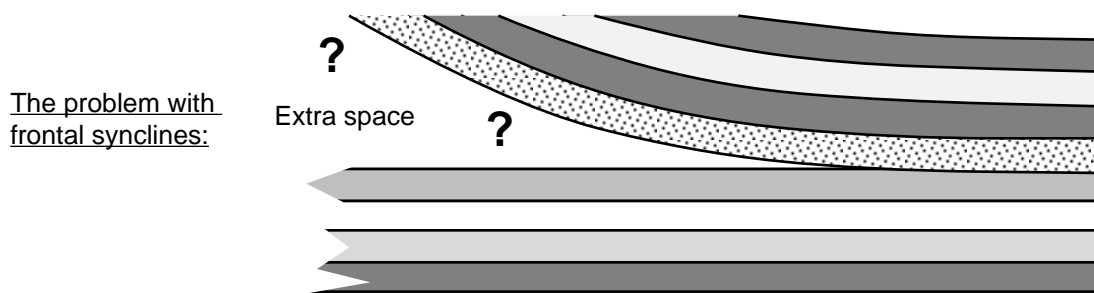
32.4.3 Imbrication

Imbrication means the en echelon tiling or stacking of thin slices of rocks. Imbricate zones are similar to duplexes except that they do not all join up in a roof thrust. There are two basic types of imbrications, illustrated below:

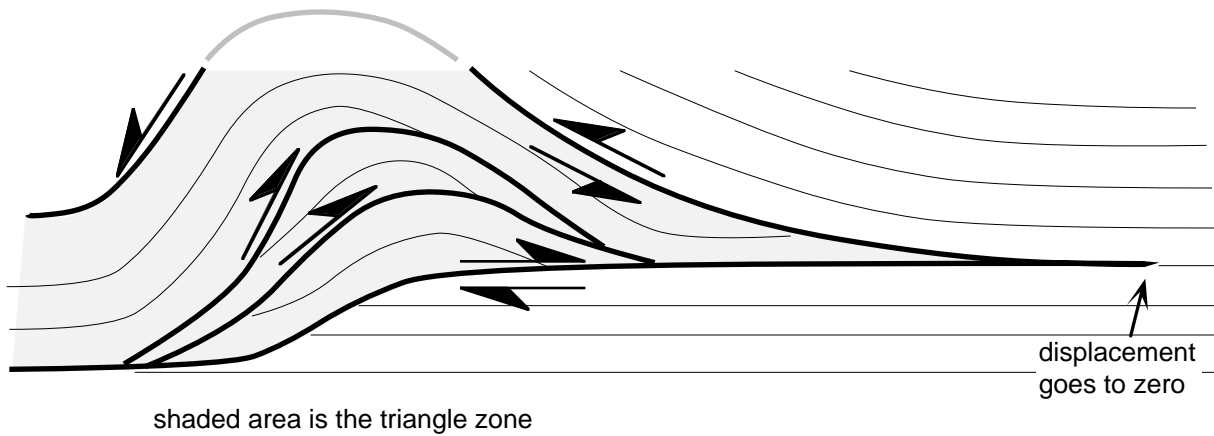


32.4.4 Triangle Zones

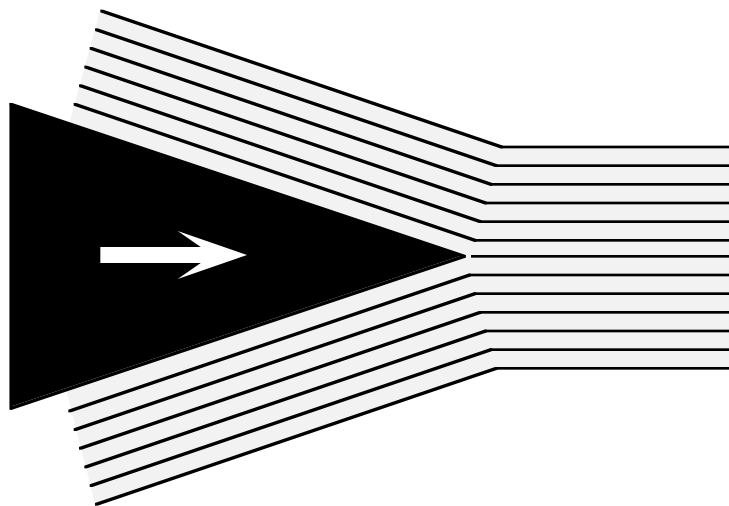
At the leading edge of a thrust belt, one commonly sees a curious syncline (or monocline). The best documented example is in the southern Canadian Rockies, where the Alberta syncline forms the eastern edge of the orogen:



The problematical space is triangular in shape so it is known as a **triangle zone**. The solution to this dilemma of frontal synclines is to fill the space with a type of duplex:



This duplex differs from the ones that we discussed above, in that the roof thrust has the opposite sense of shear than the floor thrust, whereas in "normal" duplexes they have the same sense of shear. For this reason, triangle zones have sometimes been referred to as **passive roof duplexes**. You can best visualize the kinematics of this structure by imagining driving a wedge into a pack of cards:

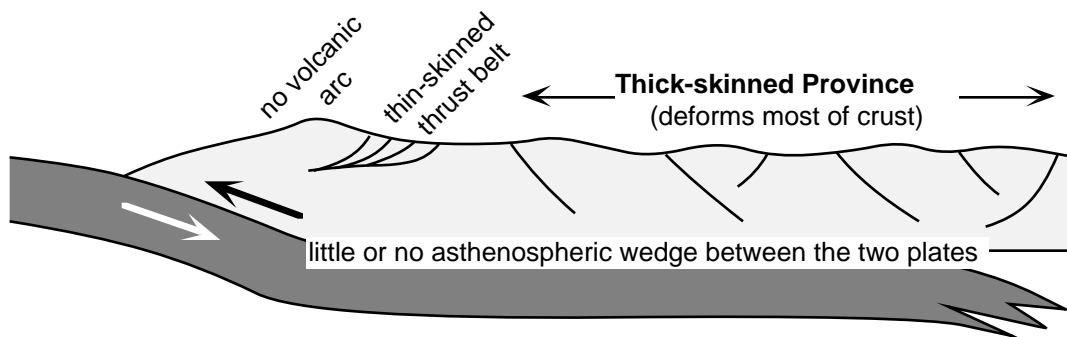


There is more than academic reasons to be interested in triangle zones. They can be prolific hydrocarbon traps, and to date have been among the most productive parts of fold-thrust belts.

LECTURE 33—THRUST SYSTEMS III: THICK-SKINNED FAULTING

33.1 Plate-tectonic Setting

The two classic areas displaying thick-skinned structures are the Rocky Mountain Foreland (“Laramide Province”) of Wyoming, Colorado, and surrounding states, and the Sierras Pampeanas of western Argentina. Both of these areas are associated with flat subduction beneath the continent and a gap in arc magmatism:



Note that coeval thin and thick-skinned deformation can be found in both the Argentine and western US examples. Some workers have proposed that the flat subduction is related to, or caused by, subduction of buoyant pieces of oceanic crust such as ridges and oceanic plateaus; this relationship has not been definitely proven.

There are parts of many other mountain belts in the world which have thick-skinned style geometries. It is not clear that flat subduction plays a role in many of these cases. These include:

- Mackenzie Mountains, Canada
- Wichita-Arbuckle Mountains, Oklahoma, Texas
- Foreland of the Atlas Mountains, Morocco
- Iberian-Catalán Ranges, Spain
- Cape Ranges, South Africa
- Tien Shan, China

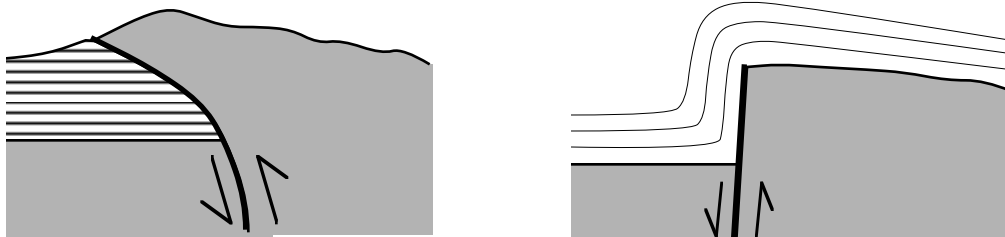
33.2 Basic Characteristics

1. Involve crystalline basement;
2. Commonly occur in regions of thin sedimentary cover;
3. Structural blocks commonly only two or three times longer than they are wide;
4. Blocks exhibit a variety of structural orientations;
5. Bounding structures commonly reverse faults with a wide variety of dips (<math><5^\circ</math> to - 6. Broad flat basins separate the mountain blocks.

33.3 Cross-sectional Geometry

In the western United States, there has, for many years, been a debate about the structural geometry of the uplifts in vertical sections. Several hypotheses have been proposed, but they can be grouped in two basic categories:

“Upthrust” Hypothesis



33.3.1 Overthrust Hypothesis



A large amount of seismic reflection and borehole data basically confirm that the overthrust model is more correct. In the Rocky Mountain foreland, the deepest overhang of basement over Paleozoic strata that has been drilled is ~14,000 ft (the total depth of the hole was 19,270 ft).

33.3.2 Deep Crustal Geometry

Insight into the deep crustal geometry of thick-skinned uplifts has come from three basic sources of information:

- seismic reflection profiling
- earthquake hypocenters and focal mechanisms
- inferences from the dip slope of the blocks.

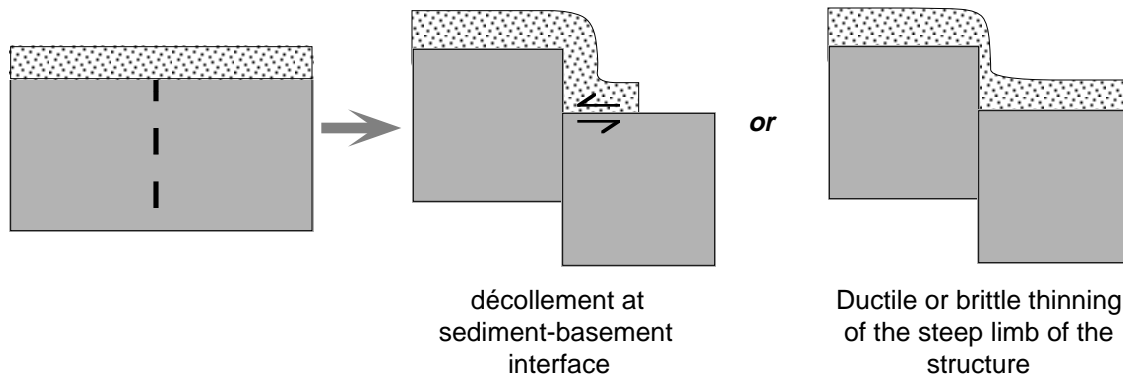
The COCORP deep seismic reflection profile across the Wind River Mountains of western Wyoming provided the most complete look at the deep structure of the uplift. That profile showed a 36°-dipping thrust fault which could be traced on the seismic section to times of 8 - 12 s (24 - 36 km). More recent processing and a reinterpretation of that seismic line indicates that the fault may have a listric geometry and flatten at between 20 and 30 km depth. This listric geometry would help explain the dip slope of the range.

Earthquake focal mechanisms from the still-active Sierras Pampeanas of western Argentina uniformly show thrust solutions with dips between 30 and 60°. There is virtually no evidence for seismic faulting on near vertical planes or with normal fault geometries. The earthquakes also provide important insight into the crustal rheology during deformation. They occur as deep as 35 - 40 km in the crust, indicating that virtually the entire crust is deforming by brittle mechanisms, at least at short time scales. These depths are deeper than would be predicted from power law creep equations, unless the strain rate was unusually fast, the heat flow were abnormally low, or the lithology were unusually mafic. All three of these are reasonable possibilities for this part of the Andean foreland.

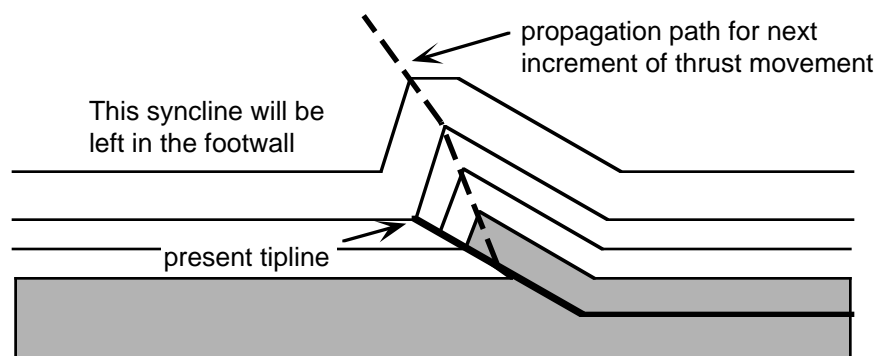
Finally the dip slope observed on many thick-skinned blocks is useful because it suggests that the blocks have been rotated. This rotation can be accomplished by listric faults or faults with bends in them. The scale of the ramp part of the fault, or the depth at which the fault flattens, can be deduced from the scale of the dip slope.

33.4 Folding in Thick-skinned Provinces

Older views of folds in thick-skinned regions suggested that the folds were formed by “draping” of the sedimentary section over faulted basement, hence the term “drape folds”. This interpretation, however, runs into problems, particularly if the fault beneath the sedimentary section is thought to be steep. It would require one of the following geometries:

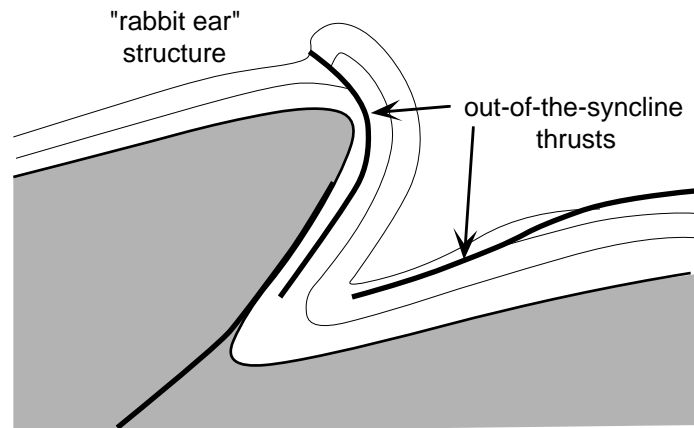


The most successful modern view is that the folds are **fault-propagation folds**, formed at the tip of a propagating thrust fault. In this scenario, overturned beds beneath basement overhangs can be interpreted to have formed when the fault propagated up the anticlinal axis, leaving an overturned syncline in the footwall.

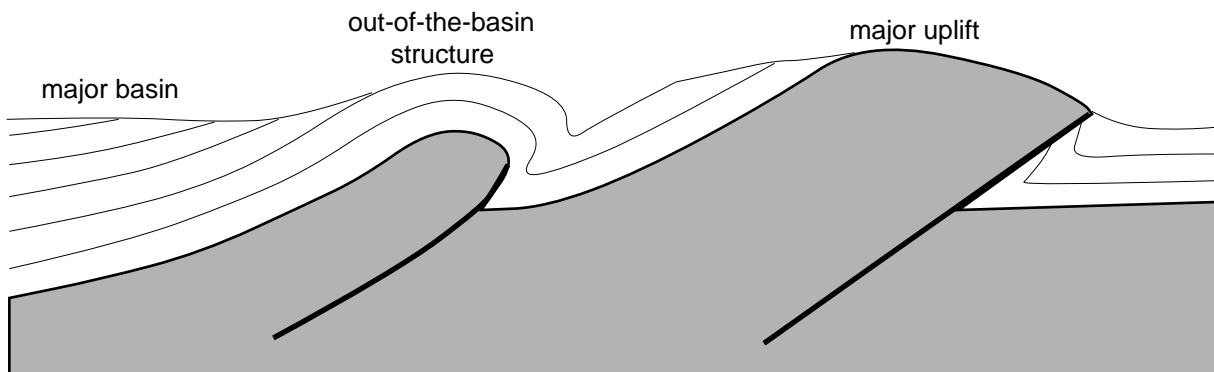


33.4.1 Subsidiary Structures

A very important family of structures are formed because the synclines underlying many of the uplifts are very tight and their deformation can no longer be accommodated by strictly layer-parallel slip. These structures are known as **out-of-the-syncline** or “crowd” structures. Basically, in the core of a syncline, there is not enough room so some of the layers get “shoved out”.



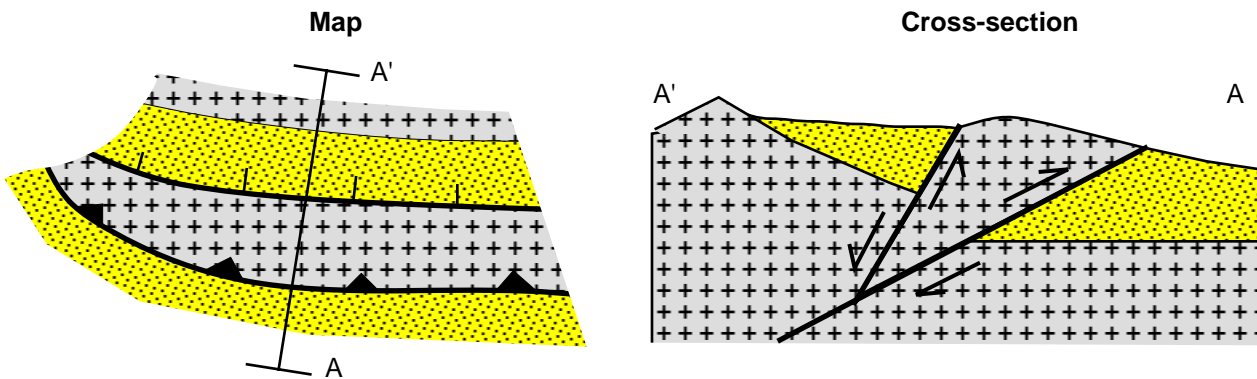
Similar structures can occur on a larger scale, where they are called out-of-the-basin faults. An example of this latter type of structure would be Sheep Mountain on the east side of the Bighorn Basin in northwestern Wyoming:



33.5 Late Stage Collapse of Uplifts

In the Rocky Mountain foreland, at least, and perhaps in other thick-skinned provinces which are no longer active, it is common to see the uplifts "collapse" by normal faulting. Thus, certain major structural blocks such as the Granite Mountains of central Wyoming have relatively little morphologic expression because most the structural relief has been destroyed by normal faulting.

In map and cross-section, this looks like:



33.6 Regional Mechanics

In the Rocky Mountain foreland, basement surfaces define regional “folds” at 100 - 200 km length scales. A model by Ray Fletcher suggests that the wavelength of the first order flexures should be four to six times the thickness of the highly viscous upper layer (i.e. the upper crust). In a rough sense, this model fits the basic observations from Wyoming if one uses a reasonable depth to the frictional crystal plastic transition zone. It is not highly successful everywhere.

Just like thrust belts, thick-skinned uplifts load the crust, producing subsidence and creating a sedimentary basin. The mechanics of these basins, known as **broken foreland basins**, is somewhat different, however, because one must model a broken beam, rather than an unbroken elastic beam.

LECTURE 34—EXTENSIONAL SYSTEMS I

34.1 Basic Categories of Extensional Structures

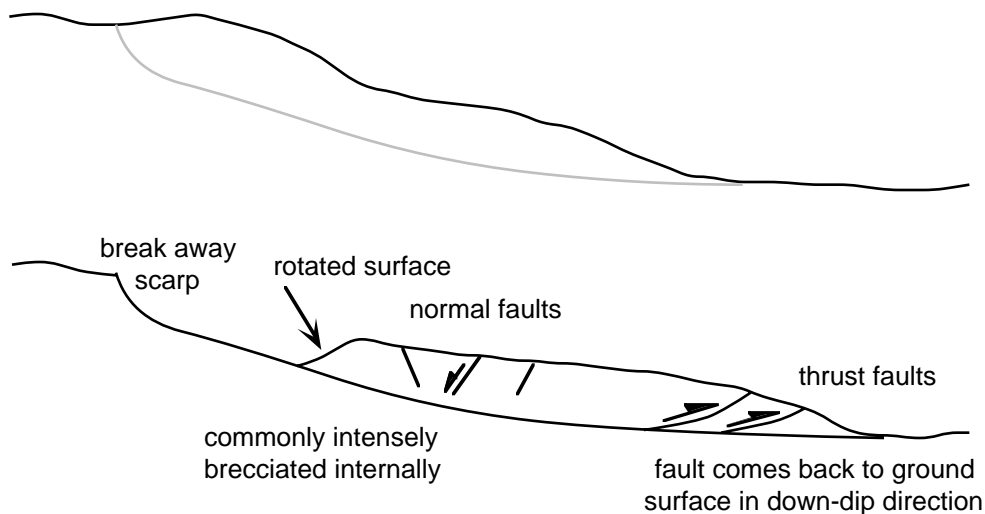
There are three basic categories of extensional structures. They differ primarily in how deep they affect the lithosphere:

1. Gravity slides (i.e. landslides, etc.)
2. Subsiding passive margins (Gulf coast growth structures)
3. Tectonic rift provinces
 - Oceanic spreading centers (e.g. Mid-Atlantic Ridge)
 - Intracontinental rifts (e.g. Basin and Range)

All are produced by essentially vertical σ_1 and horizontal σ_3 .

34.2 Gravity Slides

Subaerial gravity slides include landslides, slumps, etc., as well as much larger scale regional denudation features. Only the last one is commonly preserved in the geologic record.

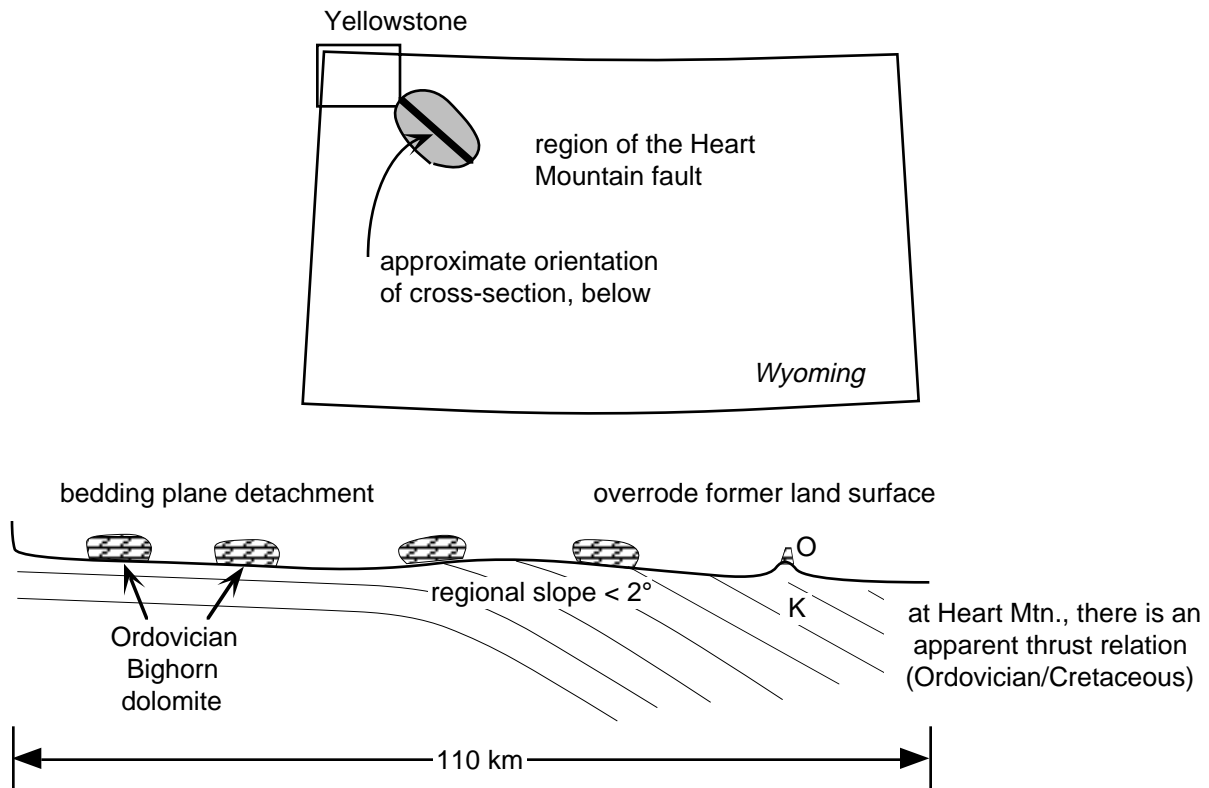


These can occur at all different scales. The underlying similarity is that the fault cuts the ground surface at both its up-dip and its down-dip termination so that only very shallow levels of the crust are involved. Although commonly caused by tectonic deformation, these are not, themselves considered to be “tectonic

structures". At the very largest scales, gravity slides are difficult to distinguish from thrust plates in mountain belts.

34.2.1 The Heart Mountain Fault

One of the largest known detachment structures is located in northwestern Wyoming and is called the Heart Mountain fault.



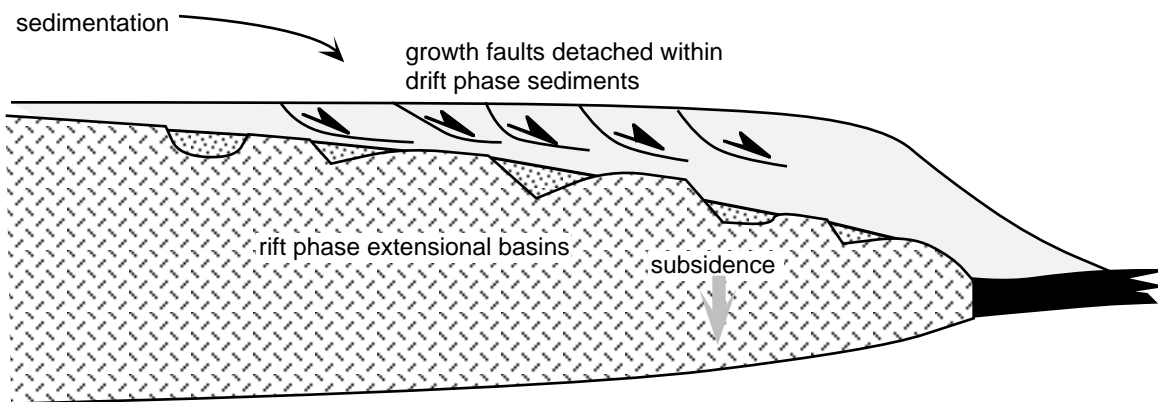
The mechanism of emplacement of the detachment is still much debated. It is possible that it was emplaced very rapidly.

34.2.2 Subaqueous Slides

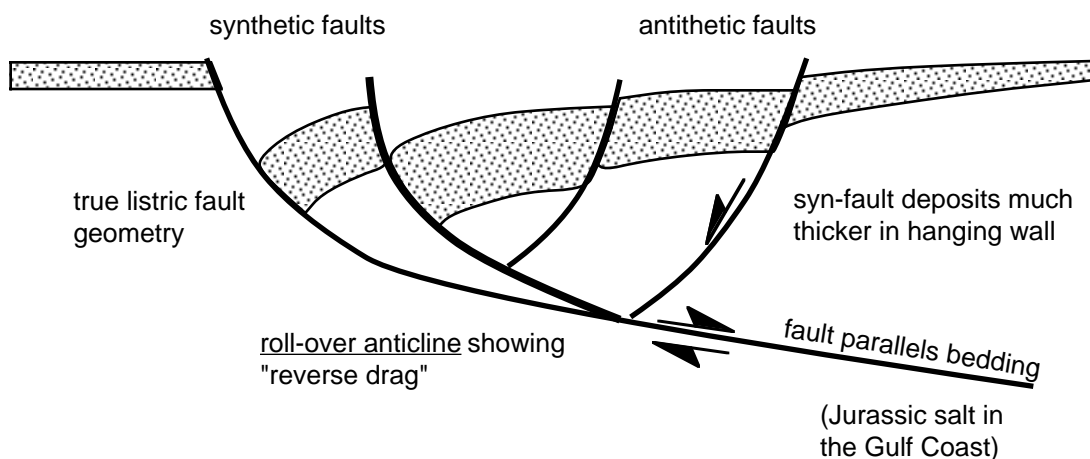
Gravity slides of unlithified or semi-lithified sediments on submarine slopes produces a very intensely deformed rock which has been termed an **olistostrome**. These are also known as "sedimentary mélanges", the term *mélange* being French for mixture. Mélanges can also be tectonic in origin, forming at the toe of an accretionary prism in a subduction zone.

34.3 Growth Faulting on a Subsiding Passive Margin

Passive continental margins with high sedimentation rates commonly experience normal faulting related primarily to the local loading by the additional sediments. The Gulf Coast is an excellent example. Such structures are commonly called “**down-to-the-basin**” faults. You should be careful to distinguish them from rift-stage structures describe in detail in the next lecture.



In detail, an individual growth fault looks like:

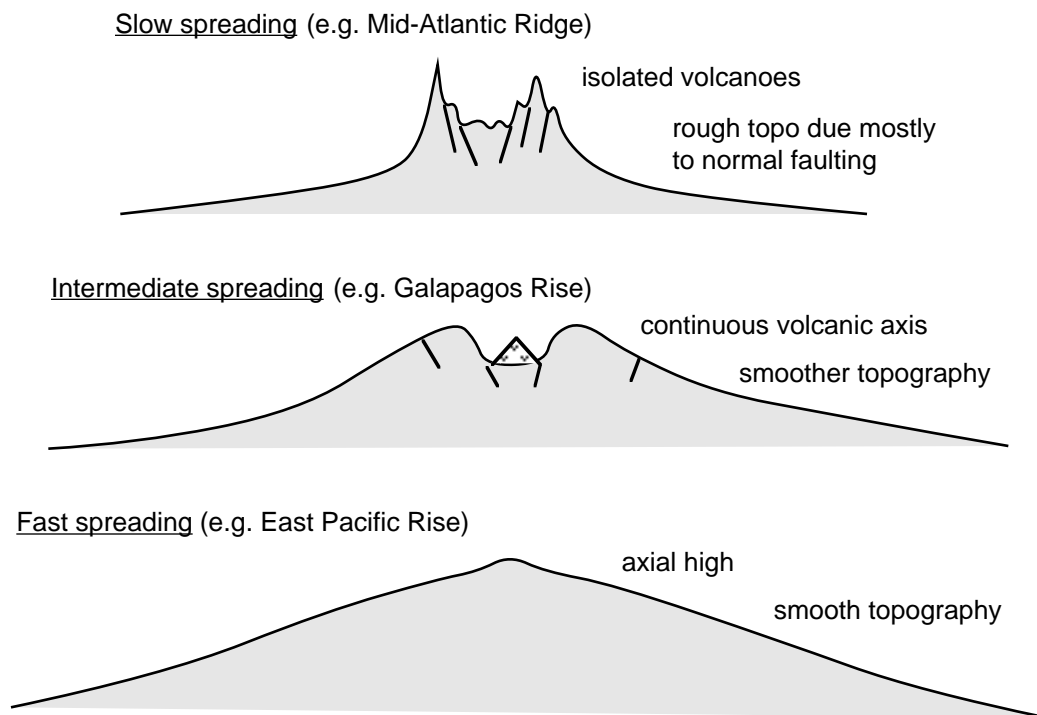


The key to recognizing growth structures is that sediments of the same age are much thicker on the hanging wall than they are on the footwall. This means that the fault was moving while the sediments accumulated preferentially in the depression made by the fault.

34.4 Tectonic Rift Provinces

34.4.1 Oceanic Spreading Centers

The largest tectonic rift provinces in the world are represented by the earth's linked oceanic spreading centers. These are sometimes inaccurately referred to as "Mid-ocean ridges" because the spreading center in the Atlantic happens to be in the middle of the ocean. We know about the structure of the oceanic spreading centers primarily from studies of their topography (or really their bathymetry). That topography represents an important interplay between structure, magmatism, and thermal subsidence.



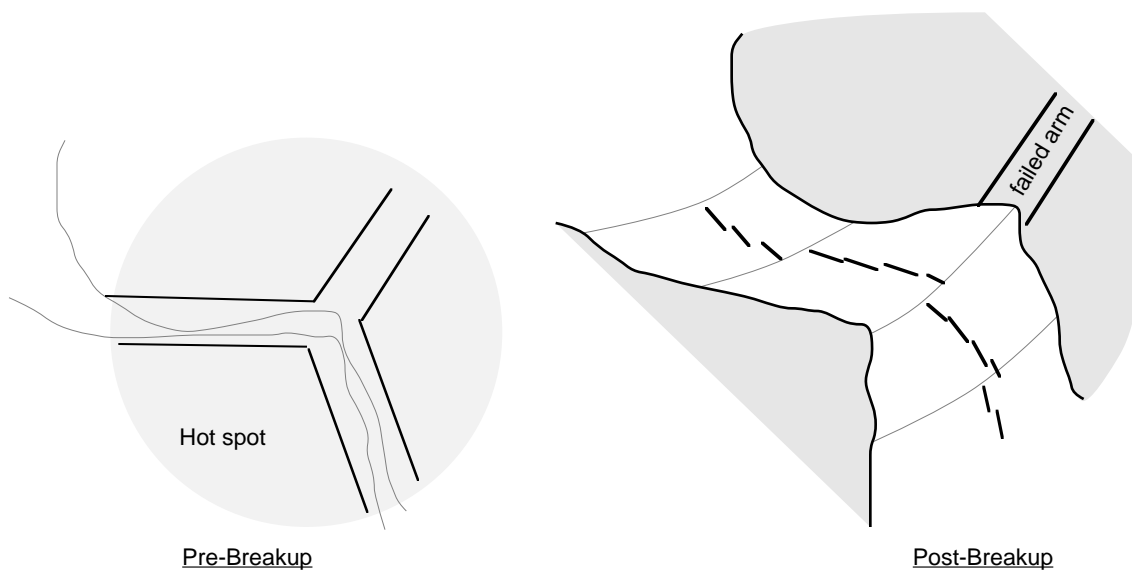
At *slow spreading* rates (~ 2.5 cm/yr), normal faulting dominates the topography. There is a distinct rift valley. Even though there are greater local reliefs, overall the ridge is lower because there is a smaller thermal component to the topography.

At *intermediate spreading rates* (7 cm/yr half rates), volcanic processes become more important as magma can reach the surface every where along the axis. There is still a subdued rift valley due to normal faulting but the topography is smoother and higher.

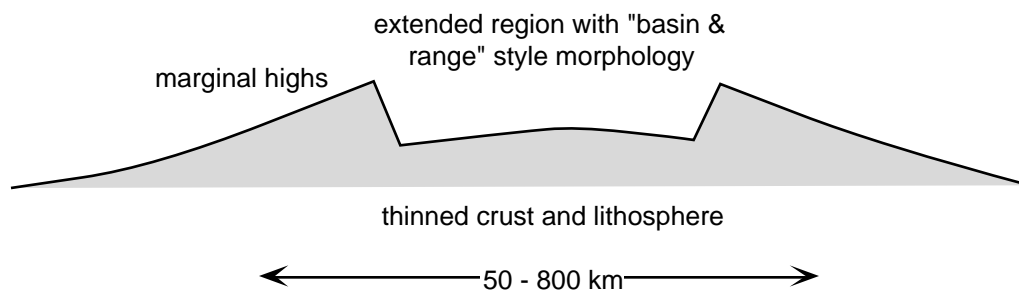
At *high spreading rates* (~15 cm/yr) the regional topography is dominated by thermal effects and abundant volcanism, with little or no axial rift valley.

34.4.2 Introduction to Intracontinental Rift Provinces

Intracontinental rift provinces form within continental crust (hence the prefix “intra”). They may lead to the formation of an ocean basin, but there are many examples which never made it to that stage. Such rifts are called failed rifts or aulacogens. Many such features are found at hot spot triple junctions formed during the breakup of the continents:



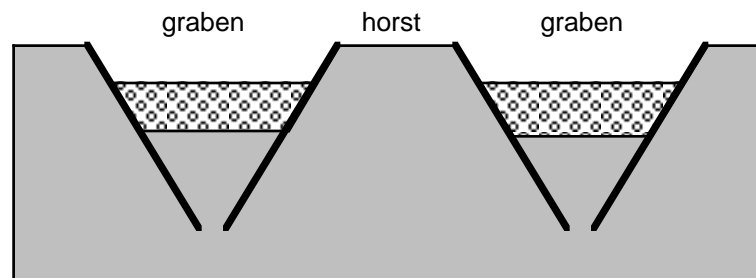
Most intracontinental rifts have a gross morphology similar to that of their oceanic counterparts. This reflects the importance of lithospheric scale thermal processes in extensional deformation. Generally, the regional thermal upwarp is much larger than the zone of rifting.



LECTURE 35—EXTENSIONAL SYSTEMS II

35.1 Basic Categories of Extensional Structures

Until about 15 years ago, our understanding of extensional deformation was dominated by Anderson's theory of faulting. The resulting geometric model is known as the horst and graben model:



Faults in this model are planar and dip at 60° (assuming an angle of internal friction of 30°). Superficially, this model appeared to fit the observations from many rifted areas (e.g. the Basin and Range, Rhine Graben, etc.).

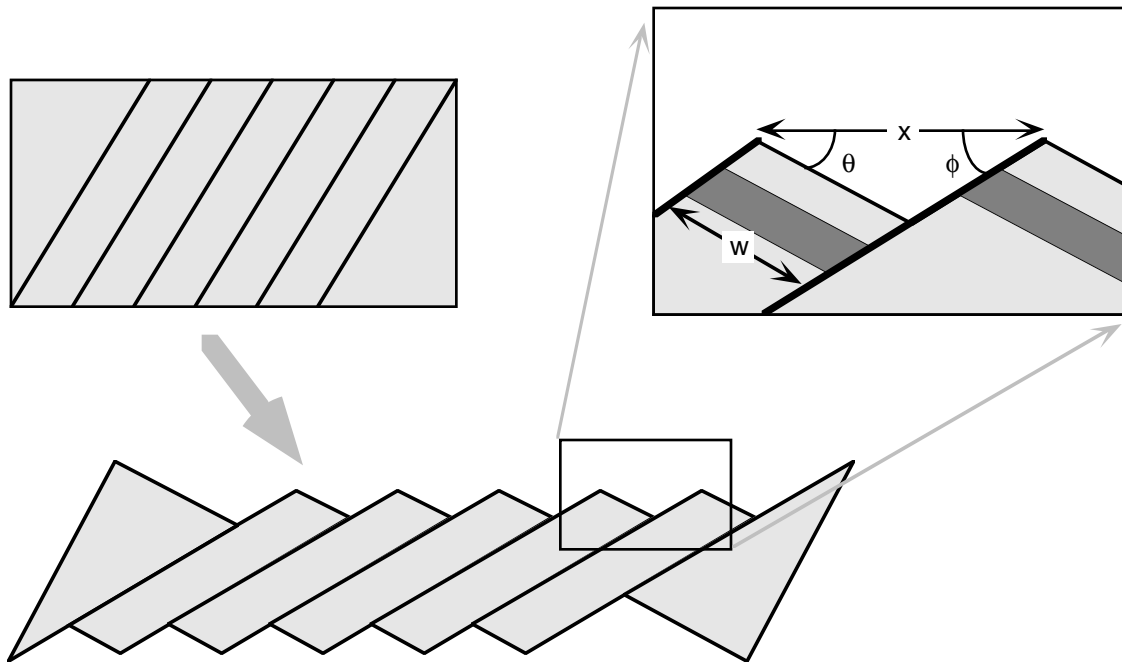
The basic problems with it are:

- non-rotational, even though tilted beds are common in rift provinces
- only small extensions are possible, and we now know of extensions $>100\%$

These problems forced people to seek alternative geometries

35.2 Rotated Planar Faults

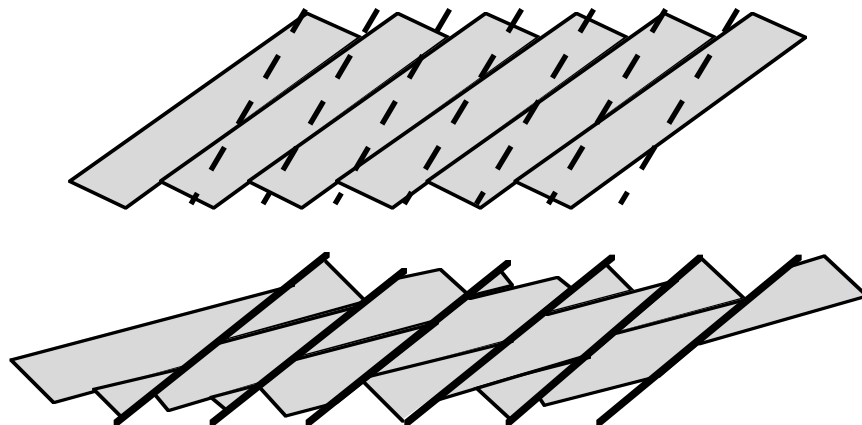
In this geometry, the faults are planar but they rotate as they move, much as a stack of dominoes collapses. For that reason it is commonly called the **domino model**. The resulting basins which form at the top of the dominoes are called **asymmetric half graben** because they are bounded by a fault only on one side. This model produces the commonly observed rotations in rift provinces:



If you know the dip of the rotated bedding and the dip of the fault, you can calculate the horizontal extension assuming a domino model from the following equation (from Thompson, 1960):

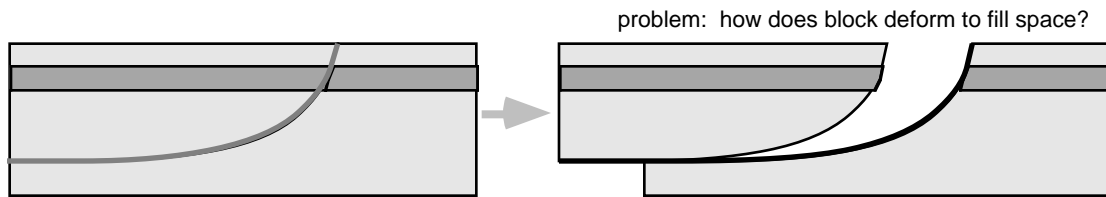
$$\% \text{ extension} = \frac{(x - w)}{w} 100 = \left(\frac{\sin(\phi + \theta)}{\sin \phi} - 1 \right) 100 .$$

When the faults rotate to a low angle, they are no longer suitably oriented for slip. Then, a new set of faults may form at a high angle. Several episodes of rotated normal faults can result in very large extensions.

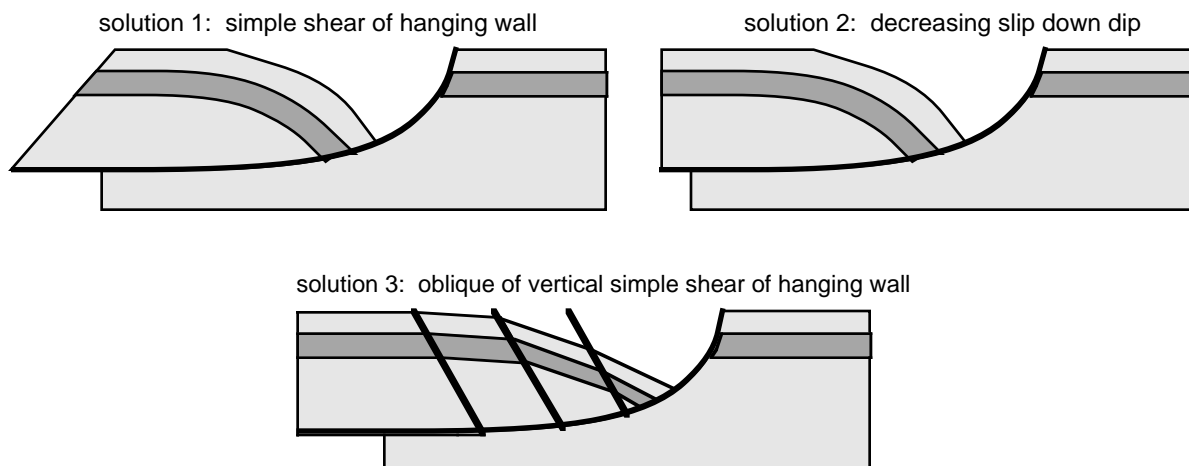


35.3 Listic Normal Faults

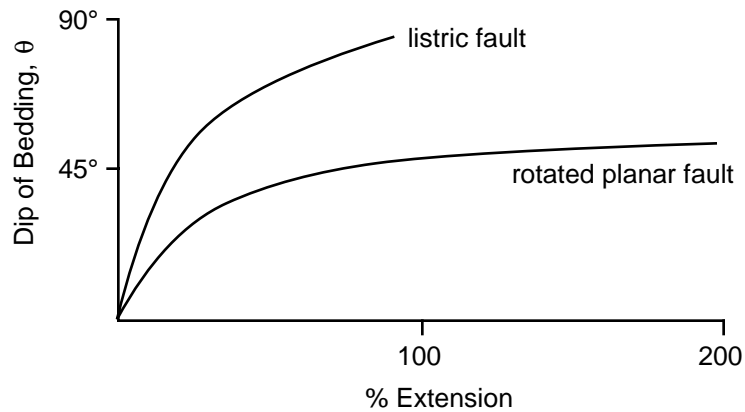
In listric normal faults, only the bedding in the hanging wall rotates. This is in contrast with the domino model in which the faults and bedding in both hanging wall and footwall rotate.



The shape of a listric block poses interesting space problems. How does the hanging wall deform to fill the space. The solutions to this problem are illustrated below.

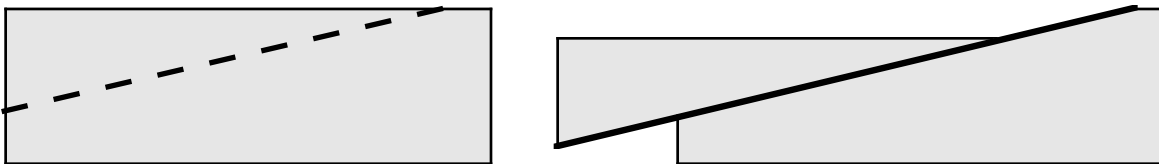


In both the listric and the rotated planar faults cases, the dip of bedding is directly related to the percent horizontal extension. For the same bedding dip, the amount of extension predicted by the rotated planar faults is much greater than that predicted by the listric faults as shown schematically by the graph below [the graph is not accurate, but is for general illustration purposes only].

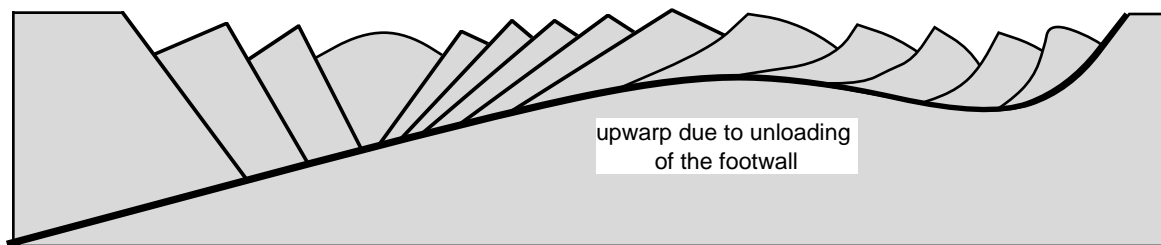


35.4 Low-angle Normal Faults

Planar, or very gently listric, normal faults which formed initially at a low angle (in contrast to faults rotated to a low angle) and move at a low angle are called **low angle normal faults**. These faults are very controversial because they are markedly at odds with Anderson's Law of faulting. Given the weakness of rocks under tension, it seems likely that they move under their own weight and over virtually friction-free surfaces (which could be simulated by pore pressure close to lithostatic, i.e. $\lambda \approx 1$). Their mechanics are still poorly known and much debated. These faults accommodate more extension than high-angle normal faults, but less than either of the geometries discussed above.



All of the above structural styles can be combined in a single extensional system. The picture, below, is similar to cross-sections drawn across many of the metamorphic core complexes in the western U.S.



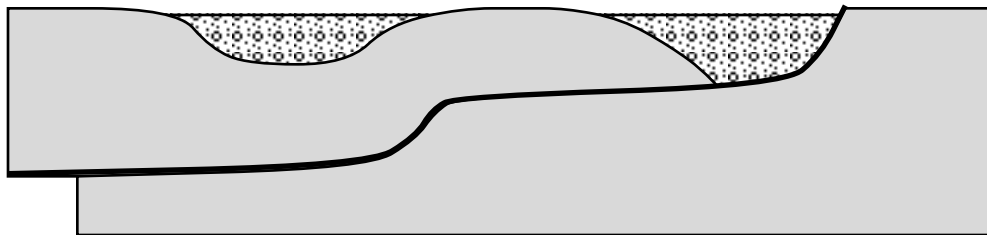
35.5 Review of Structural Geometries

The following table, after Wernicke and Burchfiel, summarizes the structural styles discussed above:

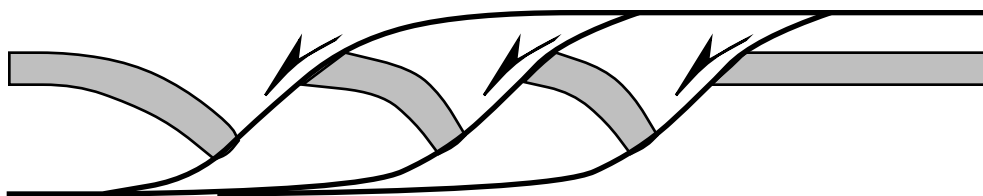
	Rotational	Non-rotational
Planar fault	Faults (domino style) & strata both rotated	High-angle & low-angle normal faults
Curved fault	Faults (listric-style) HW strata only rotated	compaction after faulting

35.6 Thrust Belt Concepts Applied to Extensional Terranes

35.6.1 Ramps, Flats, & Hanging Wall Anticlines:



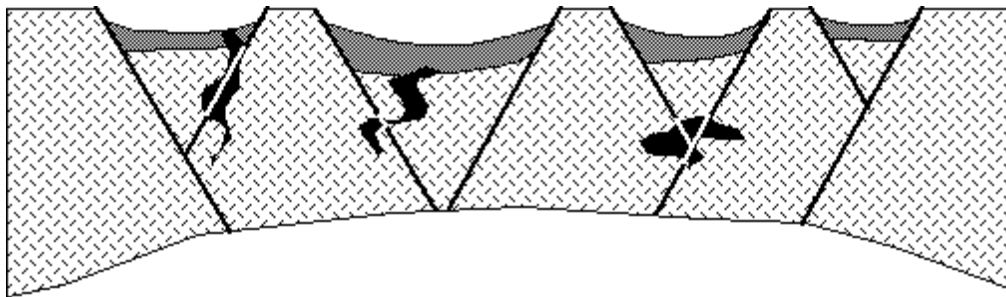
35.6.2 Extensional Duplexes:



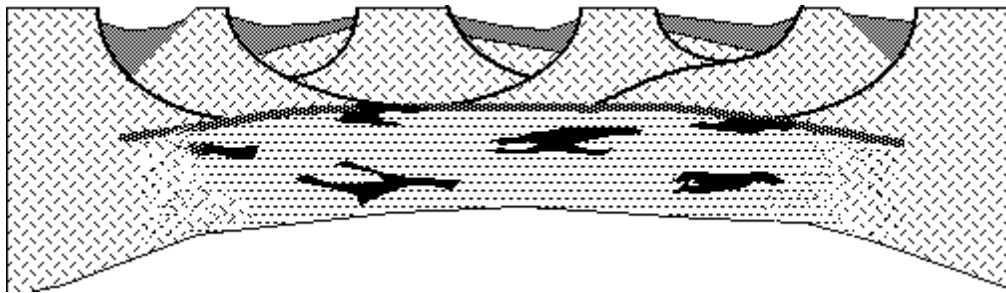
35.7 Models of Intracontinental Extension

A major question is, “what happens in the middle and lower crust in extensional terranes?” Because extensional provinces are generally characterized by high heat flow and therefore probably a weak plastic rheology at relatively shallow depths, it is not at all clear that the faults that we see at the surface should continue deep into the crust. There are now four basic models:

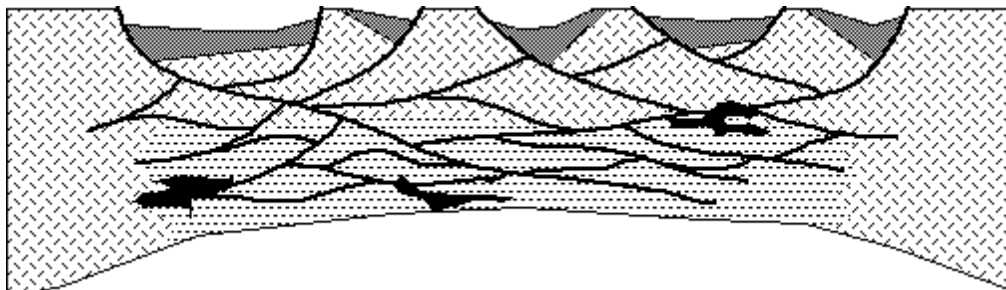
35.7.1 Horst & Graben:



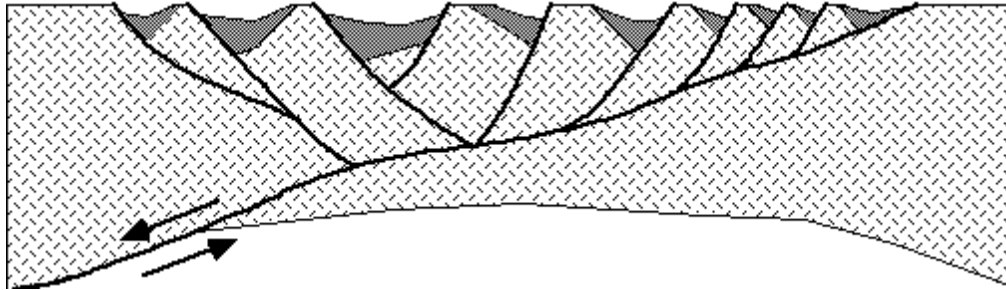
35.7.2 “Brittle-ductile” Transition & Sub-horizontal Decoupling:



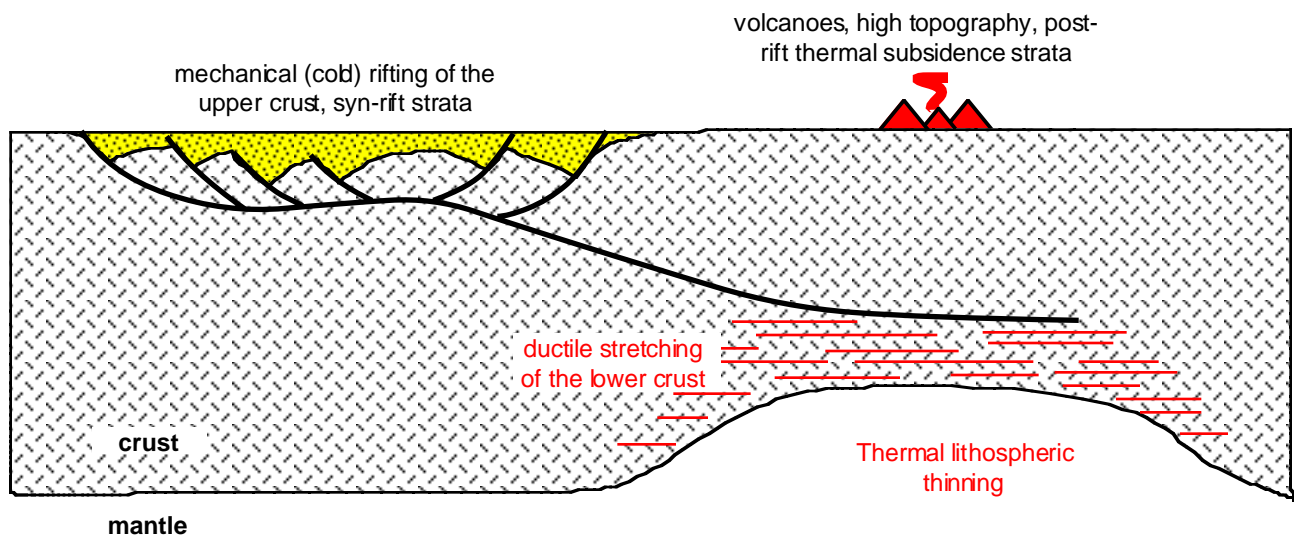
35.7.3 Lenses or Anastomosing Shear Zones:



35.7.4 Crustal-Penetrating Low-Angle Normal Fault:



35.7.5 Hybrid Model of Intracontinental Extension



LECTURE 36—STRIKE-SLIP FAULT SYSTEMS

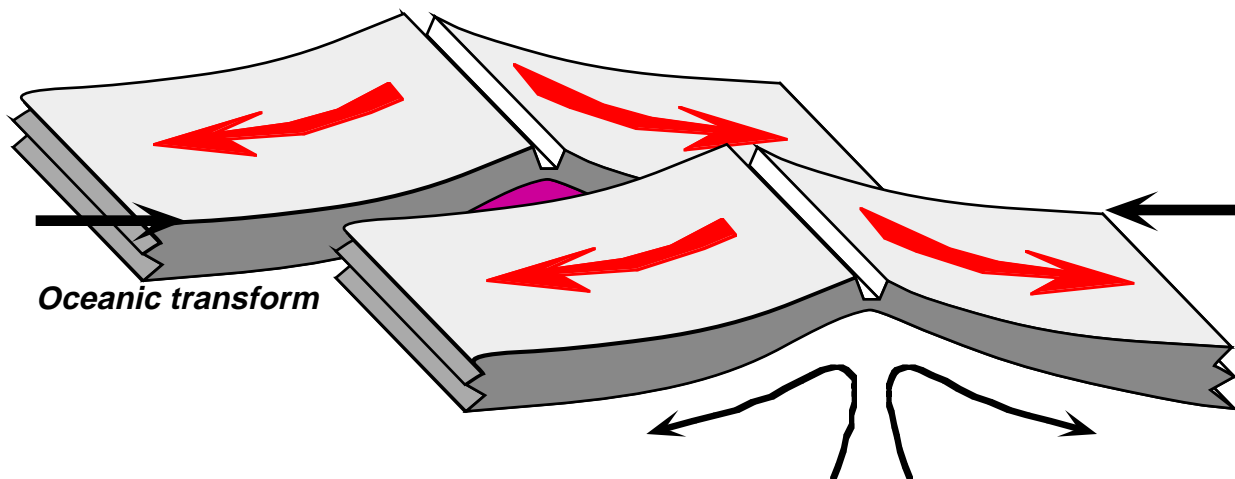
36.1 Tectonic setting of Strike-slip Faults

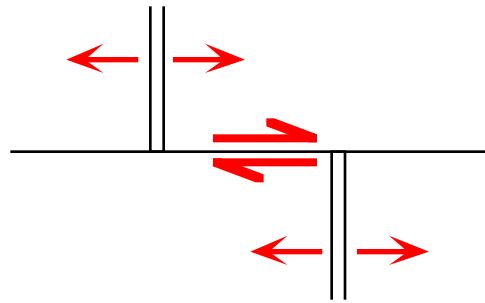
There are three general scales of occurrence of strike-slip faults:

1. Transform faults
 - 1a. Oceanic transforms
 - 1b. Intracontinental transforms
2. Transcurrent faults
3. Tear faults

36.1.1 Transform faults

Oceanic transforms occur at offsets of oceanic spreading centers. Paradoxically, the sense of shear on an oceanic transform is just the opposite of that implied by the offset of the ridge. This arises because the ridge offset is probably inherited from the initial continental break-up and is not produced by displacement on the transform.





36.2 Transcurrent Faults and Tear Faults

Large strike-slip faults within continents which are parts of plate boundaries are called **intracontinental transforms**. Examples include:

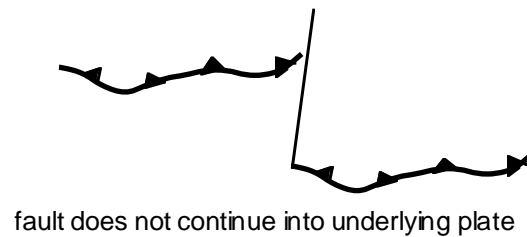
- San Andreas fault (California)
- Alpine fault (New Zealand)
- North Anatolian fault (Turkey)

Other large intra-continental strike-slip faults —called **transcurrent faults** by Twiss and Moores— are not clearly the plate boundaries include

- Altyn Tahg fault (China)
- Atacama fault (Chile)
- Garlock fault (California)
- Denali fault (Alaska)

All of these structures have a characteristic suite of structures associated with them.

A **tear fault** is a relatively minor strike-slip fault, which usually occurs in other types of structural provinces (e.g. thrust or extensional systems) and accommodates differential movements of individual allochthons. When a tear fault occurs within a thrust plate, it usually is confined to the hanging wall and does not cut the footwall:



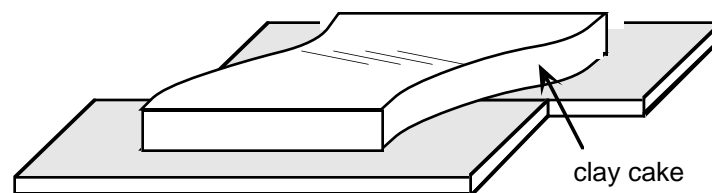
A **wrench fault** is basically a vertical strike slip fault whereas a strike slip fault can have any orientation but must have slipped parallel to its strike.

36.3 Features Associated with Major Strike-slip Faults

In general there are three types of structures, all of which can occur along a single major strike slip fault:

1. **Convergent** -- the blocks move closer or converge as they slide past each other
2. **Divergent** -- the blocks move apart as they move past one another
3. **Parallel** -- they neither converge nor diverge.

36.3.1 Parallel Strike-slip

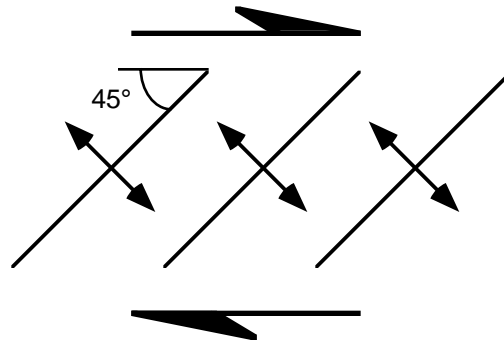


Much of our basic understanding of the array of structures that develop during parallel strike-slip faulting comes from experiments with clay cakes deformed in shear, as in the picture, above. These experiments show that strike-slip is a two stage process involving

- pre-rupture structures, and
- post-rupture structures.

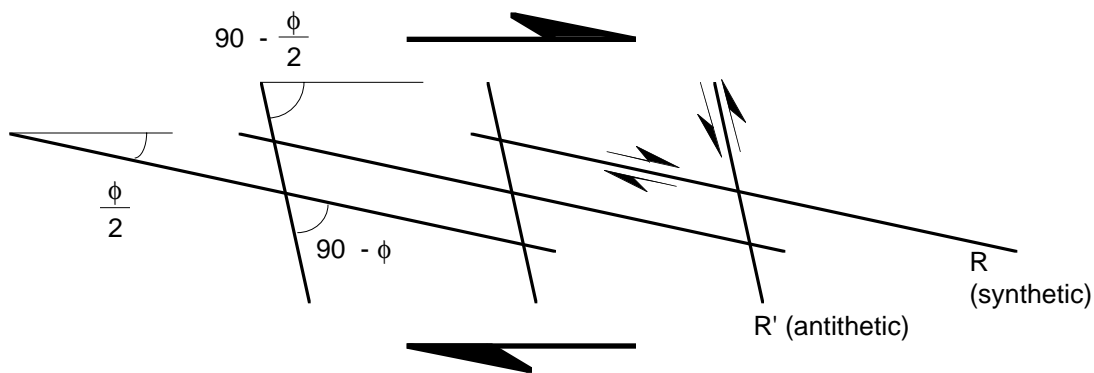
1 Pre-rupture Structures

1. En echelon folds:



The folds in the shear zone form initially at 45° to the shear zone walls, but then rotate to smaller angles.

2. Riedel Shears (conjugate strike-slip faults):

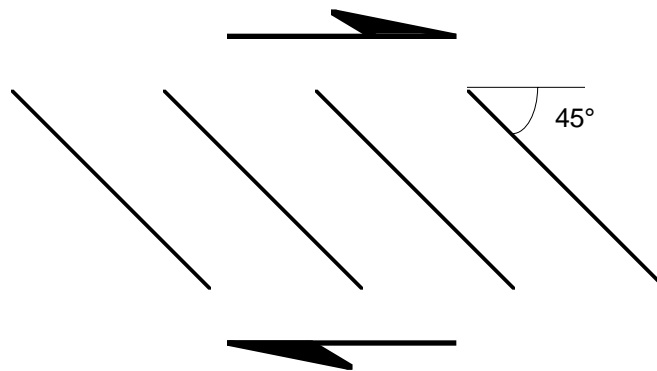


The initial angles that the synthetic and antithetic shears form at is controlled by their coefficient of internal friction. Those angles and the above geometry mean that the maximum compression and the principal shortening axis of infinitesimal strain are both oriented at 45° to the shear zone boundary.

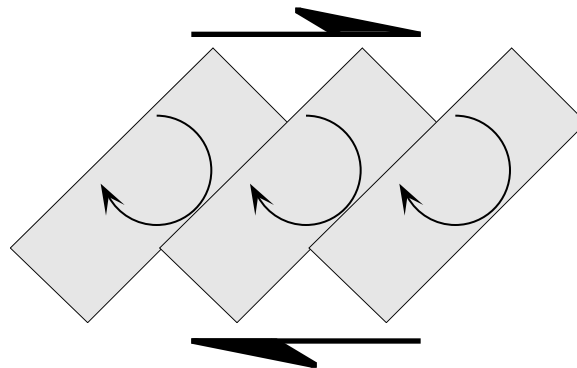
With continued shearing they will rotate (clockwise in the above diagram) to steeper angles. Because the R' shears are originally at a high angle to the shear zone they will rotate more quickly and become inactive more quickly than the R shears. In general, the R shears are more commonly observed, probably because they have more displacement on them.

Riedel shears can be very useful for determining the sense of shear in brittle fault zones.

3. **Extension Cracks:** In some cases, extension cracks will form, initially at 45° to the shear zone:



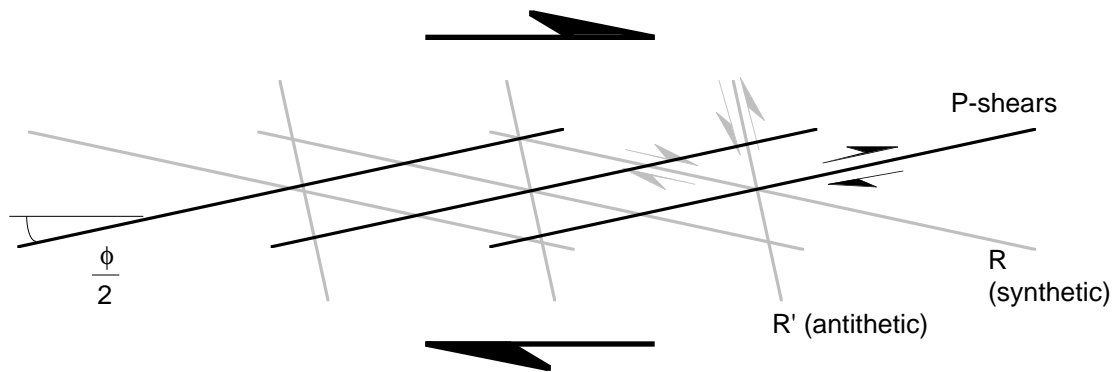
These cracks can serve to break out blocks which subsequently rotate in the shear zone, domino-style:



Note that the faults between the blocks have the opposite sense of shear than the shear zone itself.

2 Rupture & Post-Rupture Structures

A rupture, a new set of shears, called “P-shears”, for symmetric to the R-shears. These tend to link up the R-shears, forming a through-going fault zone:



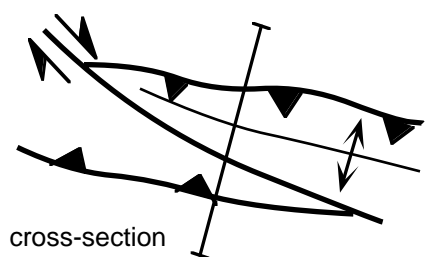
36.3.2 Convergent-Type

Convergent type structures have sometimes been referred to as transpressional structures, a horrible term which is both genetic and confuses stress and strain.

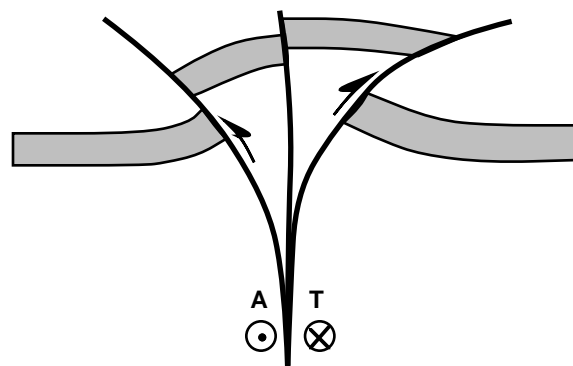
In convergent structures, you see

- enhanced development of the en echelon folds
- development of thrust faults sub-parallel to folds axes
- formation of “flower structures”

In map view:



In cross-section:



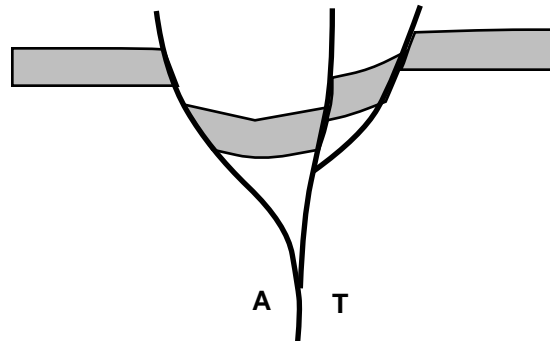
36.3.3 Divergent Type

In the divergent type, extensional structures dominate over compressional. It has the following characteristics:

- folds are absent
- development of normal faults

- formation of “inverted flower structures”

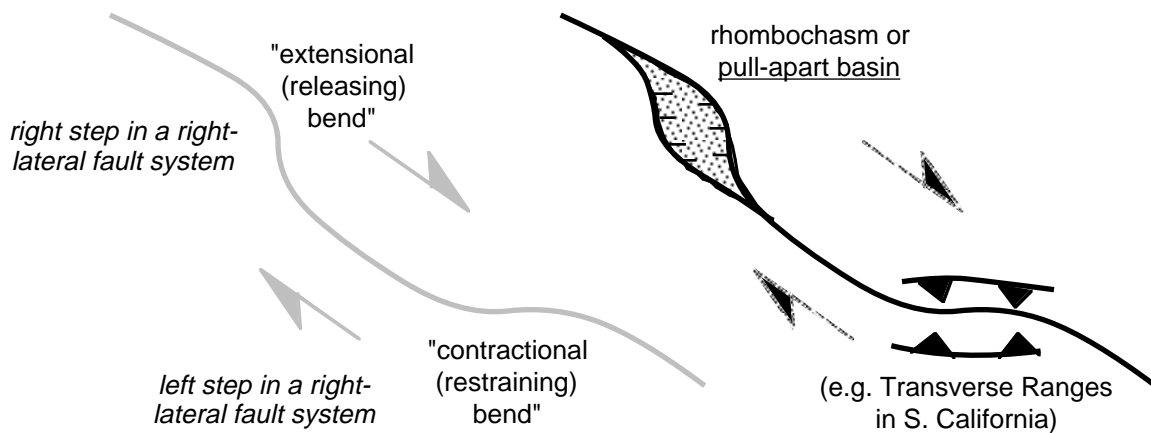
In cross-section:



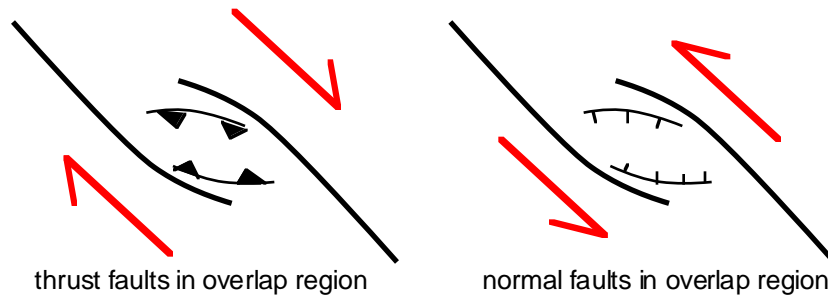
Extensional basins formed along strike-slip faults are called “pull-apart” basins.

36.4 Restraining and Releasing bends, duplexes

You can have both convergent and divergent structures formed along a single strike-slip fault system. They usually form along bends in the fault:

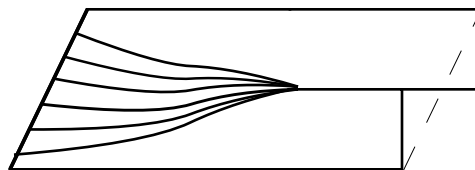


Restraining or releasing bends can be the site of formation of strike-slip duplexes, in which the faults can either be contractional or extensional, respectively. Extensional or contractional structures can also be concentrated at the overlaps in an echelon strike-slip fault segments:



36.5 Terminations of Strike-slip Faults

Transform faults, either oceanic or intracontinental, can only terminate at a triple-junction. Transcurrent faults may terminate in a splay of strike-slip faults sometimes referred to as a horsetail structure:



In this way, the deformation is distributed throughout the crust. Alternatively, they may terminate in an imbricate fan of normal faults (for a releasing bend) or thrust faults (for a restraining bend).

LECTURE 37—DEFORMATION OF THE LITHOSPHERE

So far, we've mostly talked about "horizontal tectonics", that is horizontal extension or horizontal shortening. Yet the most obvious manifestation of deformation is the mountains! That is the vertical displacements of the lithosphere.

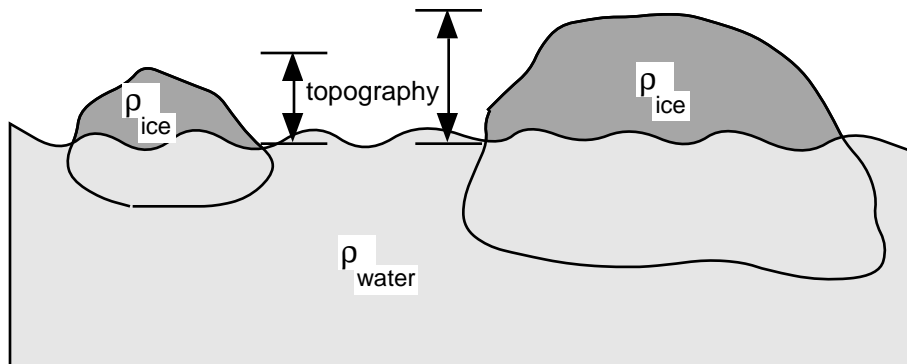
There are two parts to the topographic development question:

1. What are the mechanisms by which mountains are uplifted? and
2. Once they are uplifted, how do they evolve?

37.1 Mechanisms of Uplift

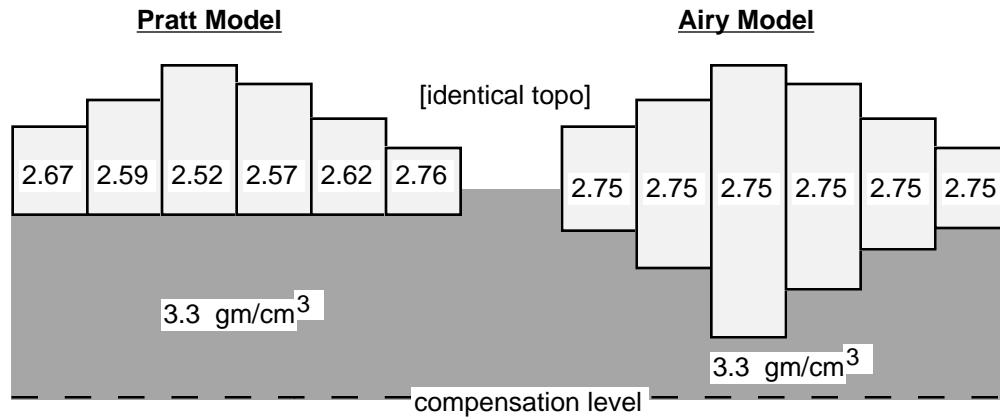
37.1.1 Isostasy & Crust-lithosphere thickening

Imagine that you have an object (an iceberg, piece of wood, etc.) floating in water:



The way to get more topography is to make the ice (or wood) thicker. The topography itself and the ratio of the part of the iceberg above and below water is a direct function of the ratio of the densities of ice and water. This basic principle is known as isostasy.

There are two basic models for isostasy. The Pratt model assumes laterally varying densities; the Airy model assumes constant lateral densities:



We now know that, in general, Airy Isostasy applies to the majority of the world's mountain belts. Thus most mountain belts have roots, just like icebergs have roots.

37.1.2 Differential Isostasy

Two relations make it simple to calculate the isostatic difference between two columns of rock:

1. The sum of the changes in mass in a column above the compensation level is zero:

$$\Delta(\rho_w h_w) + \Delta(\rho_s h_s) + \Delta(\rho_c h_c) + \Delta(\rho_m h_m) = 0$$

where "w" refers to water, "s" to sediments, "c" to crust, and "m" to mantle.

2. The changes in elevation of the surface of the earth, ΔE , equals the sums of the changes in the thickness of the layers:

$$\Delta E = \Delta h_w + \Delta h_s + \Delta h_c + \Delta h_m$$

This gives us two equations and two unknowns. Thus, if we know the densities and the changes in elevations, we can predict the changes in crustal thicknesses.

Take as an example the Tibetan Plateau, which is 5 km high. If we assume a crustal density of 2.75 gm/cm³ and a mantle density of 3.3 gm/cm³ then:

$$\Delta E = \Delta h_c + \Delta h_m = 5 \text{ km}$$

and

$$\Delta(\rho_c h_c) + \Delta(\rho_m h_m) = 2.75\Delta h_c + 3.3\Delta h_m = 0.$$

Solving for Δh_c :

$$\Delta h_c(2.75 - 3.3) = 5 * 3.3$$

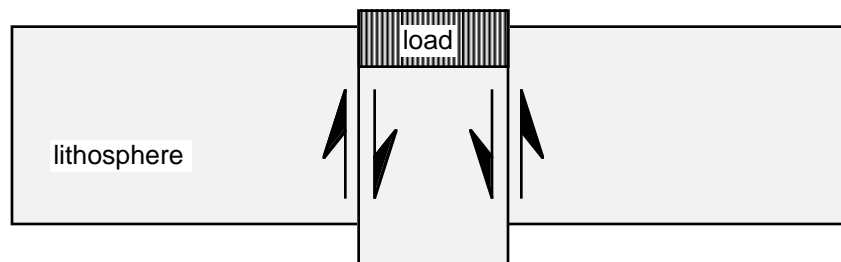
and

$$\Delta h_c = 30 \text{ km}.$$

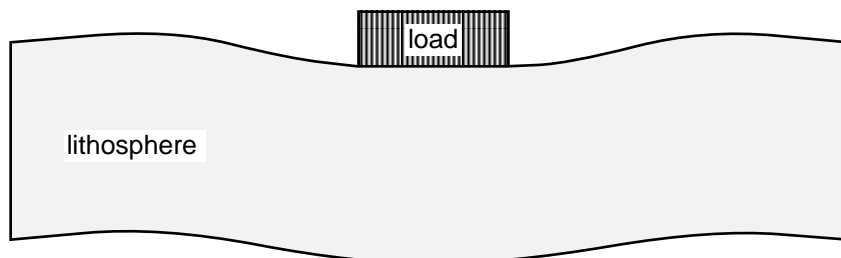
What this means is that the crust beneath the Tibetan Plateau should be 30 km thicker than a crust of equivalent density, whose surface is a sea level. The base of the crust beneath Tibet should be 25 km deeper than the base of the crust at sea level (because of the 5 km elevation). *Note that the root is about five times the size of the topographic high.*

37.1.3 Flexural Isostasy

So far in our discussion of isostasy we've made the implicit assumption that the crust has no lateral strength. Thus, when we increase the thickness by adding a load, you get vertical faults:



The Earth usually doesn't work that way. More commonly, you see:



In other words, the lithosphere has finite strength and thus can distribute the support of the load over a much broader area. The bending of the lithosphere is call flexure and the process of distributing the load

is called flexural isostasy. The equations which, to a first order, describe flexure are:

$$z = z_o \left[\cos\left(\frac{x}{\alpha}\right) + \sin\left(\frac{x}{\alpha}\right) \right] \exp\left(\frac{-x}{\alpha}\right)$$

Where x is the distance from the center of the load, z is the vertical deflection at x , and z_o is the maximum deflection at $x = 0$. z_o , α , and related constants are given by the following equations:

$$z_o = \frac{V_o \alpha^3}{8D}$$

$$\alpha = \left[\frac{4D}{(\rho_m - \rho_w)g} \right]^{\frac{1}{4}}$$

and

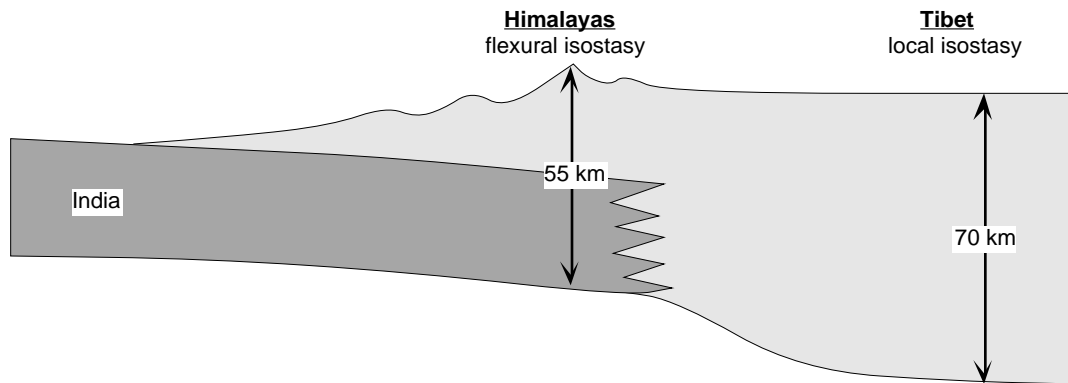
$$D = \left[\frac{Eh_e^3}{12(1 - \nu^2)} \right]$$

This last equation is what really determines the amplitude and wavelength of the deflection. D is known as the flexural rigidity, a measure of a plate's resistance to bending. The flexural rigidity is in fact the plate's bending moment divided by its curvature. A high flexural rigidity will result in only very gentle flexure.

As you can see from the above equation, D depends very strongly on h_e , the thickness of the plate being bent, or in the case of the earth, the effective thickness of the elastic lithosphere; it varies as the cube of the thickness. In simple terms, thin plates will flex much more than thick plates will.

If a mountain range sits on a very strong or thick plate, the load is distributed over a very broad area and the mountains do not have a very big root.

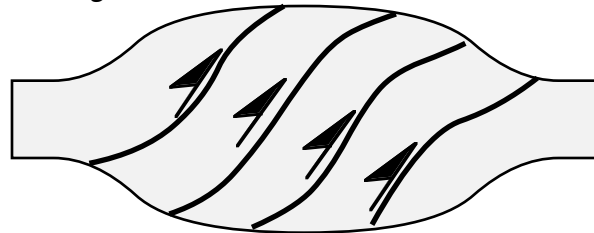
In the Himalayan-Tibetan system we see both types of isostasy:



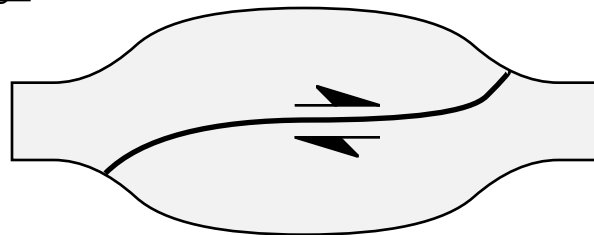
In general, the degree to which flexural vs. local isostasy dominate depend on a number of factors, including heat flow, the age of the continental crust being subducted and the width of the mountain belt.

37.2 Geological Processes of Lithospheric Thickening

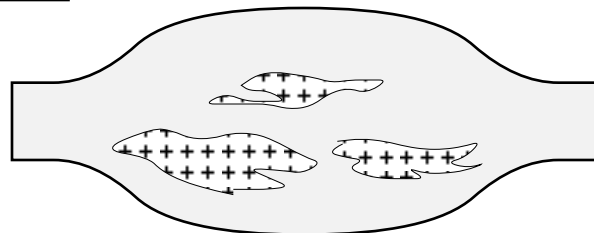
37.2.1 Distributed Shortening:



37.2.2 "Underthrusting":



37.2.3 Magmatic Intrusion:



37.3 Thermal Uplift

Because things expand when they are heated, their density is reduced. This has a profound effect on parts of the Earth's lithosphere which are unusually hot, thin, or both. Thermal uplift is most noticeable in rift provinces such as the oceanic spreading centers or intracontinental rifts where the lithosphere is being actively thinned and the asthenosphere is unusually close to the surface. It can also, however, be an important effect in compressional orogens with continental plateaus such as the Andes or the Himalaya.

For the oceanic spreading centers, the change in elevation with time can be computed from:

$$\Delta E = \frac{\rho_a}{\rho_a - \rho_w} \left[2\alpha(T_w - T_a) \left(\frac{kt}{\pi} \right)^{\frac{1}{2}} \right],$$

where, α is the coefficient of thermal expansion, k is the thermal diffusivity ($8 \times 10^{-7} \text{ m}^2 \text{ s}^{-1}$), T_w is the temperature of seawater, T_a is the temperature of the asthenosphere ($\sim 1350^\circ\text{C}$), and t is time. In continental areas the maximum regional elevation which you commonly can get by thermal uplift alone is between 1.5 and 2.0 km.

37.4 Evolution of Uplifted Continental Crust

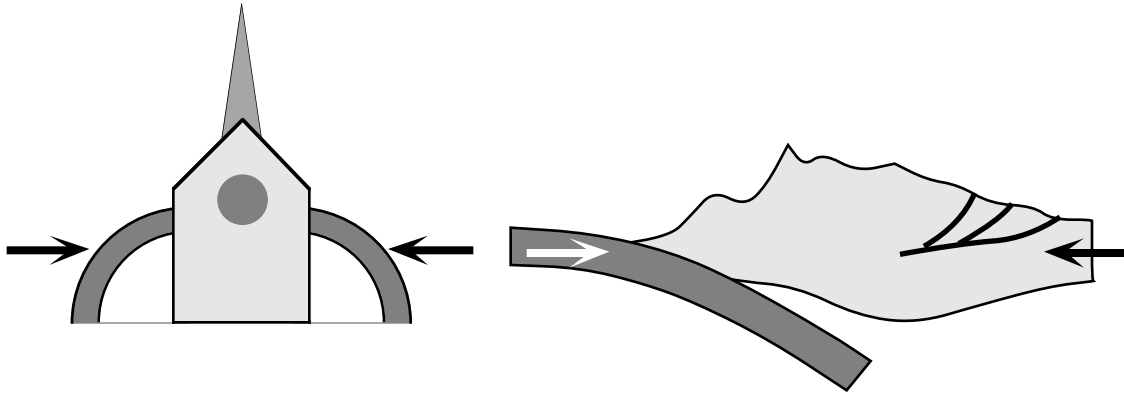
Once uplifted what happens to all that mass of rock in mountain belts? There are some simple physical reasons why mountain belts don't grow continuously in elevation. At some point the gravitational potential of the uplifted rocks counteracts and cancels the far field tectonic stresses and then the mountain belt grows laterally rather than vertically.

Generally, the higher parts of mountain ranges, especially in the Himalaya and the Andes are in a delicate balance between horizontal extension and horizontal compression. Small changes in plate interactions, rheology of the crust, or erosion rates can cause the high topography to change from one state to another.

We used to think of orogenies as being all "compressional" or all extensional. However, with this understanding of the simple physics of mountain belts, it is clear the you can easily find normal faults forming in the interior of the range at the same time as thrust faults are active along the exterior margins.

Peter Molnar makes an excellent analogy between mountain belts and medieval churches. Both are built up high enough so that they would collapse under their own weight if it weren't for their

external lateral supports. In the case of the churches, flying buttresses keep them from collapsing. In the case of mountain belts, plate convergence and the horizontal tectonic stresses that it generates, keeps the mountains from collapsing.



Many people now think that a very common sequence of events is for large scale intracrustal rifting to follow a major mountain building episode. When the horizontal compression that built the mountains is removed, the uplifted mass of rocks collapses under its own weight, initiating the rifting. This sequence of events is observed, for example in the Mesozoic compressional deformation and the Cenozoic Basin and Range formation in the western United States.

It is important to realize that there can be two type of extension in over-thickened crust: (1) a superficial effect just due to the topography, and (2) a crustal-scale effect in which the positive buoyancy of the root contributes significantly to the overall extension.

A

activation energy127
 Alberta syncline.....237
 albite twins.....120
 allochthon.....225
 Alpine fault258
 Amontons.....113-114
 analytical methods.....3
 Anderson's theory.....159-160
 Anderson's theory of faulting.....250
 Andes.....241, 270
 angle of internal friction.....107, *See also*
 fracture
 angular shear40
 annealing.....126
 anticline.....178
 antiform.....178
 Appalachians134
 Appalachians225
 Argentina.....239, 241
 asperities.....114
 asthenosphere.....270
 asymmetric half graben.....250, *See also*
 extensional structures
 asymmetric porphyroclasts220-221
 Atacama fault.....258
 Athy's Law104, *See also* compaction
 Atlas Mountains239
 augen.....152
 aulacogens.....249
 autochthon.....225
 axes.....12

B

b-value6
 basalt103
 Basin and Range250, 271
 Basin and Range3
 bedding.....207
 bending moment268
 Bighorn Basin.....243
 bond
 attraction.....100, 102
 force.....101
 length.....102
 potential energy.....100-102
 repulsion.....100, 102
 boudinage.....206

boudinage, chocolate tablet206
 boudins203, 205
 Bowden.....114
 Britain, coast of.....5
 brittle.....98
 "brittle-ductile transition"131
 Brunton compass.....15
 buckling.....192-193
 Burgers vector.....122
 Busk method.....186

C

calcite.....120
 Canada.....239
 Canadian Rockies.....226, 231, 237
 Cape Ranges.....239
 Cartesian coordinates10, 14, 17
 cataclasis.....98
 Cauchy's Law.....64, 68
 CDP23-24
 Chamberlain, T. C.225
 characteristic equation.....73
 China.....239
 cleavage203, 207-208
 anastomosing.....210
 conjugate.....210
 crenulation.....211, 216
 climb.....98
 Coble creep.....119
 COCORP.....241
 COCORP.....25
 coefficient of friction112
 coefficient of internal friction 110, *See also*
 fracture
 coefficient of thermal expansion.....102
 cohesion.....110, 112
 cold working.....125
 Colorado239
 Colorado Plateau.....135
 columnar joints.....103
 compaction.....103-104
 confining pressure.....95, 97, 107
 continuum mechanics.....36
 coordinate transformation71
 cosine.....17
 cracks, modes I, II, III.....133
 creep.....94
 creep curve95

- Crenulation cleavage216
 cross product.....18-19
 crust.....131
 crystal plastic98, 146
 curvature191
 cylindrical fold.....12
- D**
- Dahlstrom.....231
 décollement.....177, 187
 décollement.....225, 228
 defects117
 impurities118
 interstitial.....118
 linear.....121
 planar119
 point118
 substitution118
 vacancies.....118
 deformation bands.....119
 deformation lamellae.....119
 deformation map.....129
 deformation paths.....55
 deformation, crystal plastic .127, 146, 152
 Delaware Water Gap116, 214
 Denali fault.....258
 denudation245
 deviatoric stress.....65
 diagenesis.....104, 116-117
 diffractions27-28
 diffusion.....98, 118, 125-126, 129
 diffusion
 diffusion coefficient148
 erosional147
 diffusion creep.....127, 129
 crystal lattice119, 126, 129
 grain boundary116, 119, 126
 Dilation33, 41
 dip and dip direction.....15
 dip isogon.....185
 direction cosines.....14, 16, 82
 dislocation glide98, 123
 dislocation
 jogs.....124
 climb.....125
 edge123
 glide.....125-126
 glide and climb125-127
 pinning.....124
 screw123
 self stress field.....123
 strain hardening123
 dislocations.....119, 121-122
 displacement gradient tensor71-72
 displacement vector37
 Distortion.....33
 Dix equation.....25
 dolomite.....120
 dome and basin190
 dominos220
 dot product.....18
 drag folds.....195
 ductile98
 dummy suffix notation.....69
 duplex235, *See also* thrust belt
 extensional.....254
 passive roof238, *See also* triangle zone
 dynamic analysis.....161
- E**
- earthquake.....6
 earthquake.....95
 east-north-up convention.....11
 eigenvalues.....73
 eigenvectors73
 Einstein summation convention69-70
 elastic.....93
 elastic deformation.....100
 electrical conductivity.....68
 ellipticity.....50
 en echelon.....134
 engineering mechanics.....1
 exfoliation.....136
 Experimental.....3
 extension.....39
 domino model.....250
 down-to-the-basin.....247
- F**
- fabric.....203
 failed rifts.....249
 failure envelop.....108, 110, 113, *See also*
 fracture
 fault bend folding232, *See also* thrust belt
 fault plane solutions.....161
 fault rock.....146

fault rocks.....144
 fault scarp.....147
 fault-line scarp.....147
 fault-propagation folds.....242
 faults.....133
 anastomosing.....141
 blind.....149
 branch line.....142
 conjugate sets.....158
 dip slip.....143
 emergent.....147
 footwall.....141
 hanging wall.....141
 hinge fault.....144
 left lateral (sinistral).....143
 listric.....141
 listric.....160
 normal.....143
 oblique slip.....143
 piercing points.....142
 planar.....141
 reverse.....143
 right lateral (dextral).....143
 rotational.....144
 scissors.....144
 sense-of-slip.....151
 separation.....142
 slip vector.....142
 surface trace.....142
 tip line.....141
 wrench.....143
 fenster.....225
 flat irons.....148
 flexural rigidity.....268
 flexure.....267
 Flinn diagram.....59
 fluid inclusions.....138
 fluid pressure. 104, *See also* pore pressure
 fluid pressure ratio.....175
 fluids.....96
 fold axis.....186
 folding
 “competence”.....199
 buckling.....193
 dominant wavelength.....200
 elastic.....200
 flexural flow.....194
 flexural slip.....194

multilayers.....199
 neutral surface.....193
 nucleation.....200
 passive flow.....197
 theoretical analysis.....199
 viscous.....200
 folds
 anticlinoria.....180
 asymmetric.....179
 axial surface.....181-182
 axial trace.....182
 axis.....192
 class 1.....185
 concentric.....186
 conical.....188
 cylindrical.....186
 dip isogon.....185
 drag.....195
 enveloping surface.....179
 facing.....179
 hinge.....180
 interlimb angle.....183
 isoclinal.....183
 kink.....187, 195
 non-cylindrical.....188
 parallel.....186
 parasitic.....195
 plunging.....182
 reclined.....182
 recumbent.....182
 sheath.....188
 similar.....187
 superposed.....189
 symmetric.....179
 synclinoria.....180
 vergence.....179
 foliation.....203, 207
 folium.....207
 footwall.....232
 force.....2
 force.....61
 foreland.....227, 235
 foreland basin.....230
 broken.....244
 foreland basins.....229
 foreland thrust belts...226, *See also* thrust
 belt
 FORTRAN.....70

fractal dimension.....5
 fractals..... 4, 6, *See also* scale invariance
 fracture.....106, 126
 brittle.....106
 Coulomb.....110-111
 ductile.....106
 ductile failure.....111
 tensile.....108
 transitional tensile.....109
 fractures, pre-existing.....112
 Fresnel Zone.....27
 Fresnel zone.....27
 friction.....113-114

G

Garlock fault.....258
 Gaussian curvature.....191
 geometry.....2-3
 geothermal gradient.....129
 Gibbs notation.....12
 gneissic layering.....207
 graded beds.....208
 grain boundaries.....119
 grain size.....110, 129
 Granite Mountains.....243
 gravity slides.....245
 Griffith Cracks.....109
 Griffith cracks.....110
 growth faulting.. 247, *See also* extensional structures
 Gulf Coast.....247

H

hand sample.....4
 hanging wall.....232
 Heart Mountain detachment.....176
 Heart Mountain fault.....246
 Herring Nabarro creep.....119
 Himalaya.....270
 hinterland.....227, 235
 homocline.....180, 183
 horse.....235, *See also* thrust belt
 horsetail structure.....264
 horst and graben.....250
 hot working.....125
 Hubbert & Rubey.....170
 hydraulic fracturing.....112
 hydrostatic pressure.....175

hydrostatic pressure.....65

I

Iberian-Catalán Ranges.....239
 Idaho.....230
 indicial notation.....13
 interval velocity.....25
 isostasy.....265
 Airy.....265-266
 differential.....266
 flexural.....229, 267-269
 local.....269
 Pratt.....265

J

Jeffery Model.....214
 jelly sandwich.....131
 joint sets.....134
 joint systems.....134
 joints.....133
 butting relation.....135
 cooling.....136
 cross joints.....134
 sheet structure.....136
 systematic joints.....134
 twist hackles.....135
 joints.....203
 joint zone.....134
 Jura Mountains.....226

K

kinematic analysis.....161
 kinematic analysis.....33
 kinematics.....2
 klippe.....225

L

laboratory.....97
 landslides.....245
 Laramide Province.....239
 latitude.....10
 left-handed coordinates 11, *See also* right-handed coordinates
 linear algebra.....67
 lineation.....203
 lines.....14
 listric normal faults.....252
 lithosphere.....130

lithosphere.....229, 270
 lithostatic pressure.....65
 longitude.....10
 low angle normal faults.....253

M

Mackenzie Mountains239
 magnitude2
 magnitude, earthquake6
 Mandelbrot, B.5
 mantle131
 March model.....214
 Martinsburg Formation.....214, 216
 material properties.....1
 mean stress.....65
 mechanics2-3
 mélange.....246
 mélanges.....223
 metamorphic core complexes.....253
 metamorphic foliation.....113
 metamorphism117
 mica “fish”219
 mica fish.....152
 microlithon.....215, 217
 microlithons211
 mid-ocean ridges.....248
 migration25-26
 mineral fibers.....152, 203
 mineral lineations.....152
 minor structures203
 miogeocline228
 Modulus of Rigidity.....89
 Mohr’s Circle.....82
 Mohr’s Circle, 3-D.....86
 Mohr’s Circle, finite strain47
 Mohr’s circle, for stress.....106
 Mohr’s Circle, for stress.....107, 111
 Mohr’s Circle, stress.....78-79, 85, *See also*
 stress
 moment, earthquake.....6
 monocline180
 Morocco239
 Mother Lode.....138
 movement plane.....161
 mullions.....203
 multiple.....30
 multiples.....29
 mylonite.....146

N

neutral surface193
 New England136
 Newton61
 Newtonian fluid93
 non-penetrative4
 North Anatolian fault258
 north-east-down convention11, 14
 numerical methods3

O

oceanic spreading centers248
 Oklahoma239
 olistostrome.....246
 olivine130
 optical microscope4
 orientation2
 orientations.....14
 orthogonality relations82

P

P and T axes161
 P-shears.....151
 P-shears.....261
 P-waves.....22
 paleocurrent indicators12
 paleomagnetic poles12
 parallelogram law18
 parasitic folds.....195
 parautochthon.....225
 particle path37
 particle paths.....34
 passive margin.....228, 247
 pencil structure.....206
 penetrative.....4
 permeability112
 piercing points.....142
 pitch.....15
 plagioclase.....120
 plane strain.....58
 plane trigonometry8
 planes14
 plastic, perfect.....94
 plate convergence rates229
 point source.....27
 Poissons Ratio.....89
 poles12, 14

- pore fluid97
 pore fluid pressure175
 pore pressure105, 111-112
 pore space96
 porosity103-104, 112
 power law creep127
 pressure solution115-117, 126
 pressure solution213, 215-217
 grain size117
 impurities117
 temperature117
 principal stresses63
 pure shear54
- Q**
- quadrangle map4
 quadratic elongation39, *See also* strain
- R**
- R-shears151
 R-shears261
 rake15
 reflection coefficient21
 reflectivity23
 rheology87
 Rhine Graben250
 Rich, J. L.231
 Riedel Shears150, 152, 260
 rift provinces249
 right-hand rule15, 19-20
 Right-handed coordinates 11, *See also* left-
 handed coordinates
 rigid body deformation33
 rock bursts136
 Rocky Mountain Foreland239
 Rocky Mountain foreland243
 Rodgers, J.225
 rods203
 rotation1
 Rotation33
 rotation34
 left-handed34
 right-handed34
 rupture stress96
- S**
- S-C fabrics152
 S-C fabrics203, 207, 219
- S-surfaces207
 S-waves22
 sag ponds148
 San Andreas fault258
 sandstone dikes214
 scalar17-18, 67
 scalar product18, *See also* dot product
 scale3, 36
 scale invariance4-5, *See also* fractals
 scale
 global3
 macroscopic3
 map3-4
 mesoscopic4
 microscopic4
 provincial3
 regional3
 submicroscopic4
 schistosity207
 secular equation73
 sedimentary basin104
 seismic reflection
 artifacts29
 fold24
 shear strain40
 shear stress158
 shear zone140
 displacement221
 sense-of-shear219
 sheath folds152, 188
 Sheep Mountain243
 Sierras Pampeanas239, 241
 sign conventions
 engineering61
 geology61
 simple shear139
 simple shear54
 sine17
 slickenlines152
 slickensides152
 slip system123
 slip vector142
 soil mechanics105
 Spain239
 spalling136
 spherical coordinates10, 14, 17
 stacking24
 stereographic projection12

strain.....1-2
 strain.....100
 strain.....68
 strain ellipse42
 strain ellipsoid217
 strain hardening123
 strain rate.....3
 strain rate..... 92-93, 96-97, 127, 129
 strain softening.....125
 strain
 angles39-40
 coaxial54
 continuous.....34
 discontinuous.....35
 finite53
 heterogeneous.....35
 homogeneous.....35
 infinitesimal53
 lines39
 lines of no finite elongation51
 maximum angular shear49
 non-coaxial54
 non-commutability.....58
 non-rotational54
 principal axes.....48
 pure shear.....54
 rotational54
 simple shear54
 superposition58
 volume39
 volumetric103
 stress.....1-2
 stress.....100, 107, 110, 114
 stress.....61, 67-68
 stress field.....86
 stress tensor.....63-64
 stress trajectory87
 stress vector.....61
 stress
 axial65
 biaxial.....65
 deviatoric.....64
 differential.....95
 effective.....105
 isotropic106
 mean.....64-65
 normal.....77
 principal.....63

principal plane.....86
 shear77
 spherical.....66
 triaxial65
 uniaxial65
 units.....61
 stretch.....39
 striae152
 strike and dip.....14
 strike-slip, convergent259
 strike-slip, convergent type262
 strike-slip, divergent.....259
 strike-slip, divergent type262
 strike-slip, en echelon folds260
 strike-slip, parallel.....259
 strike-slip, transpression262
 structural domains36
 stylolites.....115
 stylolites.....203
 sub-grain walls126
 Sub-Himalayan Belt.....226
 Subandean belt226
 subduction, flat.....239
 subgrain boundaries119
 syncline178
 synform.....178

T

tangent vector122
 tear fault..... 258, *See also* strike-slip fault
 temperature.....117
 temperature.....96, 102, 127, 129
 tension gashes.....139
 tensor transformation70, 81
 tensor
 antisymmetric72
 asymmetric.....72
 infinitesimal strain72
 invariants.....73
 principal axes.....73, 83
 symmetric.....72
 tensors.....68
 Terzaghi.....105
 Texas.....170
 Texas.....239
 Theoretical.....3
 thermal conductivity.....68
 thermal diffusivity270

thermal expansion.....270
 thermal subsidence248
 thermodynamics.....3
 thrust belt
 Andean-type227
 antiformal stack236
 antithetic227, 229
 basic characteristics.....228
 Dahlstrom's rules231-232
 duration229
 folded thrusts.....234
 Himalayan-type.....227
 imbrication237
 ramp and flat geometry.....231
 rates229
 synthetic.....227, 229
 timing.....229
 triangle zones.....237
 types of folds in233
 thrust faults170
 gravity gliding176
 gravity sliding.....176
 paradox of170
 wedge shape176
 thrusts
 out-of-the-syncline242
 thick-skinned225, 239
 thin-skinned225
 Tibetan Plateau266-267
 Tien Shan239
 tool marks.....152
 topography, pre-glacial136
 traction vector61
 traction vectors62
 transcurrent fault.....258
 transform, intracontinental .. 258, *See also*
 strike-slip fault
 transformation matrix.....82-83
 transformation of axes.....81
 translation.....1, 33
 transposition222-223
 trend and plunge.....15
 triangle zone.....238
 triple-junction264
 twin glide.....120
 twin lamellae.....119-120

U

unit vector13-14, 16, 19
 universal gas constant127

V

vacancies.....118, 125, *See also* defects
 Valley & Ridge Province226
 vector.....13, 14, 17, 67
 vector product. 19, *See also* cross product
 addition.....18
 cross product.....18-19
 dot product.....18
 magnitude13
 scalar multiplication17
 subtraction.....18
 veins115, 133, 137
 antitaxial138
 sigmoidal.....139
 syntaxial.....138
 "tension" gashes.....139
 veins203
 velocity.....26
 pullup/pushdown.....29
 rock.....22
 vergence.....179
 viscosity200
 viscosity93
 viscous, perfect94
 void ratio104
 Von Mises.....111

W

wavelength.....26
 wedge taper.....177
 wedge, critical taper.....177
 Wichita-Arbuckle Mountains.....239
 Wind River Mountains.....241
 window.....225
 wrench fault259
 Wyoming.....230, 239, 241, 243-244, 246

Y

yield stress.....96-97
 Young's modulus200
 Young's Modulus.....89